# Morphogenetic mechanisms in zebrafish inner ear neurogenesis

Laura Fargas Madriles

TESI DOCTORAL UPF / 2016

DIRECTORS DE LA TESI

Dra. Berta Alsina Español

Dr. Esteban Hoijman

Departament de Ciències Experimentals i de la Salut

Universitat Pompeu Fabra
Barcelona

**A la meva germana Mireia**

**i als meus pares Salut i Joan**

## Agraïments

Primer de tot m'agradaria donar les gràcies a la Berta, per haver-me donat la oportunitat de fer el projecte de màster al seu laboratori i per haver-me deixat quedar a fer el doctorat. Ha estat una experiència dura, però molt gratificant. He après moltes coses, més de les que m'hauria imaginat, i la Berta ha estat sempre al meu costat guiant-me i donant-me suport. Ha estat un plaer poder ser la seva doctorand i conèixer-la, ja que a més de ser una gran directora i científica, és una gran persona.

Vull donar les gràcies a l'Esteban, co-director de la tesis i un gran amic. Hem estat treballant colze a colze i he après molt al seu costat. Les hores de confocal muntant i desmuntant embrions no ens les treu ningú. Sempre m'has transmès una gran passió per la ciència.

Agraeixo també a les persones que formen i han format part del laboratori de Biologia del Desenvolupament pel seu suport, les discussions, els dinars i per totes les bones estones de cafès i riures: Laura, Esteban, Davide, Ivan, Adrià, Héctor, Simone, Cova, Maria, Sylvia, Javi, Gina, Jelena, Àlex, Andrea, Marta, Sara i Miquel. Gràcies també al Fernando Giráldez i a la Cristina Pujades.

Especialment a "las gordas" Malmusi, Simo i Giulia pels sopars, les tonteries, els "piques" i per ser uns grans amics. A l'Adrià pels dies de surf i els que encara ens queden. A l'Ivan, pels dies de riures infinits, els musicals, les llistes compartides, per mil coses i perquè som "los favoritos de acuáticos".

Moltíssimes gràcies a les persones que he conegut a Viena. A la Gerlinde i a la Viktoria per la seva acollida al laboratori i per la seva paciència. A l'Eirini i a l'Ogi per tots els moments inoblidables que hem viscut, per les històries, riures i aventures. Sou uns amics per sempre.

Gràcies a la Theresa, la Cristina i l'Anna R, persones puntals a la meva vida, que per molt lluny que estiguin sempre estan al meu costat.

Gràcies al "Valls team", Clàudia i Eli, per les mil estones juntes, pels moments inoblidables de sopars al Ganxo, les Xamores, dies de platja i per ser unes persones que sempre formareu part de la meva vida.

Gràcies al Gonzalo, la Laura, el Carlos i en Fran per les hores de desconnexió i de ballar sense parar. Sou uns cracks!

Vull donar les gràcies a totes aquelles persones que d'alguna manera han compartit moments importants de la meva vida i que han estat presents durant aquests anys de tesis: Sara B, Karen, Noelia, Valèria, Paola, Vicky, Eriong, Marcel, Igna, Anna M, Maria, Anton, Gemma, Vangelis, Stavros, Alexis, Albert, Mario.

Especialment vull agrair a en Fran el seu suport durant aquests mesos d'escriptura. Gràcies per estar dia a dia al meu costat, aguantar els moments d'estrès, que no són pocs, i fer-me riure. Gràcies per tots els moments viscuts. Aquesta tesis no hagués estat el mateix sense tu.

Vull donar les gràcies a tota la meva família per fer-me sempre costat i pels moments de felicitat que m'han donat. Als tiets Robert i Montse per haver-me cuidat tant, per donar-me tant d'amor i pels estius a Calella que tot nen voldria. Al tiet Manel, amb qui sempre he sentit que tenim un vincle especial, per estimar-me tant. A la tieta Montse per estar sempre tan pendent de mi. A la Judith per transmetre'm sempre tanta confiança en mi mateixa i pels seus ànims. Al Guigo, la Tate, l'Ot i l'Abril per les mítiques nits de sopars i xerrades i pels caps de setmana de desconnexió que m'omplen d'energia.

Finalment, vull donar les gràcies als meus pares i a la meva germana perquè gràcies a vosaltres tot el que he fet ha estat possible. Sou essencials a la meva vida i us estimo moltíssim.

# Abstract

The vertebrate inner ear is a highly ordered and complex three-dimensional structure. Therefore, its development is an intricate process by which all cell types and structures involved in inner ear function are generated in a precise manner. In this work we analyze in detail the spatiotemporal regulation of the formation of the sensory and neurogenic domains and the relation of proneural genes and Notch signaling, specifically the role of *her4*, a Notch target. We show that *her4* expression is highly dynamic and spatiotemporally regulated, and that it participates in the lateral inhibition during otic neurogenesis. Moreover, by taking advantage of the powerful imaging technologies we analyze in real time the formation of the neurogenic domain, which is characterized by the restricted expression of *neurog1*. We identify pioneer cells that express *neurog1* outside the otic primordium, migrate and ingress into the epithelializing placode, becoming the first otic neuronal progenitors. These pioneer cells promote local *neurog1* expression in other otic cells, and its ingression relies in the activity of the FGF pathway. Finally, we analyze with high spatiotemporal resolution the delamination of neuroblasts from the otic epithelium, which resembles a developmental EMT.

# Resum

L'orella interna dels vertebrats és una estructura tridimensional, altament organitzada i complexa. Per aquest motiu, el seu desenvolupament és un procés intricat mitjançant el qual els diferents tipus cel·lulars i estructures involucrades en la funció de l'orella interna són generats de manera precisa. En aquest projecte analitzem en detall la regulació espaciotemporal de la formació dels dominis sensorial i neurogènic i la relació entre els gens proneurals i la via de senyalització de Notch. Específicament analitzem la funció de *her4*, que forma part de la via de Notch. *her4* presenta una expressió dinàmica regulada espaciotemporalment i participa en el procés d'inhibició lateral durant el procés de neurogènesis òtica. D'altra banda, mitjançant les noves tècniques en microscòpia, analitzem en temps real la formació del domini neurogènic, caracteritzat per l'expressió restringida de *neurog1*. Identifiquem les cèl·lules pioneres que expressen *neurog1* que es troben fora del primordi òtic, migren i ingressen dins la placoda en procés de epitelialització. Aquestes cèl·lules pioneres esdevenen els primers progenitors neuronals de l'orella interna promovent l'expressió local de *neurog1* en altres cèl·lules òtiques. El seu ingrés depèn de la via de senyalització de FGF. Finalment, analitzem amb una gran resolució espaciotemporal la delaminació dels neuroblasts de l'epiteli òtic, procés similar a una EMT.

# Preface

During embryonic development, specialized cells originate at distinct domains of the inner ear. Therefore, patterning and cell fate specification must be coupled with morphogenesis of the entire organ. Although some spatiotemporal information about expression of proneural genes and specification of neuronal progenitors in the inner ear has been reported, the dynamics of neurogenesis and the cell behaviors underlying the formation of the neurogenic domain are poorly understood.

This thesis provides new information on the formation of the sensory and neurogenic domains taking into account that these domains develop almost concomitantly. Moreover, we combine 4D analysis of cell behaviors with dynamic quantification of proneural expression and uncover the mechanism for the construction of the zebrafish otic neurogenic domain. Therefore, we disclose the impact of cell behaviors on neuronal specification proposing a novel view for initiation of otic neurogenesis integrating cell dynamics and illustrating the relevance of cell behaviors for acquisition of neuronal fate.

Moreover, unveiling the mechanisms involved in otic sensory neurons formation, we can contribute in the development of new therapies for the treatment of neuronal disorders.

# Table of contents

# 1. INTRODUCTION

## 1.1. The vertebrate inner ear

The vertebrate inner ear is one of the main sensory organs of the head and it is responsible for the senses of hearing and balance. The sense of hearing detects acoustic stimuli from vibratory movement and provides the ability to communicate and interact with the external world. Moreover, a properly functioning balance system allows humans to identify the orientation, determine the direction and the speed of movement. Through a complex mechanism involving the transformation of waves into electrical impulses, the information is transmitted to the appropriate part of the brain.

The inner ear is a highly conserved structure among vertebrates and it consists of a series of interlinked fluid-filled chambers containing patches of sensory epithelia. The number of those patches varies between animal species, but all have at least six of them which transduce specific stimuli (Wu and Oh, 1996; Lewis and Narins, 1999; Fritzsch et al., 2002) (**Figure 1**). The dorsal part of the ear is similar among all vertebrates and consists of vestibular organs comprising the gravity-sensitive maculae (placed in the central utricle and saccule) which are responsible for the sense of balance and detect linear acceleration in the horizontal and vertical axis respectively, and the three rotation-sensitive cristae (placed in the ampullary connections between each semicircular canal and the utricle) which detect angular acceleration. The morphology of the ventral part of the ear is more specific to each class of vertebrate, but it typically consists of an auditory organ that transduces mechanical stimuli associated with sound and provides the basis of hearing. The auditory system only contains one sensory organ (organ of Corti in mammals and basilar papilla in birds) placed along the cochlear duct. Fishes possess no structure homologous to the cochlear apparatus. Instead, maculae (in the

saccular and lagena pouches) appear to be regionally specialized with auditory functions, vestibular functions or both (Haddon and Lewis, 1996; Bever and Fekete, 2002; Bryant et al., 2002) (**Figure 1**).
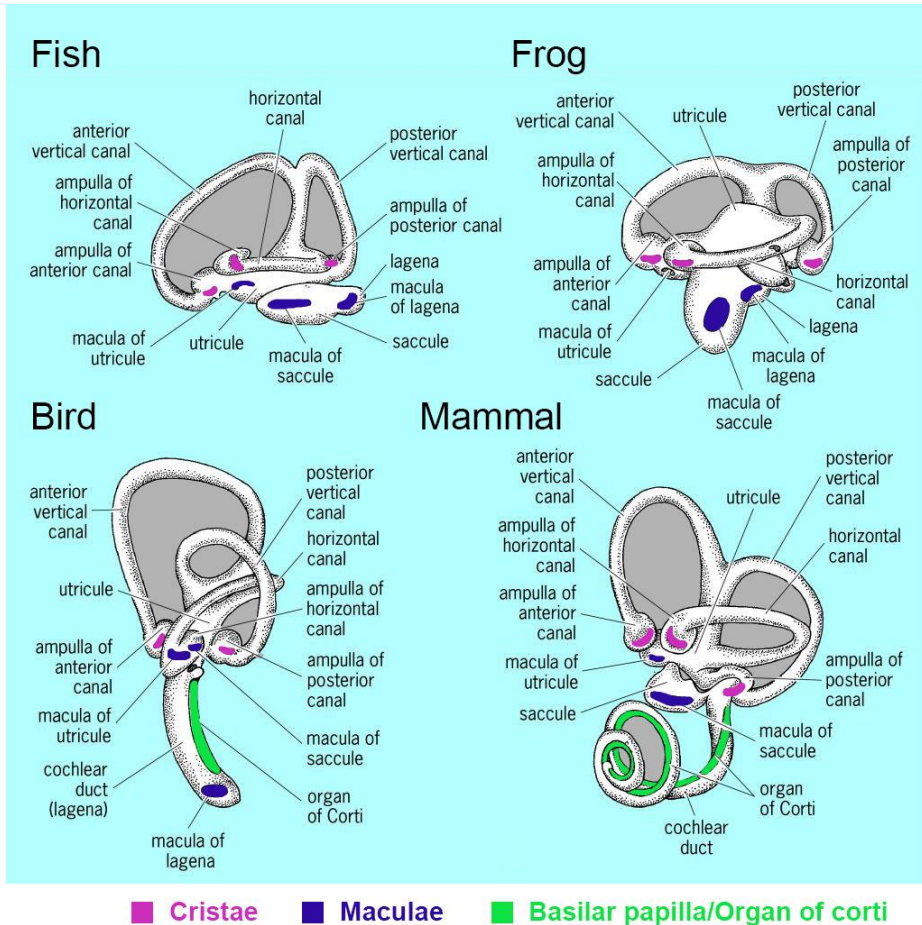


**Figure 1. Schematic representation of the adult inner ear of different vertebrate species.**

The sensory epithelium of the ear is heterogeneous in structure and function. Different specialized regions are responsible for the diverse functions of the organ. The dorsal part of the ear is a highly conserved structure among vertebrate species. The ventral part presents a prominent evolution; it is nearly absent in aquatic vertebrates and shows increasing degrees of complexity in

terrestrial animals. Left ear external view. Modified web image (http://encyclopedia2.thefreedictionary.com).

Detection of sensory stimuli in each sensory patch is mediated by the functional cellular sensory unit that is composed by an array of mechanosensory hair cells (HCs), associated supporting cells (SCs) and sensory neurons (**Figure 2**). These specialized cells are morphologically similar in all epithelial structures of the ear in all vertebrates (and in the lateral line of the fishes and amphibians), but they have either auditory or vestibular functions. HCs are specialized mechanoreceptors and are located within a highly-ordered and complex topological organization in the sensory patches. Each HC presents a hair bundle protruding from the apical surface. This comprises a single kinocilium and a bundle of stereocilia that are immersed in a mobile gelatinous matrix that overlie each of the cristae (cupula) and maculae (otolithic membrane). The movement of these gelatinous structures provokes the deflection of the hair bundles that causes the opening of the mechanosensitive ion channels and the consequent generation of electrical potential (Hudspeth, 1989). On the other side, HCs are secondary receptor cells; they do not elaborate either axons or dendrites but are innervated by axons of bipolar primary afferent sensory neurons, which transmit the information to second order neurons in the vestibular and auditory nuclei in the brainstem. Their somas are located within the statoacoustic ganglion (SAG) subdivided in two ganglia, reflecting the dual function of the organ: neurons of the vestibular ganglion innervate the vestibular HCs and project towards de vestibular nuclei, and neurons of the auditory ganglion innervate cochlear sensory epithelium and project towards the cochlear nuclei (Guth et al., 1998; Torres and Giraldez, 1998; Burighel et al., 2003, 2008, 2011). HCs are also surrounded and isolated from one another by the SCs. SCs are non-

5

sensory cells that vary greatly in morphology and present several functions: maintain epithelial integrity by generating appropriate extracellular matrix and cell adhesion molecules (Haddon et al., 1999; Whitfield et al., 2002), maintain ion homeostasis and finally, in some species possess stem-cell like function for HC renewal by induced division during regeneration (Corwin and Cotanche, 1988; Stone and Rubel, 1999; Baird et al., 2000; Williams and Holder, 2000; Rubbini et al., 2015).
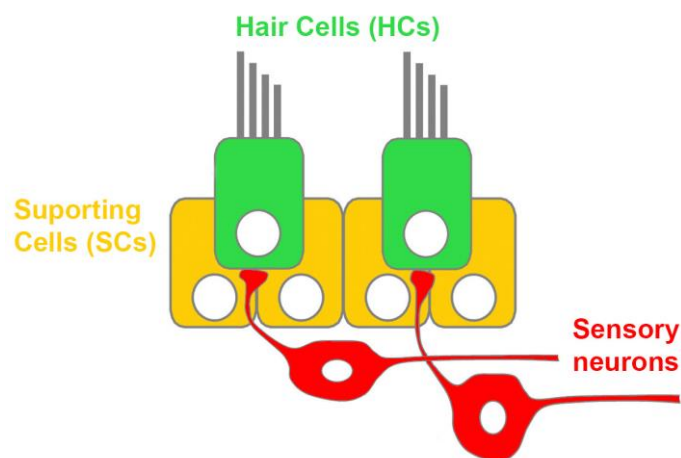


**Figure 2. The sensory patch.**

The inner ear sensory unit consists of three different cell types: hair cells (HCs, green), supporting cells (SCs, yellow) and sensory neurons (red) whose soma is located within the statoacoustic ganglion (SAG) positioned adjacent to the inner ear and innervate HCs within the epithelium. Modified from (Alsina et al., 2009).

## 1.2. The cranial placodes

Despite the high complexity of the inner ear, its origin is very simple. It derives from a transient structure in the embryonic ectoderm, the otic placode.

### 1.2.1. Placode development

Specialized sensory organs and most of the neurons in the vertebrate head derive from the cranial placodes, which are transient discrete regions of thickened columnar epithelium that form in specific positions in the head of vertebrate embryo. The most anterior placodes include the single adenohypophyseal placode, the bilateral olfactory and lens placodes and the trigeminal placodes. The posterior set of placodes consists of the otic and epibranchial placodes (Baker and Bronner-Fraser, 2001; Streit, 2004; Schlosser, 2006; Saint-Jeannet and Moody, 2014) (**Figure 3A-B**). Furthermore, in amphibians and fish additional placodes are present which form the lateral line system (Schlosser et al., 1999; Baker and Bronner-Fraser, 2001). These cranial placodes do not develop directly as individual entities from the ectoderm, they are induced at the neural plate border, in distinct but overlapping domains. Specifically, cranial placodes arise from a common zone of ectoderm; a horseshoe shaped area called pre-placodal region (PPR) originated at the border between the neural plate/neural crest established at the end of gastrulation and future epidermis (Baker and Bronner-Fraser, 2001; Streit, 2004; Schlosser, 2006; Saint-Jeannet and Moody, 2014).

The PPR is a region of competence[1] for all craniofacial sensory placodes. Spatiotemporal changes in this competence state are very important for placode induction[2]; each individual placode is induced at different times by a different combination of tissues and molecules, consistent with the diverse fates (D'Amico-Martel and Noden, 1983; Schlosser and Northcutt, 2000; Baker and Bronner-Fraser, 2001; Bhattacharyya et al., 2004; Bailey and Streit, 2006; Bailey et al., 2006; Ohyama et al., 2007; Schlosser, 2010).
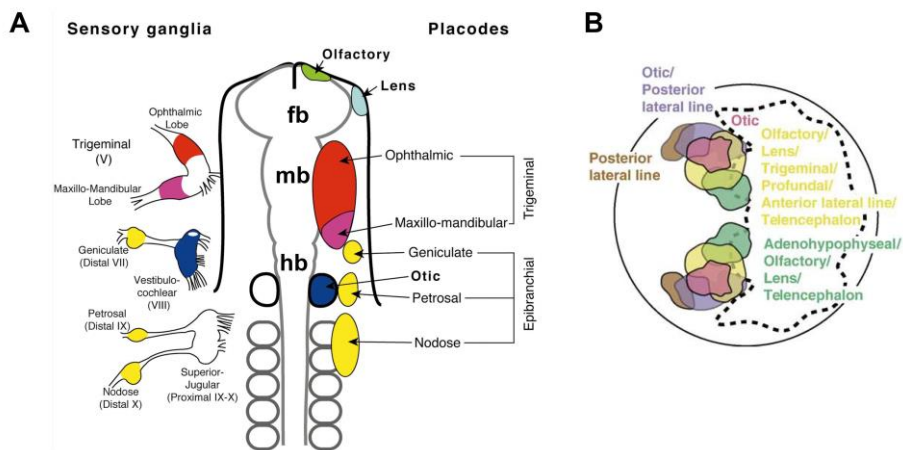


**Figure 3. The cranial placodes in vertebrates.**
**(A)** Fate map of the cranial sensory placodes and their corresponding sensory ganglia in an 8 ss chick embryo. The otic placode (right side, in blue) contributes to sensory neurons of the VIIIth ganglion (left side, in blue). Modified from (Baker and Bronner-Fraser, 2001). **(B)** Fate map of late gastrula zebrafish embryo with

---

[1] The **competence** of a tissue is defined by its ability to acquire a specific fate in response to appropriate inducing signals (Groves and Bronner-Fraser, 2000).

[2] Tissue **induction** has been defined as an interaction between an inducing and a responding tissue that alters the path of differentiation of the responding tissue (Jacobson, 1966; Gurdon, 1987; Jacobson and Sater, 1988).

substantial overlap between ectodermal regions giving rise to different placodes. The otic placode is depicted in purple. Dotted line indicates the boundary of the prospective neural plate. From (Schlosser, 2006). fb, forebrain; hb, hindbrain; mb, midbrain.

A two-step model was described for the development of the cranial placodes. The first step in placode induction is the establishment of the neural plate border region which will give rise to the PPR, and also to the neural crest (NC) cells (Baker and Bronner-Fraser, 1997). In all organisms studied, the establishment and maintenance of the border between the neural plate and the adjacent non-neural ectoderm requires an integration of signals from the organizer, the developing neural plate, the paraxial mesoderm and the non-neural ectoderm, involving FGF and Wnt signals and the controlled balance between BMP and their antagonists (Liem et al., 1995; Neave et al., 1997; LaBonne and Bronner-Fraser, 1998; Nguyen et al., 1998; Streit and Stern, 1999; Litsiou et al., 2005). Afterwards, the PPR is specified and the cells that will form the cranial placodes will be segregated from the three other ectodermal domains (epidermis, neural crest and neural plate). Placodal fate gets restricted to anterior regions of the neural plate border and at gastrula stages, all regions of the ectoderm are competent to form placodes. The PPR is defined by the expression of a combination of transcription factors belonging to the Six, Dlx, Eya, Dach, Gata, Foxi and Msx families that confer its identity and competence for specific placode-inducing signals (Esteve and Bovolenta, 1999; Kobayashi et al., 2000; David et al., 2001; McLarren et al., 2003; Woda et al., 2003; Ohyama and Groves, 2004a; Schlosser and Ahrens, 2004; Brown et al., 2005; Khatri et al., 2014). The PPR is subsequently divided along the AP axis into individual domains in which cells will adopt a fate characteristic for each sensory placode. Fate map analyses in frog, chicken and fish also show that before differentiation of different cranial placodes, the

precursors can be intermingled in this region (Kozlowski et al., 1997; Streit et al., 2000; Whitlock and Westerfield, 2000; Bhattacharyya et al., 2004; Pieper et al., 2011). The segregation of the PPR into different placodes is progressive and several studies have pointed out the importance of cell arrangements associated with sensory placode separation. In chicken embryos is documented that during the separation process cells of the PPR undergo extensive cells movements (Streit, 2002; Bhattacharyya et al., 2004). However, in *Xenopus*, analysis of cell movements by time-lapse imaging shows very little rearrangements within the PPR during initial segregation of placodal domains (Pieper et al., 2011). Another study focused on epibranchial (EB) placodes shows that placode cells undergo cell rearrangements in response to migrating NC (Theveneau et al., 2013). In zebrafish fate-mapping data indicate that at midgastrula stage (50% epiboly, 5-6 hpf) the precursors for all the different placodes are already organized in the expected AP order. Interestingly, a morpholino-based study also described the importance of precursor cell movements and convergence in the posterior otic/EB placode in which integrin-α5 (*itga5*) coordinates directed cell migration and recruitment of cells from adjacent regions (Bhat and Riley, 2011).

## 1.2.2. The otic placode

The earliest morphological evidence for the primordium of the inner ear is the otic placode that can already be visible apposed to the posterior hindbrain at mid-somite stages (9-10 ss in chick; 13.5-14 hpf in zebrafish) (**Figure 4A-B**, 10 ss). The entire inner ear, together with the neurons that innervate it, are derived during development from the otic placode (Torres and Giraldez, 1998; Baker and Bronner-Fraser, 2001).

10

As described above, once the PPR is formed is then subdivided into distinct subdomains containing shared precursors for multiple placodes (Bailey et al., 2006; Schlosser, 2006). With regard to the otic placode, previous studies suggested that their precursors might arise from a common subdomain of the PPR concomitantly with the EB placodes since prior to the appearance of the otic placode, a large *Pax2/8*-expressing domain encompasses the precursors of future EB and otic placodes, and also contains precursors for the anterior and posterior lateral line placodes (Groves and Bronner-Fraser, 2000; Streit, 2002, 2004; Ohyama and Groves, 2004b; Schlosser and Ahrens, 2004; McCarroll et al., 2012). This domain is coined otic-epibranchial precursor domain (OEPD) (Freter et al., 2008) to highlight the close developmental relationship between these placodes (**Figure 4A-B**, 4 ss). In zebrafish, it was shown that differential levels of *pax2a* and *pax8* modulate commitment and behavior of cells that eventually contribute to the otic and EB placodes. Heat-shock-induced misexpression and morpholino-based gene knockdown, demonstrated that cells with high levels of pax2a protein contribute to the otic placode, while lower levels of pax2a drive precursors to the EB placodes (McCarroll et al., 2012). Fgf signals from the neural tube and head mesoderm during early somitogenesis promote formation of the multipotent *Pax2a/8*-positive domain (Nechiporuk et al., 2006) and, in parallel with other factors such as Wnt and Notch, this territory is divided into the otic placode and the adjacent territory that gives rise to epidermis and EB placodes (Ladher et al., 2000, 2010; Ohyama et al., 2006; Freter et al., 2008; Jayasena et al., 2008; McCarroll et al., 2012).

The appearance of the morphologically visible otic placode is concurrent with the elongation of cells and the acquisition of apicobasal polarity. In chick and mouse, once the otic precursors coalesce, the otic placode becomes visible and recognizable from the surrounding non-placodal

ectoderm as a thickened region (**Figure 4A**, 10 ss) (Graham and Begbie, 2000). However, in zebrafish, the otic placode appears to emerge from the unorganized mass of ectodermal cells beneath the enveloping layer (EVL) as a compacted mass of cells, and the thickening is less obvious (**Figure 4B**, 10 ss). In higher vertebrates, such as birds and mammals, the otic placode transits into the otic vesicle through a deepening invagination as an epithelial sheet to form the otic cup which finally pinches off from the surface ectoderm as a closed vesicle sunk within the head mesenchyme (**Figure 4A**, 16 ss). In the fish, the process differs from that seen in amniotes. By contrast, no cup or pit is seen and the initial mass of placodal cells in the ectoderm appears simply to model itself into an ovoid solid ball forming the otic vesicle by hollowing just beneath the surface (**Figure 4B**, 16 ss). Presence of actin staining concentrated at the future luminal surfaces before any lumen has opened, shows that the cells already have their epithelial polarization. Small intercellular spaces generated at the apical side will be fluid-filled and expanded to generate the lumen (Haddon and Lewis, 1996; Hoijman et al., 2015). The resulting hollow epithelial structure is the otic vesicle (**Figure 4A-B**, 55 hr, 24 hpf).

It is considered that at this stage, once the otic field has become progressively committed[3] to the otic fate, it reaches an irreversible state of determination[4] (Waddington, 1937; Jacobson, 1963; Swanson et al., 1990; Gallagher et al., 1996). Once the state of determination is achieved, the otic vesicle undergoes a period of extensive cell

---

[3] A cell or tissue is **committed** to a particular fate if it adopts that fate regardless of its environment (Groves and Bronner-Fraser, 2000).

[4] **Determination** is the property of the otic field to develop into an ear independently of the embryonic environment (Waddington, 1937; Jacobson, 1963; Swanson et al., 1990).

proliferation that is under the control of several growth factors (Leon et al., 1995; Sanchez-Calderon et al., 2007). The combination of cell proliferation and the complex morphogenetic changes will shape the final organ and transform the otic vesicle into a highly organized structure with all its sensory elements placed at their specific positions.
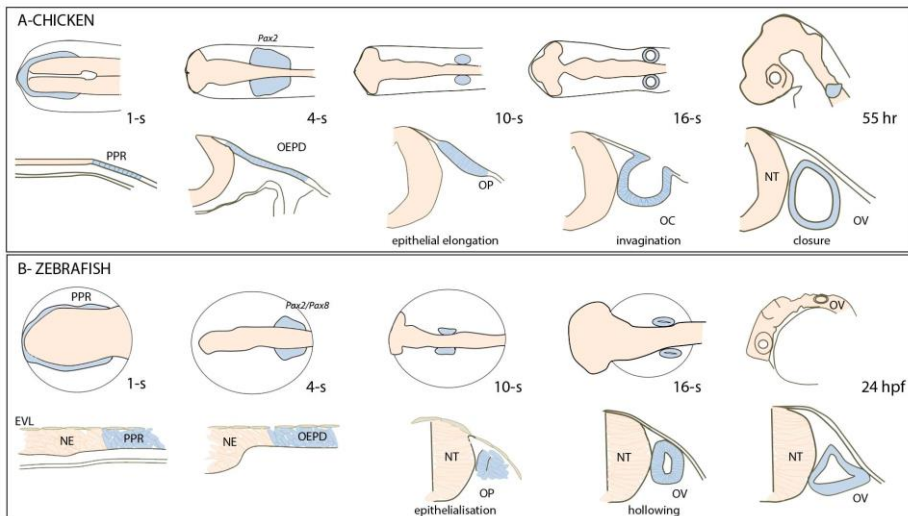


**Figure 4. Early inner ear development in chick and zebrafish.**
**(A, B)** Schematic representation of early development of the inner ear from the appearance of the PPR until the formation of the OV. **(A)** In chick **(B)** In zebrafish. In both organisms the PPR emerges adjacent to the neural plate at 1 ss. The PPR splits into larger preplacodal domains, including the OEPD, which expresses *Pax2* in chick and *pax2/pax8* in zebrafish. The otic placode is morphologically visible as a thickening of the epithelium by 10 ss. The otic vesicle appears approximately at 16 ss. First row in each panel shows dorsal views, except the last image that is a lateral view. Bottom rows show transversal sections of the hindbrain at the level of the otic region (blue). PRR, preplacodal region; NE, neuroepithelium; EVL, enveloping layer; OEPD, otic-epibranchial domain; NT, neural tube; OP, otic placode; OC, otic cup; OV, otic vesicle. From (Alsina and Whitfield, in press).

## 1.3. Inner ear development

The development of such a sophisticated structure as the inner ear from the otic placode involves a series of changes in the otic ectoderm, which require the action of inductive signals emanating from neighboring tissues and within the ear itself.

## 1.3.1. Inner ear induction

Ear induction and specification[5] are processes composed of a series of individual and overlapping steps. Within the presumptive otic placode region, inductive signals are a sequence of discrete instructions that act to specify and then commit the placodal ectoderm, leading to the complete differentiation to an inner ear fate (Gurdon, 1987; Groves and Bronner-Fraser, 2000). It is known that most of the genes expressed at the otic placode stage maintain their expression in the otic vesicle, but restricting their expression domain, suggesting their implication in the regional patterning of the otic vesicle.

Several genes have been found to be specifically expressed in the presumptive otic ectoderm and characterize the different steps of inner ear development. In chick, together with classical grafting experiments, the specification of the otic placode has been determined to occur approximately at 5-6 ss with respect to *Pax2* expression (Groves and Bronner-Fraser, 2000). In zebrafish, the earliest reported marker for the otic anlage is *foxi1*, which is expressed in otic precursor cells before the otic placode becomes visible. It regulates the expression of other early

---

[5] A tissue is said to be **specified** to a particular fate when it has already received inducing signals and can express markers of that fate in the absence of any additional signals (Groves and Bronner-Fraser, 2000; Ohyama et al., 2007).

markers such as *pax8*, *pax2a* and *dlx3b* and disruption of this gene, by homozygous *hearsay* (*hsy*) mutation, results in a reduction or loss of the otic placode and vesicle (Solomon et al., 2003). The second earliest known ear-specific markers of otic placode induction include members of the *pax2/5/8* family of transcription factor genes in both fish and mammals (Pfeffer et al., 1998). The otic precursor marker *pax8* is the first gene of the *pax2/5/8* family to be induced in the primordium of the otic placode during late gastrulation, between 8.5 and 9 hpf (85-90% epiboly). Its expression is strongly upregulated until the formation of the otic vesicle (Pfeffer et al., 1998; Phillips et al., 2001).

There is a constraining evidence that competent ectodermal cells respond to specific molecular signals coming from adjacent tissues to form different craniofacial placodes. In the case of the otic placode, some of the inducing signals come from members of the Fibroblast Growth Factor (FGF) family (Ohyama et al., 2007; Schimmang, 2007; Ladher et al., 2010). Several FGF family members are expressed in the primordium of the hindbrain or cranial mesoderm prior to otic placode formation with species-specific patterns (Fekete, 2000), and have been discussed as potential ear inducers in frog, chicken and mouse (Wilkinson et al., 1988; Represa et al., 1991; Mansour et al., 1993; Mansour, 1994; Mahmood et al., 1996; McKay et al., 1996; Lombardo et al., 1998; Fekete, 2000; Vendrell et al., 2000; Adamska et al., 2001; Abelló et al., 2010). In mouse, *Fgf3* and *Fgf10* are expressed in hindbrain and cranial mesoderm respectively and embryos lacking both of them fail to form otic vesicles (Alvarez et al., 2003; Wright and Mansour, 2003a). In chick, loss and gain of function experiments suggested that *Fgf3* is required for inner ear induction and development (Represa et al., 1991; Vendrell et al., 2000). In zebrafish, at least two members of the FGF family of peptide ligands, *fgf3* and *fgf8,* are expressed in the future hindbrain by late gastrula stages (75-85%

epiboly, 8 hpf) and appear to be essential for otic induction (Phillips et al., 2001; Léger and Brand, 2002; Maroon et al., 2002; Liu et al., 2003). Loss of either *fgf3* or *fgf8* leads to a reduction in ear size, and inactivation of both genes simultaneously blocks otic induction resulting in near or total ablation of otic tissue (Phillips et al., 2001). Misexpression of *fgf3* or *fgf8* can lead to the formation of ectopic otic placodes. Therefore, it has been demonstrated that FGF signaling is sufficient and necessary for otic induction (Phillips et al., 2001, 2004; Léger and Brand, 2002; Maroon et al., 2002; Liu et al., 2003). It has also been suggested that the competence of embryonic ectoderm to respond to FGF signaling during otic placode induction correlates with the expression of PPR genes (Martin and Groves, 2006). Previous studies have shown that competent ectodermal cells start to express *pax8* as the earliest response to Fgf signals from adjacent tissues and that this induction does not occur in the absence of it (Phillips et al., 2001). The function of fgf8 is disrupted by the *acerebellar* (*ace*) mutation, which dramatically reduces the number of pre-otic cells expressing *pax8* and *pax2a* and results in formation of small, abnormally patterned otic vesicles (Brand et al., 1996; Phillips et al., 2001). Therefore, several lines of evidence suggest that early otic markers such as *pax8* and *pax2* mediate otic induction or early differentiation in response to Fgf signaling (Phillips et al., 2001; Léger and Brand, 2002; Maroon et al., 2002; Ladher et al., 2005; Martin and Groves, 2006).

However, even though the induction of *Pax2* in cranial ectoderm is commonly thought to be synonymous of otic placode induction, studies in chick and mouse have shown that *Pax2* induction by FGF signaling can also give rise to structures other than the otocyst, such as the epidermis or EB placodes. This suggests that *Pax2*-expressing cells are not yet committed to an otic fate (Streit, 2002; Ohyama and Groves, 2004b; Ohyama et al., 2007). Therefore, Ohyama and colleagues called

"pre-otic field" this domain marked by early otic marker genes, differentiating it from the otic placode. They also reformulated the two-step model of placode induction and a new step was defined in which FGF signaling is required for the induction of the *Pax2* positive pre-otic field, while additional signals (such as Wnt) are required to subdivide the pre-otic field into the otic placode and epidermis (Ohyama et al., 2007). However, it is worth noting that Fgf signaling is required for the pre-otic expression of some, but not all, of the transcription factors involved in otic induction (Liu et al., 2003). In zebrafish induction of *foxi1*, *dlx4b* and *sox9b* is unaffected in mutants lacking fgf3 and fgf8 function (Solomon et al., 2004). Indeed, foxi1 and pax8 have been proposed to mediate early Fgf dependent otic specification and dlx3b and pax2a mediate later Fgf signaling required for maintained development (Hans et al., 2004, 2007).

Ladher and colleagues reported the first evidence of the involvement of Wnt signaling in otic placode induction. In the presumptive chick otic ectoderm it was observed that induction of otic marker genes such as *Pax2* by Fgf19 was greater in the presence of Wnt8c (Ladher et al., 2000). Other studies carried out in mouse also demonstrate that presumptive otic ectoderm is exposed to Wnt signals (Mohamed et al., 2004; Ohyama et al., 2006). It was shown that constitutive activation of the canonical Wnt signaling pathway by stabilization of β-catenin, a downstream molecule required for canonical Wnt signaling pathway, in *Pax2*-positive cells causes an expansion of the otic placode at the expense of epidermis. Moreover, it was proposed that canonical Wnt signaling could be the signal required to mediate the placode-epidermis fate decision after the induction of the *Pax2* positive pre-otic field by FGF, suggesting a potential crosstalk between Wnt and FGF pathways (Ohyama et al., 2006).

As a summary, the formation of the otic placode from the naïve ectoderm is described as a three-step model. First, it requires the formation of the PPR, a zone of competence for the craniofacial sensory placodes. Second, FGF signaling induces the "pre-otic field" which is subsequently partitioned into non-otic epidermis and committed otic placode tissue through the action of Wnt signaling and maybe by combinations of other local acting factors. It is possible that these processes overlap extensively in time and they might not be completely independent. Therefore, the same set of inducing signals, acting at different times, may serve to specify different processes during inner ear development.

## 1.3.2. Otic patterning

After the otic induction and specification phases of the otic placode, asymmetries in gene expression can already be observed in the otocyst. The anlage progressively become patterned or regionalized in distinct regions in which specific cell-types will be specified, and includes the definition of neural, sensory and non-sensory territories. The process of patterning takes place over an extended period of time, beginning at placode or even at OEPD stage to late labyrinth stage. Over time, the three axes of the ear become firmly established and can no longer be re-specified. The fixing of each axis occurs at different times, with anteroposterior (AP) and mediolateral (ML) patterning becoming permanent before the dorsoventral (DV) patterning, visible once the otic vesicle is formed. This suggests that different signals might be involved in the specification of each axis (Wu et al., 1998; Brigande et al., 2000b; Fekete and Wu, 2002). For the purpose of the thesis, I will focus on the description of the AP patterning. However, information of otic ML and DV asymmetries can be found in detailed reviews from (Bok et al., 2007; Whitfield and Hammond, 2007; Groves and Fekete, 2012).

18

Neural specification takes place only in the anterior part of the otic placode (Hemond and Morest, 1991; Adam et al., 1998; Fekete and Wu, 2002; Alsina et al., 2004). It relies on the integration of diffusive signals such as Fgf, Shh, RA and Wnt (Lassiter et al., 2014; Raft and Groves, 2014), as well as the function of intracellular proteins as Sox3, Neurog1, Delta1 and Hes5 (Alsina et al., 2004; Abelló et al., 2010), Otx1 (Maier et al., 2014), Eya1 (Friedman et al., 2005) and Six1 (Zou et al., 2004). The neurogenic region is adjacent and complementary to the posterior non-neurogenic portion of the otocyst epithelium expressing *Tbx1* (Vitelli et al., 2003; Raft et al., 2004; Radosevic et al., 2011) and *Lmx1b* (Nichols et al., 2008; Abelló et al., 2010), as well as components of the Notch signaling pathway such as *Serrate1/Jagged1* and *Hes1* (Cole et al., 2000; Kiernan et al., 2006; Abelló et al., 2007; Daudet et al., 2007; Neves et al., 2011; Radosevic et al., 2011). This region generates sensory and non-sensory regions of the cochlea and vestibular canals. Our laboratory has been working in otic patterning for several years and it was described that in chick, *Sox3* expression is restricted to an anterior otic territory, establishing neural fate and the neurogenic versus non-neurogenic AP asymmetry that characterizes the otic placode (Abelló et al., 2010). In zebrafish, *her9,* a zebrafish orthologue of *Hes1*, also acts as a patterning gene by restricting otic neurogenesis to an anterior domain. Posterior retinoic acid (RA) signaling promotes *tbx1* that, through a Notch-independent mechanism, activates *her9*, which blocks neurogenesis outside the neurogenic domain (NgD) (Radosevic et al., 2011). As in zebrafish, the chick *Hes1* orthologue, *Hairy1*, is expressed in the non-neurogenic region of the otocyst (Abelló et al., 2007). Other works in mice showed that loss of *Tbx1* causes and expansion of the neurogenic region of the otic placode; suggesting that Tbx1 posteriorizes the otocyst by inhibiting neural fate and suppressing *Neurog1* and *Delta1* expression (Raft et al., 2004; Xu et al., 2007). It has also been shown that Tbx1 is mislocalized in the ventral region of

Shh^{-/-} embryos causing loss of *Neurog1* therefore suggesting that Shh could regulate *Neurog1* permissively (Raft et al., 2004; Xu et al., 2007). Using zebrafish, our laboratory also showed that pharmacological inhibition of hedgehog signaling also causes an up-regulation of *tbx1* and reduction of *neurod* expression in the zebrafish otic epithelium (Radosevic et al., 2011).

## 1.3.3. Proneural genes

The generation of the specialized cell types of the inner ear is under tight control. Studies in *Drosophila* and vertebrates revealed that proneural genes are key regulators of sensory development, coordinating the acquisition of specific cellular fates at the appropriate time and location (Bertrand et al., 2002). Specification and differentiation of neurons and sensory cells requires distinct proneural genes which encode for the basic helix-loop-helix (bHLH) class transcription factors, which give all cells in the naïve ectoderm of the equivalence group[6] the potential to adopt a primary neural cell fate (Ghysen and Dambly-Chaudière, 1988; Skeath and Carroll, 1994). Proneural genes were first identified in *Drosophila* as a complex of genes that are involved in regulating early steps of neural development (Garcia-Bellido, 1979). Molecular analysis led to the isolation of the members of the *achaete-scute* complex (*asc*) (Garcia-Bellido, 1979; Villares and Cabrera, 1987; Ghysen and Dambly-Chaudière, 1988). The products of these genes share sequence similarities used for their DNA binding and dimerization, the bHLH domain (Murre et al., 1989). A further *Drosophila* proneural gene, *atonal* (*ato*), was isolated later in a PCR-based screen to identify bHLH

---

[6] An **equivalence group** is a zone of neural competence formed by a set of unspecified cells that have the same developmental potential or ability to adopt various fates (Greenwald and Rubin, 1992; Jarman et al., 1995).

sequences related to that found in *asc* genes (Jarman et al., 1993). The vertebrate bHLH orthologues genes of the *Drosophila* proneural genes *asc* and *ato* have been identified. The vertebrate asc family includes: *Mash*, *Cash*, *Zash* and *Xash;* and the *ato* family includes *Math* and other genes that can be grouped into distinct families: *Neurogenin*, *Neurod* and *Olig* families (Lee, 1997; Guillemot, 1999; Hassan and Bellen, 2000). The orthologues of the *ato* gene subfamily have been shown, by loss-of-function analysis, to be critical for ear development (Jarman et al., 1993; Ma et al., 1998; Bermingham et al., 1999; Kim et al., 2001).

Proteins of the bHLH families share several features that define and qualify their function as proneural genes. First, proneural genes are expressed in the neuroephitelium before any neural fate determination becomes apparent. They modulate the transition from a proliferating neural progenitor to a post-mitotic cell, generally by activating the expression of cyclin-dependent kinase (Cdk) inhibitor and promoting cell cycle exit (Farah et al., 2000; Ohnuma et al., 2001; Kageyama et al., 2005; Nguyen et al., 2006). Second, they are both required and sufficient to promote the generation of neural progenitor cells from the ectoderm. Therefore, being able to induce ectopic neural development. Third, its activity involves the activation of the Notch (N) signaling pathway, proneural genes are subject to lateral inhibition. Last, since all known proneural genes belong to the same class of bHLH transcriptions factors, they present similar biochemical properties (Campuzano and Modolell, 1992; Jimenez and Modolell, 1993; Jan and Jan, 1994; Artavanis-tsakonas et al., 1999; Bertrand et al., 2002; Westerman et al., 2003; Niwa et al., 2004). This type of analysis was used to place bHLH genes in temporal and, whenever possible, epistatic cascades which underlie the sequential steps of cell specification and differentiation (Cau et al., 1997; Lee, 1997; Roztocil et al., 1997; Kintner, 2002). Therefore, taking into account whether the gene is expressed before or

after the terminal mitoses it is known that *Neurogenins* (*Neurog1, Neurog2*), *Mash1* and *Math1* are expressed in proliferative progenitors and are sensitive to lateral inhibition, whereas *NeuroD* and *Math2* have characteristics of differentiation genes (Lee et al., 1995; Kageyama and Nakanishi, 1997; Brunet and Ghysen, 1999; Farah et al., 2000). In mouse, *Neurog1* and *Neurog2* are expressed in precursors of both placode and NC-derived sensory neurons and are required for the expression of *Math3*, *NeuroD* and *NeuroM* (Ma et al., 1996, 1997, 1998; Sommer et al., 1996; Fode et al., 1998). In the inner ear, *Neurog1* has a similar proneural function as their *Drosophila* counterparts, define the otic neurogenic domain where otic progenitors will acquire a neuronal lineage (Andermann et al., 2002; Abelló et al., 2007), and Notch signaling regulates the final number of otic sensory neurons (Adam et al., 1998; Haddon et al., 1998a; Abelló et al., 2007; Daudet et al., 2007). However, other proneural bHLH genes, such as *NeuroD*, are involved in neuronal differentiation and survival (Bertrand et al., 2002; Cau et al., 2002). In fish, *ato* homologous genes accomplish their function as proneural genes since their expression precedes and coincides with the selection of sensory progenitors, their expression is regulated by Notch signaling and their function is both necessary and sufficient for sensory cell development (Hassan and Bellen, 2000; Itoh and Chitnis, 2001; Whitfield, 2002; Whitfield et al., 2002; Millimaki et al., 2007; Sweet et al., 2011).

Finally, an essential role of proneural proteins is to restrict their own activity to single progenitors. As it has been mentioned above, proneural genes inhibit their own expression in adjacent cells through Notch-mediated lateral inhibition. This is achieved by transcriptional activation of the *Delta* (*Dl*) genes in specified cells, which activate Notch signaling in neighboring cells resulting in the expression of repressors that directly inhibit subsequent proneural gene expression, and prevent these cells

from differentiating (Baker and Yu, 1997; Parks et al., 1997). The vertebrate Hes/Her/Esr proteins constitute, with their *Drosophila* counterparts, the Hairy and Enhancer of Split (Espl) factors. These genes encode for another family of bHLH proteins which act as proneural gene inhibitors (Kageyama and Nakanishi, 1997; Davis and Turner, 2001); acting as classical DNA-binding repressors of proneural gene transcription (Ohsako et al., 1994; Van Doren et al., 1994; Chen et al., 1997) and antagonizing proneural activities of the *Neurogenin*, *Atonal*, and *Achaete scute* families of bHLH proteins (Fischer and Gessler, 2007). Two mouse genes homologous to the *Drosophila Hairy* and *Enhancer of Split* (Hes) genes are *Hes1* and *Hes5*, which are both expressed in the inner ear and play important roles in neurogenesis and sensorigenesis. HES genes are considered direct targets of Notch pathway and they have been used to monitor Notch activity (Jarriault et al., 1995, 1998; Ohtsuka et al., 1999; Zheng and Gao, 2000; Zine et al., 2001). The products of these genes act as negative regulators of neurogenesis in vertebrates (Ohtsuka et al., 1999), and also as negative regulators of HC differentiation. It has been shown that *Hes1* interacts with *Math1* to inhibit HC differentiation, that an increase in HC number is observed in *Hes1*$^{-/-}$ and *Hes5*$^{-/-}$ mutant mice, and that upon Notch activation *Hes5* is induced and suppresses HC fate while promoting SC fate (Zheng et al., 2000; Zine et al., 2001; Hartman et al., 2009; Tateya et al., 2011). Similarly, *Hes5* is expressed complementary to *Delta1* expressing cells in the neurogenic domain (Abelló and Alsina, 2007). *hairy-related* (*her*) genes are the highly evolutionarily conserved zebrafish counterparts of the *Hairy* and *Enhancer of split* type genes in *Drosophila*, and of the *Hes* genes in mammals (Müller et al., 1996). One of the zebrafish orthologues of mammalian *Hes5* is *her4* and it has been shown to be implicated in the control of primary neurogenesis, brain regeneration and neuronal target innervation (Takke et al., 1999; So et al., 2009; Kroehne et al., 2011). In the CNS *her4* expression depends

on Notch, while does not in the trigeminal sensory ganglia (Yeo et al., 2007).

In summary, the balance between the activator (*proneural*) and repressor (*Hes*) bHLH genes allows only subsets of cells to undergo differentiation while keeping others as neural stem cells. Also it should be taken into account that a crucial determinant for proneural gene function is the context in which it operates, and that proneural function can combine with positional information to provide neural specificity since proneural expression patterns vary along the nervous system (Ma et al., 1997, 1998; Fode et al., 1998; Niwa et al., 2004).

The early otic patterning step generates a domain with neurogenic and sensory potential. Therefore, this early domain is coined neurosensory domain, which is characterized by the expression of the transcription factors *Sox2 and Sox3* belonging to the SoxB1 family of Sox proteins defined by their ability to maintain neural progenitor or stem cell identity. *Sox2* and *Sox3* are initially expressed in regions of the otocyst that will give rise to both sensory and non-sensory components (Neves et al., 2007) and then, become restricted to the neurosensory competent domain. Therefore, they give competence to respond to either neuronal or sensory-inducing signals (Kiernan et al., 2005b; Abelló and Alsina, 2007; Neves et al., 2007; Abelló et al., 2010).

The neurosensory domain in amniotes initiates neurogenesis, marked by the expression of *Neurog1,* preceding sensorigenesis, marked by the expression of *Atoh1*. It is important to mention that the temporal and spatial relationship between neurogenic and sensory patch formation is not constrained across phylogeny. In zebrafish the sequence of neuronal and HC differentiation is reversed compared to amniotes; HC formation occurs slightly earlier or concomitantly with neurogenesis (Adam et al., 1998; Haddon et al., 1998a).

24

## 1.3.4. Otic sensory development

Otic sensory patches are thickened regions of epithelium containing two major cell types HCs and SCs. Sensory epithelia of the zebrafish inner ear develop not only in spatially restricted and well-defined domains, but also in a highly controlled temporal order. The two maculae are the first sensory patches to develop. The three cristae differentiate slightly later but appear before the lagena and macula neglecta (Haddon and Lewis, 1996; Whitfield et al., 2002).

The different sensory patches are all derived from a single common region in the otocyst. Therefore, the first step in the development of the sensory epithelia is the specification of this common prosensory anlage within the otic epithelium, also known as sensory equivalence group, which can be defined by the expression of one of the *atonal* orthologs, *atoh1* (Jarman et al., 1995; Shailam et al., 1999). Either the loss or overexpression of *atoh1* results in a complete absence or ectopic differentiation and supernumerary HCs (Bermingham et al., 1999; Zheng and Gao, 2000; Woods et al., 2004; Cai et al., 2013). In zebrafish, two *atonal* homolog genes are found, *atoh1a* and *atoh1b* (Whitfield, 2002; Whitfield et al., 2002; Adolf et al., 2004; Millimaki et al., 2007), which act in two distinct phases of inner ear sensory development. Early in the otic placode, *atoh1b* appears at 10 hpf in a broad territory across the entire AP axis stablishing a single prosensory domain. Subsequently, it gets restricted to two smaller sensory domains (opposite poles of the otic AP axis prefiguring the utricular and saccular maculae) where, later in development (at 14 hpf), it will induce *atoh1a* to direct differentiation of HCs (Millimaki et al., 2007) (**Figure 5**). Riley and colleagues also show that refinement of the initial prosensory domain is dependent on Delta-Notch (Dl-N) signaling since upon transient Notch blockade the two prosensory domains appear later and larger than in control animals (Millimaki et al., 2007). Later on, during

sensory epithelia differentiation, Notch signaling is involved in cell fate specification and regulates the decision to become either a HC or a SC by means of the lateral inhibition process (Haddon et al., 1998a) (**Figure 5**). Disrupting the Notch signaling at this stage results in premature differentiation and overproduction of HCs. In zebrafish *atoh1* genes are required for normal activation of the Notch ligand *delta* (Dl) gene expression. Therefore, it has been shown that knocking down either *atoh1b* or *atoh1a* strongly inhibits expression of *dlA* and *dlD* in the ear resulting in an increase in HC number and loss of most of the SCs (Millimaki et al., 2007). The same result was observed in a dominant negative mutant for the *dlA* gene, *deltaA*$^{dx2}$ (Riley et al., 1999). In *mind bomb* (*mib*) mutants the Notch signaling is impaired and an enlarged domain of *atoh1b* and *atoh1a* is observed (Millimaki et al., 2007). The *mib* gene encodes an E3 ubiquitin ligase essential for Dl-N signaling (Itoh et al., 2003). Since both *atoh1* genes remain fully active in these mutants and the *delta* gene expression is also expanded, all cells in the equivalence group differentiate as HCs (Haddon et al., 1999; Riley et al., 1999). However, in these mutants the sensory patches consist of an array of HCs without SCs (Haddon et al., 1999). Thus, the expression of *delta* in HCs, and the overproduction of HCs seen in mutants, indicate that HCs use Notch signaling to inhibit laterally their neighboring cells and thereby prevent them from adopting the same fate. Therefore, Notch activation makes the patch sensory-competent, and prevent the premature differentiation of HCs.

In zebrafish, FGF signaling could act as a key player on driving the formation of sensory domains. *fgf3* and *fgf8* begin to be expressed as the otic vesicle forms in domains that include the prospective sensory epithelia (Léger and Brand, 2002). In the *fgf3-/-* mutants, the utricular and saccular maculae remain undivided, and supernumerary HC form in the saccular macula (Hammond and Whitfield, 2011; Maier and

26

Whitfield, 2014). Moreover, analysis of Fgf signaling requirement at different developmental stages placed this pathway upstream of otic *atoh1b* and *atoh1a* expression, implicating this signaling in both the otic prosensory specification and maintenance of *atoh1* expression after placode formation (Millimaki et al., 2007).

Following commitment, once the sensory epithelium is clearly pseudostratified (by 24 hpf), the nuclei of the two cell types are arranged in distinct layers. SCs present basally positioned nuclei, but span the full thickness of the epithelium. Sensory HCs sit apically within the epithelium, where they are identified by *brn3c* expression (also called *brn3.1* or *pou4f3*), a POU-domain transcription factor that is specifically expressed by HC (Erkman et al., 1996; Sampath and Stuart, 1996; Xiang et al., 1997). *Brn3c* null mutant mice contain immature HCs but cochlear innervation develops normal (Xiang et al., 1997, 2003). Moreover, the ectopic overexpression of *brn3c* does not lead to the production of HC, suggesting that *brn3c* is only required for the later aspects of HC differentiation and survival (Xiang et al., 1998; Zheng and Gao, 2000).
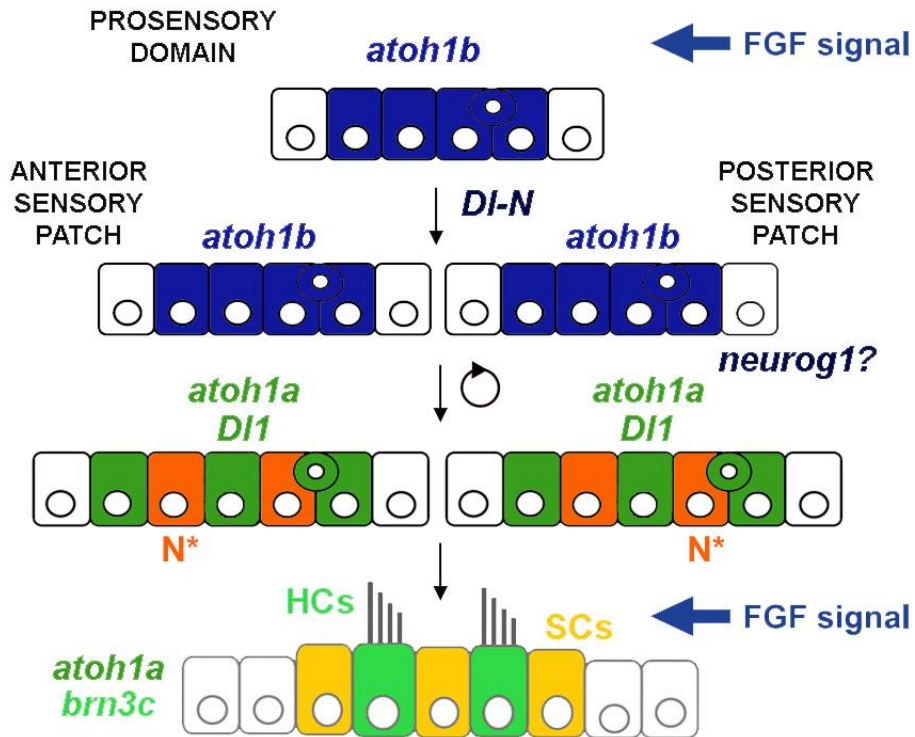
**Figure 5. Early otic sensory development.**

The diagram shows how sensory HCs and SCs are formed during zebrafish inner ear sensory development. Specification of sensory epithelia starts with *atoh1b* expression stablishing a single prosensory domain. Later on, Notch-mediated lateral inhibition through Dl ligand refines the prosensory domain in two sensory patches and, at later stages, regulates the decision to become a HC (light green) or a SC (yellow). HCs are singled out within *atoh1a* clusters, under the sustained expression of *Dl. neurog1* expression is also required for sensory lineage in the posterior macula. N*, Notch active. Fgf signaling is required at different stages of sensorigenesis.

## 1.3.5. Otic neurogenesis

Otic neurogenesis is a highly regulated and progressive multi-step process, which begins with the specification of neural progenitors, followed by their proliferative expansion, and subsequent steps of differentiation and migration of daughter cells*.*

Inner ear sensory neurons of the VIIIth cranial ganglion, also known as the statoacoustic ganglion (SAG), develop from the NgD and connect sensory HCs with the central neurons in auditory and vestibular brainstem nuclei. Formation of SAG neurons begins with the specification of otic neural precursors within the otic epithelium, which requires the expression of proneural gene *neurog1* (Ma et al., 1998; Andermann et al., 2002). Unlike those in other cranial sensory ganglia, SAG neurons are thought to have their origin in the otic placode, with very little contribution from the NC (D'Amico-Martel and Noden, 1983; Karpinski et al., 2016).

The first visible output of otic neurogenesis is the delamination[7] of otic neuroblasts[8] from the otic vesicle and the formation of the SAG. However, cell fate specification starts much earlier in otic development, at the otic placode stage, as indicated by the expression of both *Neurog1* and *Delta1* which corresponds to the specification of neuronal precursors from multipotent progenitor cells (Adam et al., 1998; Ma et al., 1998; Alsina et al., 2004). In zebrafish, *neurog1* expression is visible in the otic epithelium by 15 hpf (Radosevic et al., 2014).

---

[7] **Delamination** defines the exit of neuroblasts from the otic epithelium.

[8] **Epithelial neuroblast** are epithelial cells that are committed to the neuronal fate (Alsina et al., 2004).

In null mutant mice for *Neurog1*, both auditory and vestibular neurons are completely absent, showing that this gene is essential for the development of all inner ear sensory neurons (Ma et al., 1998, 2000). Mice lacking *NeuroD* exhibit deficient neuroblast delamination and near or complete loss of cochlear and vestibular ganglia, but do not display alterations in the generation of neuronal precursors (Liu et al., 2000; Kim et al., 2001), suggesting that *NeuroD* acts after the selection and specification of neural precursors being required for the survival and differentiation of the inner ear sensory neurons during later stages of development. Indeed, it was suggested that *Neurog1* is required for the specification of neuronal fate and activation of *NeuroD*, the latter being part of the same cascade but regulating neuronal differentiation and delamination (Ma et al., 1998, 2000; Liu et al., 2000; Kim et al., 2001).

In zebrafish, SAG neuroblasts begin to specify approximately at 15 hpf (13 ss) and neuroblast delamination extends over a period of 25 hr (approximately from 17 hpf to 42 hpf) (Haddon and Lewis, 1996; Radosevic et al., 2011; Vemaraju et al., 2012; Raft and Groves, 2014). Upon delamination, neuroblasts lose *neurog1* expression and upregulate *neurod* (Korzh et al., 1998; Andermann et al., 2002). The *neurod*-expressing cells continue proliferating to expand the neuronal population and constitute a group of migrating and proliferating precursors. This phase, termed transit-amplification, is characterized by co-expression of *neurod* and proliferation markers. Neuroblast will finally exit the cell-cycle and differentiate within the SAG into mature bipolar neurons. They lose *neurod* expression and upregulate *islet1* (*isl1*) and *islet2b* (*isl2b*) (also known as *islet3*), transcription factors belonging to the LIM homeodomain (LIM-HD) family, which are defined as neuronal identity determinants and are expressed in early differentiating cell lineages (D'Amico-Martel and Noden, 1983; Inoue et al., 1994; Alsina et al., 2003; Li et al., 2004; Vemaraju et al., 2012) (**Figure 6**). In contrast

with amniotes, in which cell amplification and expression of *neurod* and *isl1/2* begin while neuroblasts still reside within the otic epithelium (Ma et al., 1998; Alsina et al., 2004; Radde-Gallwitz et al., 2004), in zebrafish the markers of later differentiation stages do not seem to be expressed within the otic epithelium (Korzh et al., 1998; Andermann et al., 2002; Vemaraju et al., 2012).

Several studies show that different FGFs, such as FGF2, FGF3, FGF5, FGF8, FGF10 and FGF19 are required for the neurogenesis process and SAG maturation (Mansour et al., 1993; Pirvola et al., 2000; Adamska et al., 2001; Alvarez et al., 2003; Wright and Mansour, 2003b; Alsina et al., 2004; Sanchez-Calderon et al., 2007; Vemaraju et al., 2012; Wang et al., 2015). They regulate the sequential steps of neurogenesis starting from *neurog1* expression to later events involving neuroblast expansion (Léger and Brand, 2002; Alsina et al., 2004; Vemaraju et al., 2012). In chick, FGF receptor inhibition affects early specification of otic neuroblasts due to a severe reduction in *Neurog1*, *Delta1* and *Hes5* expression, but there is no effect on *NeuroD* expression in the SAG and neuroblast delamination. On the other hand, it is described that FGF10 induces neuronal differentiation genes *NeuroD* and *NeuroM*, promoting commitment to neuronal fate (Alsina et al., 2004). In *FGF3* and *FGFR-2(IIIb)* mutant mice the size of the SAG is diminished concomitantly with other morphogenetic defects (Mansour et al., 1993; Pirvola et al., 2000). *Fgf2* is expressed in mouse and chick otic vesicles (Vendrell et al., 2000), and its involved in the migration and differentiation of SAG neurons (Hossain et al., 1996; Zheng et al., 1997; Adamska et al., 2001). Also, in zebrafish *ace* mutants, the number of otic *neurog1*-positive cells is reduced and present a smaller SAG (Léger and Brand, 2002). Moreover, *Fgf8* is also expressed in cells migrating out of the antero-medio-ventral region of the chick otocyst to produce the SAG (Adamska et al., 2001). It is worth mentioning that when

Adamska and colleagues show that ectopic FGF promotes a significant increase in size of the SAG is not due to an increase in cell proliferation but a recruitment of epithelial cells into the neuronal lineage (Adamska et al., 2001). Recently, it has also been proposed that could be the levels of FGF signaling which dictate the outcome of neurogenesis (Brumwell et al., 2000; Vemaraju et al., 2012; Kantarci et al., 2015; Wang et al., 2015). For example, in zebrafish, low activity of fgf5 signaling is initially required for neuroblast specification in the neurogenic domain. However, later on, increased levels of *fgf5* expressed in SAG neuroblasts feed back onto the neurogenic epithelium inhibiting *neurog1* expression and restricting neuroblast specification. This is suggested to ensure maintenance of progenitors and steady production of an appropriate number of mature neurons (Vemaraju et al., 2012). Interestingly, conditional manipulation of FGF signaling using heat shock-inducible transgenes and pharmacological interference revealed that, in zebrafish, Fgfr/PI3K/Akt signaling is responsible of otic neurogenesis and SAG development, while the Fgfr/Erk1/2 signaling is involved in HC production (Wang et al., 2015). It has also been shown that the transcription factor Tfap2a is expressed in the ventrolateral domain of the otic vesicle and that through Bmp7a, modulates Fgf and Notch signaling to control SAG neural development and balance the rates of maturation and proliferation (Kantarci et al., 2015).

Notch signaling is also required during otic neurogenesis to regulate the number of neural cells committed to neuronal differentiation. Members of the Notch pathway are expressed during early stages of otic neurogenesis and sensory patch formation in the chick and zebrafish (Adam et al., 1998; Haddon et al., 1998b; Riley et al., 1999). In zebrafish *mind bomb* mutants SAG neuron number increases due to dysregulation of the N-Dl pathway. As with HCs, high levels of *Dl1* expression correlate with the selection of a neuronal fate, whereas high

levels of Notch activity repress acquisition of this fate (Haddon et al., 1998a; Abelló et al., 2007; Daudet et al., 2007). Raft and colleagues also provided evidence that Neurog1, aside from promoting neurogenesis, also maintain uncommitted progenitor cell population through Notch-mediated lateral inhibition. Progenitors expressing a high amount of *Neurog1* inhibit *Neurog1* accumulation in their immediate neighbors before delaminating from the epithelium as committed neural precursors (Raft et al., 2007).

To summarize, the segregation of neurogenic otic tissue and adjacent non-neurogenic tissue and the following neurogenic process appear to involve activated FGF and attenuated Notch signaling concomitantly with effects of patterning signals, which restrict neurogenesis to an anteroventral portion of the otocyst. Also, it is very important to stress the importance of a tight regulation of neurogenesis in order to define the place and time in which neural progenitors appear (origin and pattern), how they divide (proliferation) and migrate (cell movements), to generate the precise number of neurons and place them at specific positions.
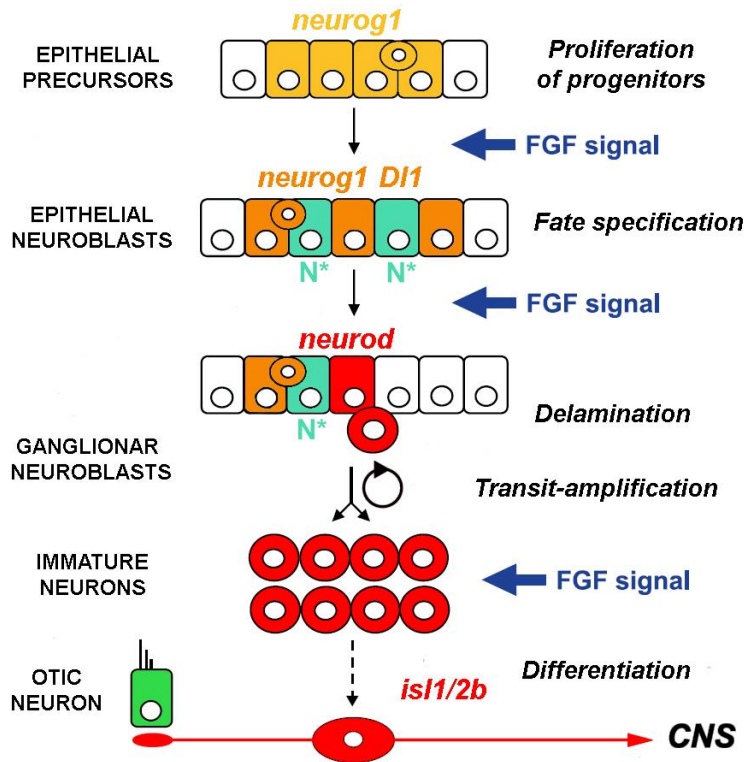
**Figure 6. Early otic neurogenesis.**

The diagram shows how sensory neurons arise from epithelial precursors during zebrafish inner ear neurosensory development. States of cell commitment and differentiation are summarized along with molecular markers. Neuronal specification takes place by the enhanced expression of *neurog1* via Dl-N pathway, and the subsequent expression of *neurod*. Epithelial neuroblast are specified in the otic epithelium to subsequently delaminate and coalesce into the SAG. Neuronal cells populating the SAG express *islet1/2b* as well as *neurod*. This cell state constitutes a transit-amplifying population of cells, determined as proliferative neurons. FGF signaling is required to shift multipotent precursors toward a state of full commitment (epithelial neuroblasts) characterized by the expression of *neurod*. Other FGF ligands are critical then for transit amplification, giving rise to post-mitotic immature neurons and starting their differentiation into mature otic neurons that connect sensory HCs with the specific CNS nuclei. N*, Notch active. Modified from (Alsina et al., 2004).

34

## 1.4. Cell behaviors during otic neurogenesis

## 1.4.1. Neurogenic cell divisions

The generation of the proper number of neurons depends on a carefully regulated spatial and temporal balance between progenitor cells proliferation and differentiation. This balance is controlled by the cumulative activities of numerous extracellular and intracellular factors. Neural progenitors also express neural fate determinants such as transcriptional regulators, and transmit these factors by means of their particular mode of division to their progeny, where they control differentiation. Thus, the relationship between cell division and cell fate specification is an important aspect of early neurogenesis since neurons are typically specified within growing and proliferating tissues (Pearson and Doe, 2004; Paridaen and Huttner, 2014; Hartenstein and Stollewerk, 2015).

Progenitor cells can divide either symmetrically or asymmetrically, as judged by daughter cell identity (**Figure 7**). In symmetric divisions, a cell generates two daughter cells with the same identity, which is not necessarily the same as that of the mother cell. If it is the same as the mother, this is a symmetric proliferative division. If it is not, this is a symmetric consumptive/terminal division (Miyata et al., 2004; Noctor et al., 2004; Roszko et al., 2006). In asymmetric divisions, the two daughter cells have different identities. In an asymmetric self-renewing division, one daughter cell has the same identity as the mother cell, and the other daughter cell has a different identity. By contrast, in an asymmetric consumptive division, the daughter cells differ in identity from one another, as well as from the mother cell (Hansen et al., 2010; Taverna et al., 2014).

Therefore, neurons can be produced by symmetric terminal divisions that produce two neurons or by asymmetric divisions that produce a neuron and a progenitor (Wildner et al., 2006).
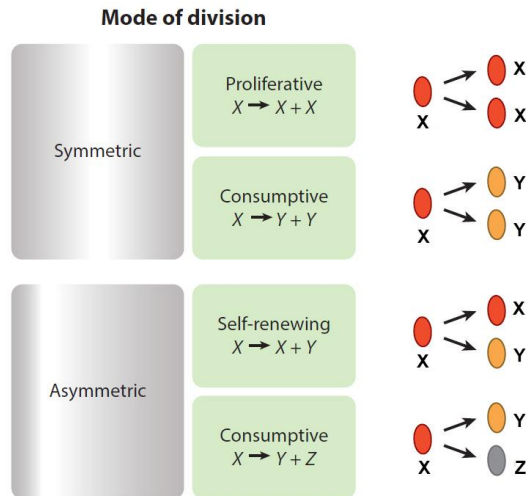


**Figure 7. Modes of cell division.**
The modes of cell division: symmetric or asymmetric. Symmetric divisions can be either proliferative or consumptive. Asymmetric divisions can be either self-renewing or consumptive. Modified from (Taverna et al., 2014).

Whether divisions are symmetric or asymmetric in terms of daughter cell fate appears to be linked to the polarized organization of the progenitor, the equal versus unequal inheritance of cell fate determinants, subcellular components and molecules by daughter cells (Li and Gundersen, 2008; Macara and Mili, 2008; Knoblich, 2010; Lancaster and Knoblich, 2012) (**Figure 8B**). Therefore, asymmetric cell division is thought to be one mechanism by which the diversity of cell fates in the nervous system is generated, since in asymmetric divisions, cell fate determinants are unequally segregated resulting in one daughter cell becoming post-mitotic while the other continues to proliferate (Das et

al., 2003; Huttner and Kosodo, 2005). Cell polarity, established prior to mitosis, not only segregates fate determinants but also dictates the orientation and position of the mitotic spindle through the interaction of microtubules with polarized cortical components (**Figure 8A**). In turn, the mitotic spindle specifies the position of cleave plane (Huttner and Kosodo, 2005; Lancaster and Knoblich, 2012; Peyre and Morin, 2012; Shitamukai and Matsuzaki, 2012; Li, 2013) and it is known that perturbing the spindle core components, such as microtubules and centrosomes, affects neurogenesis (Woods et al., 2005). Work in the vertebrate cortex and retina suggest that a division generates either a symmetric or asymmetric cell fate depending on the mitotic spindle orientation and hence cleave plane positions with respect to the apical surface of the neuroepithelium. Thus, a parallel cleave plane generates an asymmetric division, placing one daughter cell at the apical surface and the other more basally, whereas a perpendicular cleave plane generates daughter cells that inherit equal portions of apical and basal membrane (Chenn and McConnell, 1995; Das et al., 2003; Götz and Huttner, 2005; Alexandre et al., 2010). Time-lapse studies of dividing cells show that perpendicular cleave plane divisions give rise to two progenitors and parallel divisions generate and apical progenitor and a basal daughter cell becoming a post-mitotic neuron (Chenn and McConnell, 1995; Kosodo et al., 2004). During development of the *Drosophila* CNS, asymmetric division of neuroblast also presents parallel cleavage planes mediating unequal division of polarity proteins and fate determinants to give rise to a ganglion mother cell basally and a neuroblast apically (Lu et al., 2000; Doe and Bowerman, 2001). Evidence that these parallel divisions are asymmetric comes from observations that Notch signaling components such as Delta, Mind bomb, and the Notch antagonist Numb, and polarity proteins such as Par3 are differentially segregated between daughter cells (Chenn and McConnell, 1995; Zhong et al., 1996; Wakamatsu et al., 1999;

Johansson et al., 1999; Cayouette et al., 2001; Silva et al., 2002; Kosodo et al., 2004; Bultje et al., 2009; Alexandre et al., 2010; Das and Storey, 2012; Dong et al., 2012; Kawaguchi et al., 2013). Interestingly, the cell fate related to Par3 inheritance appears to vary between species. In mouse, Par3 is asymmetrically distributed and thus differentially inherited by the two daughter cells. Par3 acquisition promotes high Notch signaling activity and the cell remains as a progenitor (Bultje et al., 2009). In contrast, in the zebrafish brain, the daughter cell inheriting the apical domain, including Par3, also inherits the Notch inhibitor mind bomb and differentiates (Alexandre et al., 2010; Dong et al., 2012). Therefore, mitotic spindle orientation is suggested to mediate cell fate choice as a result to the unequal segregation of determinants localized at the apical or basal surfaces, suggesting a link between division orientation and acquisition of neurogenic fate. Moreover, it has been suggested that only divisions that produce two neurons have an exclusively perpendicular orientation, in contrast with divisions that generate two progenitors or a progenitor and a neuron that exhibit a wide range of cleave plane orientations, and that mitotic spindle orientation does not correlate with acquisition of neurogenic fate, but allows neurogenic cells to distinguish modes of neuron production in chick spinal cord (Wilcock et al., 2007).

38
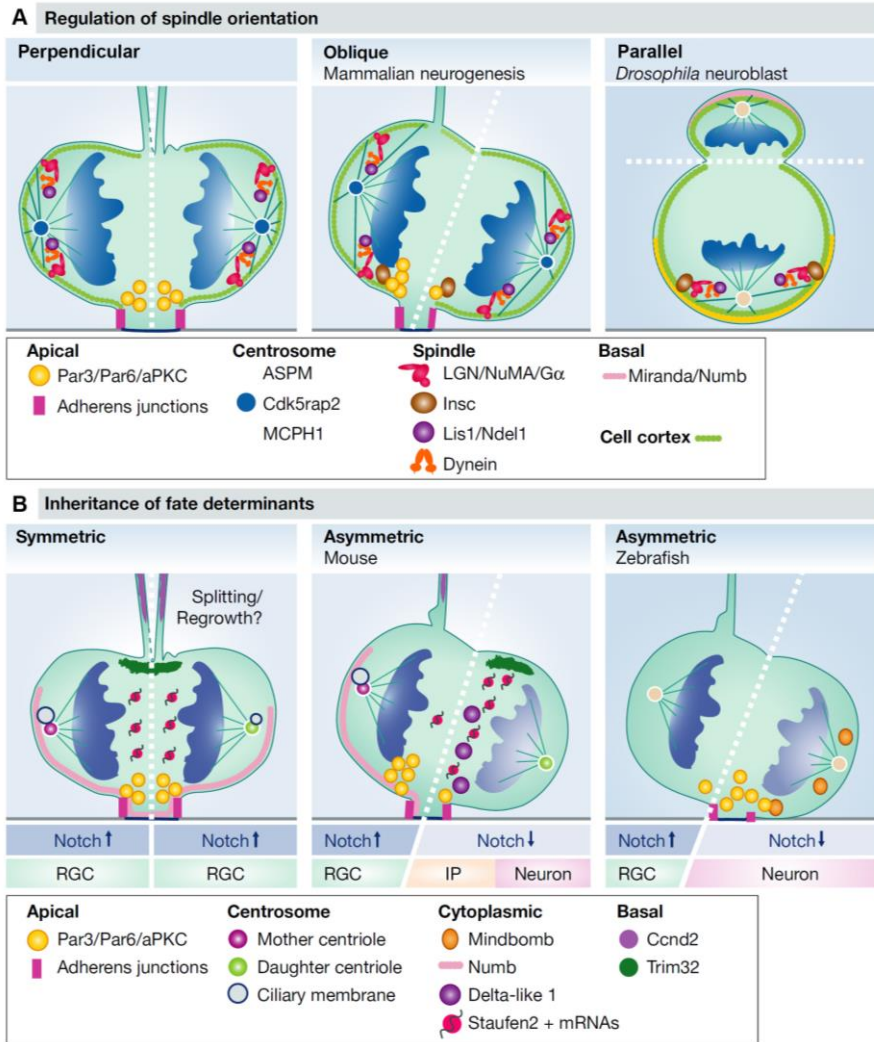
**Figure 8. Division types are determined by spindle orientation and inheritance of cell fate determinants**.

**(A)** Spindle orientation in symmetric versus asymmetric divisions is regulated by centrosomal proteins and spindle orientation complexes in perpendicular and oblique divisions of vertebrates and parallel neuroblast divisions in *Drosophila*. **(B)** Cell fate determinants may be equally (symmetric division, left) or unequally (asymmetric division, middle, mouse; right, zebrafish) distributed between daughter cells. Asymmetric inheritance is characterized by differently acquisition of centrioles and ciliary membrane, and Par3 and Notch signaling components. Modified from (Paridaen and Huttner, 2014).

Tissue polarity also allows the classification of stem and progenitor cells based on the location of mitosis: apical versus non-apical (or basal). In the mouse cortex, apical progenitors (APs) undergo mitosis at (or very near to) the luminal surface of the ventricular zone (VZ) while being integrated into the apical adherens junction belt and exposing part of their plasma membrane to the ventricular lumen (Kriegstein and Götz, 2003; Götz and Huttner, 2005), and basal progenitors (BPs) undergo mitosis at the subventricular zone (SVZ), and delaminate from the adherens junctional belt and lack apical plasma membrane (Miyata et al., 2004; Noctor et al., 2004; Roszko et al., 2006; Hansen et al., 2010; Fietz and Huttner, 2011; Shitamukai et al., 2011; Wang et al., 2011a; Reillo and Borrell, 2012; Betizeau et al., 2013).

Neuroepithelial cells present a pseudostratified structure with their nuclei located at various positions along the apicobasal axis. However, during interphase, cells extend from the luminal (apical) surface to the basal lamina, describing a dynamic oscillatory movement of nuclei within the elongated cells (Sauer and Walker, 1959; Baye and Link, 2008; Miyata, 2008). This nuclear movement is known as interkinetic nuclear migration (INM) in which the nucleus moves in concert with the cell cycle using actomyosin and microtubule motor proteins (Taverna and Huttner, 2010). Nuclei are situated near or very close to the apical surface of the neuroepithelium during mitosis, whereas S phase takes place at a more basal location. Therefore, nuclei stay basal during S phase, in G2 nuclei migrate basal-to-apical, undergo mitosis at the apical side, and migrate back to basal side in G1 (Sauer and Walker, 1959; Baye and Link, 2008; Miyata, 2008; Ladher et al., 2010; Leung et al., 2012). It has been proposed that INM-mediated pseudoestratification functions to maximize the number of progenitor mitoses within a small surface and, therefore, allows greater cell density in the epithelium (Grosse et al., 2011; Spear and Erickson, 2012).

40

Another possibility could be to differentially expose nuclei to signals that are present along an apicobasal gradient, such as Delta-Notch signaling (Taverna and Huttner, 2010). In chick spinal cord, cell membrane labeling revealed that during division cells round up at the apical surface retaining a thin membranous process inherited by one daughter cell. After division each daughter cell generates a new apical process and nuclei migrate to the basal side of the neuroepithelium, where cells remain in contact with both apical and basal surfaces. It is also shown that once a cell is going to differentiate into a neuron, the endfoot of its apical process releases from the apical surface and it loses tension (Wilcock et al., 2007). In zebrafish retina, in contrast with mammalian neocortex, it has been shown that nuclei undergo stochastic motion during both G1 and S, resulting in a very broad distribution of nuclear positions in the apicobasal domain at the onset of G2 (Leung et al., 2012). Interestingly, there is direct evidence that INM dynamics are dependent on actomyosin forces, since it still occurs when microtubule cytoskeleton is compromised but is blocked when myosin II activity is inhibited (Norden et al., 2009).

In the case of the inner ear, a morphologically visible otic placode appears once cells acquire an elongated structure, presenting a notable apicobasal polarity. In zebrafish, this is a progressive process by which epithelialization occurs first in cells located medially and close to the hindbrain, and then in cells located laterally. Time-lapse imaging shows that by 14 hpf the otic epithelium is already polarized presenting F-actin accumulation in the apical tissue midline together with the polarity marker Pard3 and the cell junction protein ZO-1. Moreover, it is also shown that otic cells undergo INM with nuclei migrating to the apical epithelial surface to divide (Hoijman et al., 2015).

In summary, in neurogenic tissues, cell division plays an important role during early neurogenesis, and there is a close association between proliferation and cell fate specification. Therefore, neural progenitors initially divide symmetrically to expand their pool and, at the onset of neurogenesis, switch to asymmetric neurogenic divisions. Neural progenitor cells are highly polarized. Polarity proteins such as Pard3, Pard6, and aPKC are important for their proliferation; these proteins promote self-renewing progenitor cell divisions at the expense of neurogenic differentiation (Costa et al., 2008). It is worth noting that the step of neural determination is not necessarily linked to cell division, exist the possibility that in a restricted domain which is being specified, mechanisms that are not involved in mitosis act at specific locations to specify neural fate (Hartenstein and Stollewerk, 2015). Therefore, dividing cells could only be increasing the size of the domain and by extrinsic factors being, at the same time, specified. While the role of cell division in CNS development has been extensively studied, in the inner ear this still remains unexplored.

## 1.4.2. Neuroblasts delamination

As mentioned above, sensory neurons are derived from neuroblasts that originate within the otic epithelium. Once neuroblasts are specified, they delaminate from the *neurog1* expressing region located at the anteroventral region of the otic vesicle and coalesce to form the SAG (D'Amico-Martel and Noden, 1983; Carney and Couve, 1989; Hemond and Morest, 1991; Haddon and Lewis, 1996; Vemaraju et al., 2012). Signs of delamination in the zebrafish inner ear primordium were first detected in resin sections, and it was visible at about 22 hpf. It was described that the basal side of the otic epithelium becomes irregular during delamination, being difficult to distinguish the line of the basal

lamina and the exact position of cells. Delamination was defined to occur from the ventral part of the otocyst, having its peak between 22 and 30 hpf, time in which delaminated cells accumulate just below the epithelium and differentiate into neurons (Haddon and Lewis, 1996; Vemaraju et al., 2012). It was also observed that although the cells originate from the lateral and middle parts of the vesicle floor, they soon shift medially so that by 48 hpf the ganglion appears as a single ventromedial mass extending beneath the anterior and the posteromedial sensory patches (Haddon and Lewis, 1996). In our laboratory it has also been described that delamination of chick otic neuroblasts takes place only in a particular subdomain of the neurosensory territory, at the posterior edge of the FGF10 expression domain (Alsina et al., 2004).

Neuroblasts delamination is one of the main morphogenetic events during otic placode neurogenesis, but it is unknown weather this process is or not an epithelial-to-mesenchymal transition (EMT) and follows similar steps to the delamination of NC from the neuroepithelium of the dorsal neural tube, which became the paradigm of developmental EMT process (Ahlstrom and Erickson, 2009).

An EMT is the process whereby epithelial cells become mesenchymal cells. This process produces complete loss of epithelial traits by the former epithelial cells, accompanied by changes in behavior and morphology, and total acquisition of mesenchymal characteristics. Thus, allowing cells to become mobile, so as to leave the epithelium and move through the substrate (either other cells or extracellular matrix) (Hay, 1995, 2005; Thiery and Sleeman, 2006; Ahlstrom and Erickson, 2009; Nieto and Cano, 2012) (**Figure 9**). EMT processes occur in several developmental processes such as gastrulation and NC delamination, and it is a fundamental event in morphogenesis (Shook and Keller, 2003). Moreover, EMT processes can also be activated in association

with tissue repair and pathological stresses, including those creating various types of inflammation and tumor metastasis (Acloque et al., 2008; Baum et al., 2008; Yang and Weinberg, 2008; Kalluri and Weinberg, 2009; López-Nouoa and Nieto, 2009; Nieto, 2009, 2011; Thiery et al., 2009; Brabletz, 2012).
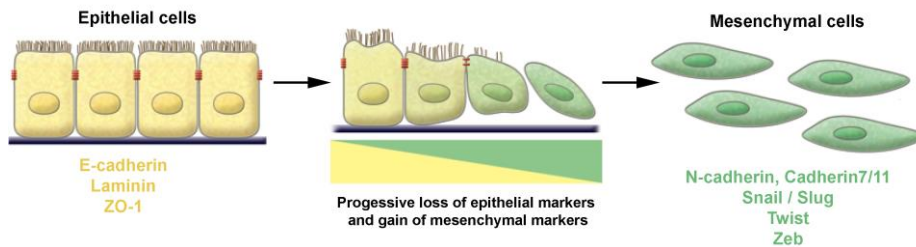


**Figure 9. EMT process.**

An EMT involves a functional transition of polarized epithelial cells into mobile mesenchymal cells. The epithelial and mesenchymal markers mentioned in the main text are listed. Colocalization of these two sets of distinct markers defines an intermedite phenotype of EMT. Modified from (Kalluri and Weinberg, 2009).

Hallmarks of EMT have extensively been described, especially in cranial NC, and involve a series of transcriptional profiles and cellular morphological changes, including a switch from an epithelial to mesenchymal cellular phenotype and migratory properties (Shook and Keller, 2003; Thiery et al., 2009; Theveneau and Mayor, 2012; Nieto, 2013; Lamouille et al., 2014). Some EMT processes are characterized by clear changes in cell shape due to an apical constriction process, which is usually driven by the contraction of actomyosin mesh across the apical surface, causing a reduction in the apical surface area and the movement of the cytoplasm to the basal region of the cell (Young et al., 1991; Keller et al., 2003; Lee and Goldstein, 2003; Martin and Goldstein, 2014). Although changes in cell shape are important, it is

suggested that are the changes in adhesive molecules which are crucial for de-epithelialization and withdrawal of cells from the epithelial surface. E-cadherin is essential for the maintenance of epithelial integrity and its repression is a crucial step for the EMT process. Therefore, there is a downregulation of E-cadherin accompanied by upregulation of mesenchymal-type cadherins, such as N-cadherin or cadherin-11, favoring cell interactions with the substrate required for puling cells out of the epithelial layer and for the migration from the site of delamination (Oda et al., 1998; Peinado et al., 2004; Nieto, 2011). The Snail genes, which encode transcription factors of the zinc finger type, were the first E-cadherin expression repressors to be described and proven to behave like master genes for EMT (Hay, 1995). The first indication came from *in vivo* studies in chick embryos, in which Slug (now called Snail2) induced NC and mesoderm delamination (Nieto et al., 1994). However, additional repressors have been identified, such as the bHLH transcription factors E47 and Twist, and the Zeb factors (Zeb1 and Zeb2) (Peinado et al., 2007; Itoh et al., 2013; Vannier et al., 2013). These factors are called EMT inducers, which repress *E-cadherin* expression and initiate the program to disassemble cell-cell junctions, and endow cells with migratory and invasive properties (Savagner et al., 1997; Batlle et al., 2000; Cano et al., 2000; Ip and Gridley, 2002; Bolós et al., 2003). However, the diversity of cellular mechanisms by which NC cells can separate from the neural tube suggests that the EMT program is a complex network of non-linear mechanisms that can occur in multiple orders and combinations to allow NC cells to escape from the neuroepithelium (Ahlstrom and Erickson, 2009).

It was described that epithelial cells exhibit apicobasal polarity and during the transformation of epithelium to mesenchyme, the transforming cells extend filopodia and pseudopodia on their basal side which allow them to exit the epithelium of origin. After delamination, the

contacts between migrating cells help to interpret directionality cues (Nieto, 2011). A good example is the coordinated migration of individual cells forming chains observed in both the chick and the mouse NC (Kulesa and Gammill, 2010). Mesenchymal cells migrate through paths imposed by signaling cues from the adjacent territories (Kulesa and Gammill, 2010; Theveneau et al., 2010; Bénazéraf, 2011). These guidance cues include chemotaxis, which involves the detection of an extracellular chemoattractant and intracellular reorganization to give directionality to the migration movement (Roussos et al., 2011). For example, during *Xenopus* NC cell migration, cells are attracted through the receptor cxcr4, towards the chemokine Sdf1 (also called cxcl12), which directionally stabilizes cell protrusions promoted by cell contact (Theveneau et al., 2010). Similarly, interneurons and zebrafish primordial germ cells (PGC), also migrate following signaling cues from adjacent cells using the SDF1/CXCRs system to control directionality (Blaser et al., 2006; Lopez-Bendito et al., 2008; Sánchez-Alcañiz et al., 2011; Wang et al., 2011b). It has recently been shown that are the cell surface filopodia which allow the interpretation of the chemotactic gradient by directing single-cell polarization in response to the distribution of cxcl12a (Meyen et al., 2015). Migrating cells also generate bleb-like protrusions that are expanded by hydrostatic pressure generated in the cytoplasm by the contractile actomyosin cortex, and they are also required for cell migration (Blaser et al., 2006; Goudarzi et al., 2012; Paluch and Raz, 2013). It is worth noting that guidance cues operate in a similar way irrespective of the type of cell or movement (individually or collective) (Nieto, 2011; Roussos et al., 2011).

When the mechanisms underlying the delamination process were analyzed in chick epibranchial placodal ectoderm, it was shown that nascent neuroblasts also move basally to exit from the basal surface of the placode through breaches in the basal lamina (Graham et al., 2007).

However, this delamination event was not considered an EMT mechanism since cells leaving the placodes do not assume a mesenchymal morphology, and they neither express Snail2 nor activate the Rho family GTPases, required for the EMT seen in NC cell delamination (Liu and Jessell, 1998; Graham et al., 2007). Aside from that, other transcription factors such as Twist, Zeb and E47 were shown to be implicated in EMT in chick and in placodes, and they could be acting instead of Snail/Slug (Lamouille et al., 2014). Finally, although Snail expression is absent in chick placodes, it is present during delamination in the zebrafish otic vesicle (Léger and Brand, 2002; Whitfield et al., 2002).

In summary, developmental EMT is required for later differentiation process that occurs at a particular time and place. It is mainly defined by the activation of the EMT inducers and subsequent E-cadherin transcriptional repression and apicobasal polarity loss. However, it has become evident in recent years that EMT is not an all-or-nothing event, and intermediate types of EMT are present during development (Nieto, 2013). In some systems, it may be that cells must be in a specific place in order to go through EMT, possibly because they require a local signal. Finally, it is very important to mention that after an EMT and further cell migration, once the cells have reached their destination, in some cases the reverse process can occur. This process is called mesenchymal to epithelial transformation (MET) and is often required for cell differentiation or in metastasis (Nieto, 2009).

## 1.5. The zebrafish as a model for studying inner ear development

The zebrafish (*Danio rerio*) emerged as in important model organism for the study of vertebrate development and morphogenesis, and also offers unique advantages for the analysis of inner ear development. The embryo is optically clear, its development is very rapid and it can be monitored and manipulated *in vivo.* Moreover, the inner ear is accessible for observation at all embryonic stages either *in vivo* or in whole mount. It offers a wide range of genetic techniques such as generation of transgenic and mutant fish lines, and its external development and embryo permeability allows the study of developmental defects after administration of synthetic small molecules. Also, many genes show similar expression patterns to those in other vertebrate species and the mutagenesis screens have yielded many mutants whose primary visible defect is in the inner ear (Haddon and Lewis, 1996; Whitfield et al., 1996; Whitfield, 2002). Moreover, zebrafish maintain continual neurogenesis and regenerative capability. Finally, the highly homology with the mammalian inner ear structure places the zebrafish as a powerful model organism for studying inner ear developmental processes and understanding of human diseases.

## 1.5.1. Developmental zebrafish stages

In Chapter 1 we analyze proneural genes expression patterns in the inner ear neurogenic and sensory domains, from the appearance of the first HC specification marker in the sensory domain (12 hpf), until both domains are completely established (24 hpf) (**Figure 10**).

In Chapter 2 we analyze the construction of the NgD. The range of developmental stages used goes from right after otic placode induction (11 hpf) until the NgD expands (20.5 hpf) (**Figure 10**).

In Chapter 3 we analyze otic neuroblasts delamination process, from its onset approximately at 18 hpf, until 24 hpf (**Figure 10**).

| 11 hpf | 12 hpf | 14 hpf | 18 hpf | 19.5 hpf | 24 hpf |
| 3 ss | 6 ss | 10 ss | 18 ss | 21 ss | |
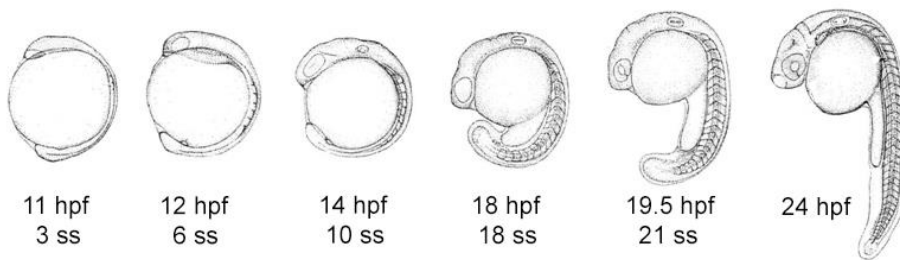
**Figure 10. Zebrafish developmental stages used in this work.**

Schematic representations of the main zebrafish developmental stages used for the experiments performed in this work. View from the left side of the embryo. Anterior to left. Dorsal to top. Modified from (Kimmel et al., 1995).

Note to the reader: Throughout the text, the nomenclature of genes changed depending whether data was obtained either in chick, mouse or zebrafish. In all species genes are referred in italic, while proteins in non-italic. Genes in mice and chick are written with the initial capital letter, while zebrafish does not.

# 2. RESULTS

52

# Chapter 1: "The role of *her4* in inner ear development and its relationship with proneural genes and Notch signalling"

Different members of the HES family were described to be expressed in the inner ear of amniotes and to play a role during neurogenic and sensory development. Our group previously investigated the expression patterns of several zebrafish *her* genes and described the role of *her9*, involved in neurogenic patterning. In this analysis it was also shown that another member, *her4*, is expressed in the neurogenic and sensory domains of the zebrafish inner ear but its role in neurosensory development was not fully characterized. Moreover, the group of Riley suggested that Notch activity was involved in the separation of a broad prosensory domain in two distinct patches, and we thought that *her4* could be the mediator of this repression.

## Aims of Chapter 1:

1. To characterize the spatiotemporal expression of *her4* in relation to proneural genes *atoh1b/a* and *neurog1* required for sensory and neuronal specification.

2. To investigate whether *her4* is Notch-dependent in the sensory and neurogenic domains.

3. To analyze the possible interaction and cross-regulation with proneural genes and other factors involved in otic neurogenesis and sensorigenesis.

4.  To determine the role of *her4* during neurosensory development.

Radosevic M\*, **Fargas L\***, Alsina B (2014) <u>The role of her4 in inner ear development and its relationship with proneural genes and Notch signalling</u>. PLoS One 9.

Radosevic M, Fargas L, Alsina B. The role of her4 in inner ear development and its relationship with proneural genes and Notch signalling. PLoS One. 2014 Oct 9;9(10):e109860.
doi: 10.1371/journal.pone.0109860

54

# Chapter 2: Pioneer *neurog1* expressing cells ingress in the otic primordium and instruct neuronal specification

Neural patterning involves regionalized cell specification. Concomitant with cell specification, neural tissues undergo phases of morphogenesis and/or growth. Thus, the cells within a given domain are not static, but perform elaborated cell behaviors. Although recent evidences hint a close relationship between cell dynamics and neural pattern refinement and progression, the impact of cell behaviors in neural specification still needs to be disclosed. To date, most information regarding the development of the otic NgD relies on the influence of patterning cues on *neurog1* induction and on the NgD specification by analyzing fixed embryos after pharmacological and genetic perturbations. The influence of dynamical changes in gene expression, proliferation behaviors or cell movements/rearrangements in the development of the otic NgD has not been addressed.

## Aims of Chapter 2:

1.  To investigate the spatiotemporal dynamics of *neurog1* activation during otic neurogenesis*.*

2.  To unveil the influence of cell dynamics in neuronal specification and the construction of the NgD.

3.  To analyze the role of cell division in the morphogenesis of the NgD.

4.  To investigate the possible role of FGF signaling in cell specification and morphogenesis of the NgD.

## 2.1. Visualizing neuronal specification dynamics

With the aim to study the influence of cell dynamics in the establishment of the NgD, we used a zebrafish BAC reporter line that expresses the fluorescent protein DsRed-Express (DsRedE, a faster maturation version of DsRed (Bevis and Glick, 2002)) upon activation of the *neurog1* promoter (Drerup and Nechiporuk, 2013). We imaged in 4D the otic development from stages of otic placode morphogenesis (15 hpf) until neuroblast delamination is abundant and the central lumen is growing (20.5 hpf, **Figure 20A-B**; Movies S1-S2 see Appendix 7.2). The overall pattern of DsRedE expression is highly preserved between embryos, being restricted to the most ventroanterolateral (VAL) region of the primordium until 19 hpf and expanding posteromedial at around 20.5 hpf (**Figure 20A-B**; Movies S1-S2 see Appendix 7.2). This DsRedE protein pattern recapitulates the endogenous spatiotemporal *neurog1* expression analyzed by *in situ* hybridization (ISH) (Andermann et al., 2002; Vemaraju et al., 2012; Radosevic et al., 2014). Moreover, DsRedE expressing cells delaminate (**Figure 27A**; Movies S1, S10 and S11 see Appendix 7.2) and incorporate into the SAG (Movie S3 see Appendix 7.2), supporting the use of this line to analyze single cell dynamics of neuronal specification upon *neurog1* expression.
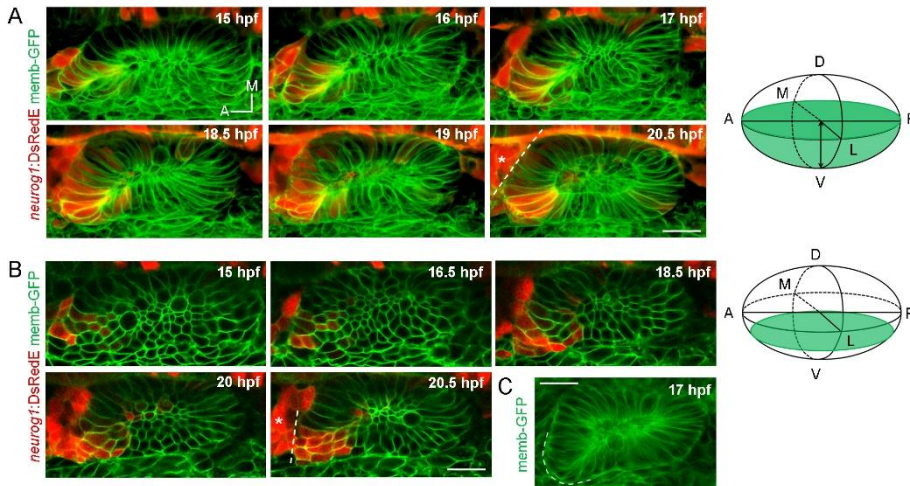
**Figure 20. Specification dynamics of the otic neurogenic domain.**

**(A, B)** Selected frames of a movie of an otic placode from a TgBAC(*neurog1*:DsRedE)[n16] embryo shown in 3D reconstructions (dorsal view) **(A)** and coronal ventral planes **(B)**. Green in the right schemes shows the region imaged. Membranes stained with memb-GFP. D: dorsal, V: ventral, A: anterior, P: posterior, M: medial and L: lateral. Dashed lines indicate the limit between the vesicle and the SAG (asterisk). Medial to the otic vesicle, DsRedE is also visible in the neural tube. **(C)** Average z-projection (dorsal view) of the inner ear at 17 hpf. Dashed line indicates the protuberance. Scale bars, 20 μm. *See also Movies S1, S2 and S3*.

## 2.2. Morphometric analysis of the NgD

We also analyzed the cellular organization of the NgD by performing a 3D morphometric analysis of this region. During the stages of neuronal specification, the shape of the otic vesicle is asymmetric, exhibiting a protuberance in the anterolateral region (**Figure 20C**). To compare the properties of the neurogenic region with the rest of the otic vesicle, we built a rectangular cuboid with the vertices of the vesicle and divided it in eight regions of equal volume (**Figure 21A**), in which we quantified

75

the number of cells and the volume of tissue. By 19 hpf, the NgD region has accumulated more cells (15.4±0.4% of cells) than the other regions (mean non-neurogenic region: 12.0±0.1% of cells, **Figure 21B**) and presents higher cellular density (**Figure 21C**; neurogenic region: 2.16±0.03 nuclei/$1x10^3\mu m^3$, mean non-neurogenic region: 1.60±0.03 nuclei/$1x10^3\mu m^3$). Quantification of all the mitotic events inside the vesicle between 14 and 18.5 hpf revealed that cell proliferation is also highly enriched in this region (**Figure 21D**). The modest increase in the number of cells in this region cannot account for the large enrichment in cell proliferation, suggesting a higher proliferation rate in the NgD region. Thus, in addition to a phase of transit-amplification of neuroblasts after delamination (Vemaraju et al., 2012), neuronal progenitors multiply inside the otic vesicle. This analysis indicates that the NgD presents a particular shape, high cell number, high cell density and an increased proliferation rate.
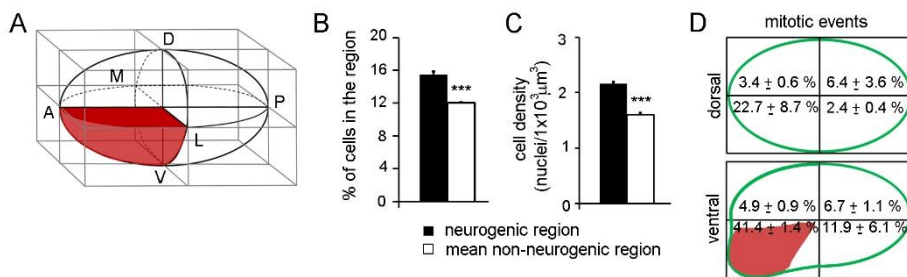


**Figure 21. Morphogenesis of the otic neurogenic domain.**
**(A)** Scheme of the rectangular cuboid used for quantifications. Neurogenic region shown in red. **(B, C, D)** Quantification of cell number **(B)**, cellular density **(C)** and mitotic events **(D)** in the indicated regions at 19 hpf (n=11) **(B, C)** or between 14 and 18.5 hpf (n=2) **(D)**. Data are mean s.e.m. ***P<0.0001 one sample t-test in (B) and unpaired t-test (C).

## 2.3. Pioneer cells specify outside the otic primordium and ingress during otic placode formation

To analyze how the NgD is built, we decided to evaluate when and where every single cell of the NgD starts to express *neurog1*. We first aimed to capture the earliest specified cells. While it has been reported that *neurog1* expression in the otic placode begins at least at 15 hpf (Radosevic et al., 2014), we found that already at 13 hpf there are rows of DsRedE expressing cells lateral to the neural tube. These cells are found anterior to the epithelializing placode (**Figure 22A**; Movie S4 see Appendix 7.2) and coincide with *neurog1* expressing cells detected by ISH assumed to belong to the anterior lateral line placode (Andermann et al., 2002). Unexpectedly, when we followed these cells, we found that some of them migrate posteriorly and incorporate into the anterolateral region of the otic placode, in a position corresponding to the NgD (red brackets in **Figure 22B**; Movie S5 see Appendix 7.2). We confirmed cell ingression by photoconversion NLS-Eos expressing nuclei outside the primordium at 13 hpf and their detection inside the vesicle at 20 hpf (**Figure S2A** see Appendix 7.1). In the same region as ingressing cells, a second pool of *neurog1*^{+} cells (expressing also *neurod*; **Figure S2B** see Appendix 7.1) moves posteromedial without ingressing (blue brackets in **Figure 22B**; Movie S5 see Appendix 7.2).

3D tracking of individual cells of the ingressing pool revealed that some cells activate *neurog1* expression while moving towards the primordium and before their epithelialization (**Figure 22C**; Movie S6 see Appendix 7.2). Immediately after ingressing into the NgD, these cells divide and delaminate, thus undergoing a complete cycle of epithelialization and de-epithelialization in only a few hours.
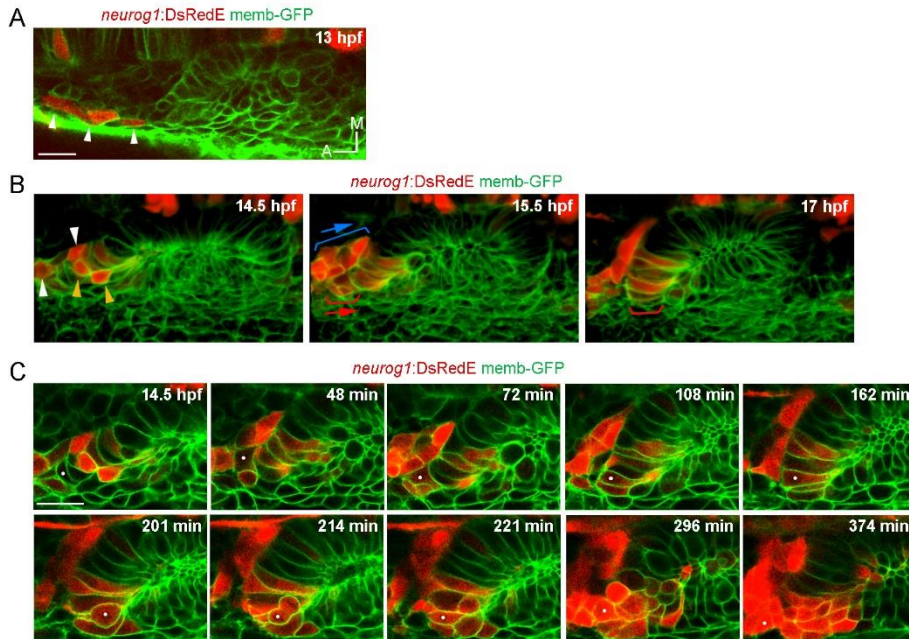
**Figure 22. Ingression of *neurog1⁺* cells.**

**(A)** The otic primordium and its anterior region at 13 hpf. Arrowheads highlight *neurog1⁺* cells outside the otic epithelium. **(B)** Selected frames of a 3D reconstruction (dorsal view) of the otic placode following the movement of the anterior *neurog1⁺* cells. Arrowheads at 14.5 hpf indicate *neurog1⁺* cells before epithelialization (white: cells outside the placode, orange: ingressing cells). At 15.5 hpf red bracket identifies cells that will ingress (shown at 17 hpf) and blue bracket cells that will not ingress. In (A) and (B) the contrast of the red signal was increased to improve visualization. **(C)** Selected planes of a 3D tracking of a single cell specifying during ingression (white dot). At 108 min the cell is already epithelialized. All scale bars, 20 μm. *See also Figure S2 and Movies S4, S5 and S6.*

Analysis of the movement of these cells suggests that their migration is an active and directional process occurring in not all but in particular cells (**Figure 23A-C**; Movie S7 see Appendix 7.2); some cells of the same region migrate in other directions (data not shown). We observed

that the cell front periodically protrudes, followed by a rapid forward translocation of the nucleus (**Figure 23D**; insets of Movie S7 see Appendix 7.2), as described during fibroblast migration (Petrie and Yamada, 2015). When tracking three neighboring cells, we observed that two of them ingress (white and pink tracks) but the third one (blue track), initially positioned closer to the otic placode, divides during migration and the daughters do not ingress (**Figure 23A-C**; Movie S7 see Appendix 7.2). These observations highlight that factors other than anteroposterior position determine whether a cell will ingress or not into the otic placode. Additionally, other morphological features particular of these stages could contribute to cell ingression (**Figure S3A-C** see Appendix 7.1).
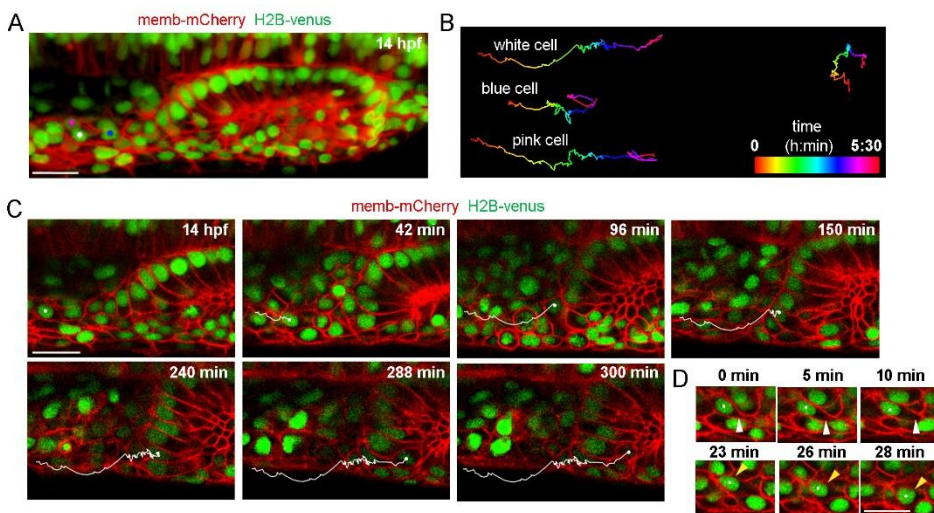


**Figure 23. Movement of ingressing *neurog1+* cells.**

**(A-C)** 3D tracking of single cells during ingression. **(A)** 3D reconstruction (dorsal view) showing the initial position of the tracked cells (white, pink and blue dots) at 14 hpf. **(B)** 2D tracks of the cells shown in (A) are displayed in a temporal color code. Each track was displaced in the y axis for better visualization. The track of the posterior vertex of the vesicle is shown on the right. **(C)** Selected frames for the cell of the white track. At 150 min the cell is ingressing and completed at 240 min. At 300 min cytokinesis occurs.

Membranes stained with memb-mCherry. Embryos are Tg(Xla.Eef1a1:H2B-Venus). **(D)** Selected planes showing cell-membrane displacements during migration of the cell tracked in (C). White arrowheads indicate protrusion of the cell front and orange arrowheads the position of the nucleus. All scale bars, 20 µm. *See also Figure S3 and Movie S7.*

In summary, our results show that a group of cells that are being specified outside the placode migrates and ingresses into the prospective NgD, constituting the earliest neuronal specified cells of the otic placode (**Figure 24**).
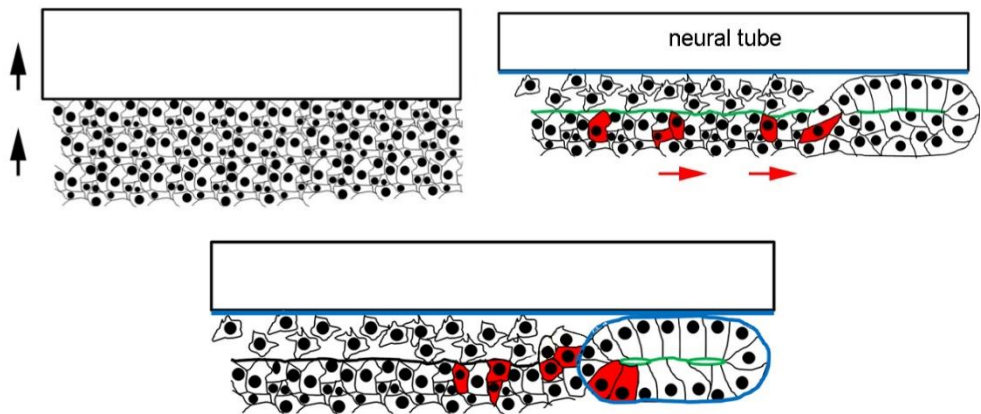


**Figure 24. Ingression of *neurog1*+ cells.**
Schematic representation of the migration and ingression during epithelialization (see Figure S3 for further details). Black arrows: medial convergence, blue line: laminin, green line: actin layer, red cells: *neurog1*+ cells, red arrows: migration of *neurog1*+ cells towards the otic placode. *See also Figure S3.*

80

## 2.4. Generation of *neurog1* expressing cells by local specification and cell division

We next evaluated if, in addition to ingressing cells, other cells start to express *neurog1* within the NgD. We visualized for the first time the activation of *neurog1* expression inside the otic vesicle in real-time (**Figure 25A**; Movie S8 see Appendix 7.2), a process that we refer to as "local specification". Dynamic quantification of DsRedE fluorescence levels in individual cells ($F_{cell}$) indicated that the rate of increase in the signal is variable among cells (**Figure 25B**, mean rate of increase = 2.3, 1.52 and 1.18 a.u./min for cells 1, 2 and 3). However, we found that when the signal reaches a certain level (between 110-150 a.u., red dots in **Figure 25B**), cells begin to delaminate (visualized by the movement of the cell body to the basal domain of the epithelium). This suggests that cells delaminate relative to *neurog1* levels and not to the time elapsed from the beginning of *neurog1* expression.
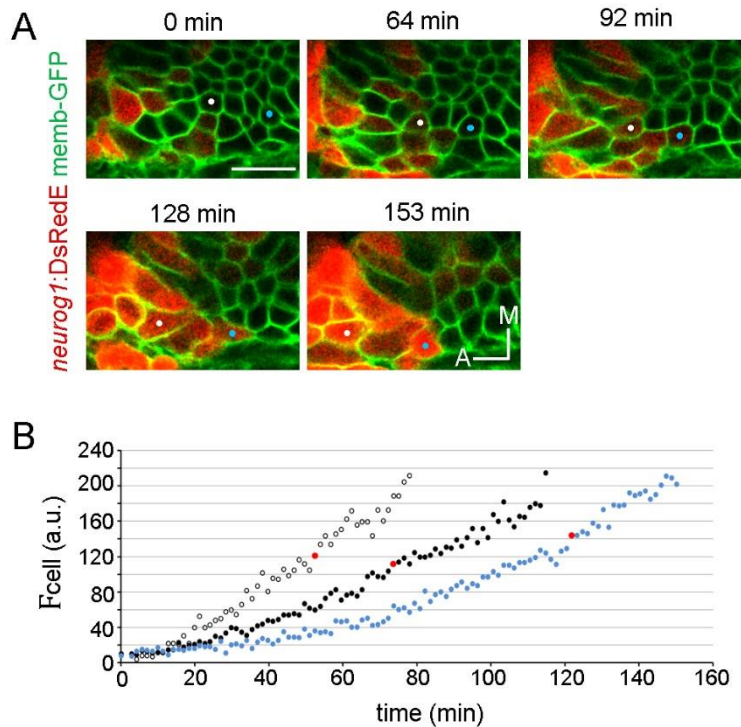
**Figure 25. Local specification of *neurog1* expressing cells.**
**(A)** Selected planes showing DsRedE expression dynamics in locally specified cells (white and blue dots) from TgBAC(*neurog1*:DsRedE)[n16] embryos expressing memb-GFP. **(B)** Quantification of DsRedE fluorescence over time for three cells of the same video (white, blue (the ones shown in (A)) and black dots). Red dots indicate beginning of delamination. Scale bar, 20 μm. *See also Movie S8.*

As we mentioned above, cells in the NgD divide at a high rate. Therefore, division could also contribute to add *neurog1* expressing cells (*neurog1*+ cells) to the domain. To address this, we performed a 4D analysis of cell divisions and found that every cell divides only once in the 7-hour period analyzed (n = 27/27). Mitotic cells are found either contacting the central lumen (**Figure 26A**) or not (**Figure 26B**). Interestingly, these later cells are apposed to an accumulation of the

apical determinant Pard3 that forms a scaffold perpendicular to the central luminal surface of the vesicle, running from the lumen to the periphery (**Figure 26C**; Movie S9 see Appendix 7.2). Thus, similar to the apical mitosis occurring in the central lumen (**Figure 26D**), peripheral divisions are also in contact with an apical surface (**Figures 26E**).
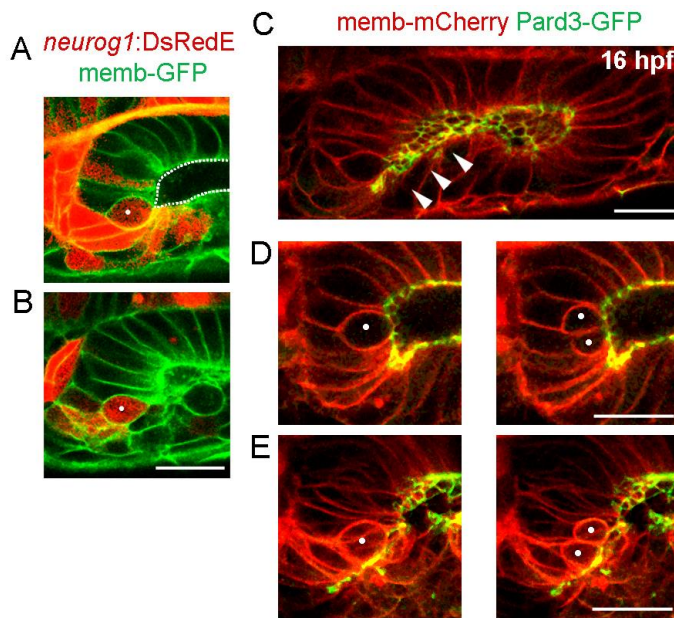


**Figure 26. Divisions of *neurog1* expressing cells.**
**(A, B)** *neurog1*^{+} mitotic cells (white dots) contacting **(A)** or not **(B)** the central lumen (dashed line). **(C)** Pard3-GFP localization in the central lumen and the AL region (white arrow heads). Membranes are stained with memb-mCherry. **(D, E)** Divisions (white dots) located in the lumen **(D)** or the apical scaffold **(E, z-projection)**. Scale bars, 20 μm.  *See also Movie S9.*

In neurogenic tissues either asymmetric (daughter cells become one progenitor and one neuron) or symmetric (both daughter cells with the same fate) divisions can occur (Chenn and McConnell, 1995; Das and Storey, 2012; Taverna et al., 2014). This depends on factors as the apicobasal position of the dividing cell and the orientation of the mitotic spindle (Das and Storey, 2012). All divisions touching the central lumen

have the cytokinesis cleavage plane perpendicular to the apical surface. Cells dividing peripheral to the central lumen seem to have the cleavage plane parallel to the central lumen, but when analyzing its cleavage plane in relation to the accumulation of Pard3 deposition, we observed that also have the cytokinesis cleavage plane perpendicular to the apical surface. Therefore, all divisions observed in the NgD have the cytokinesis cleavage plane perpendicular to the apical surface regardless of their position in the epithelium or their *neurog1* expression (**Figures 26D-E**). Moreover, when analyzing the fate of the daughter cells after division, we found all were symmetric (27/27): both daughter cells will delaminate after division (20/27 delaminate during the timeframe analyzed, 7/27 are in position to delaminate at the end of the acquisition). However, division can occur either before (13/25) or after the increase (12/25) in *neurog1* expression. Interestingly, daughter cells from mitoses of a *neurog1*$^+$ cell with high levels of DsRedE expression (*neurog1*$^{+Hi}$ cell) rapidly delaminate, remaining in close contact as they move to the periphery of the tissue (**Figure 27A-B**; Movies S10 and S11 see Appendix 7.2). Otherwise, daughter cells from mitosis of cells not expressing *neurog1* (*neurog1*$^-$) or expressing low levels of DsRedE (*neurog1*$^{+Low}$), accommodate in the epithelium after division, where they increase the DsRedE signal over a variable period of time (**Figure S4** see Appendix 7.1).

In summary, divisions in the NgD are symmetric and apical and a preferential sequence of events between *neurog1* activation and division does not occur.

Altogether, our analysis of the origin of *neurog1*$^+$ cells revealed that they are added to the NgD by three different mechanisms: cell ingression, local expression and cell division.
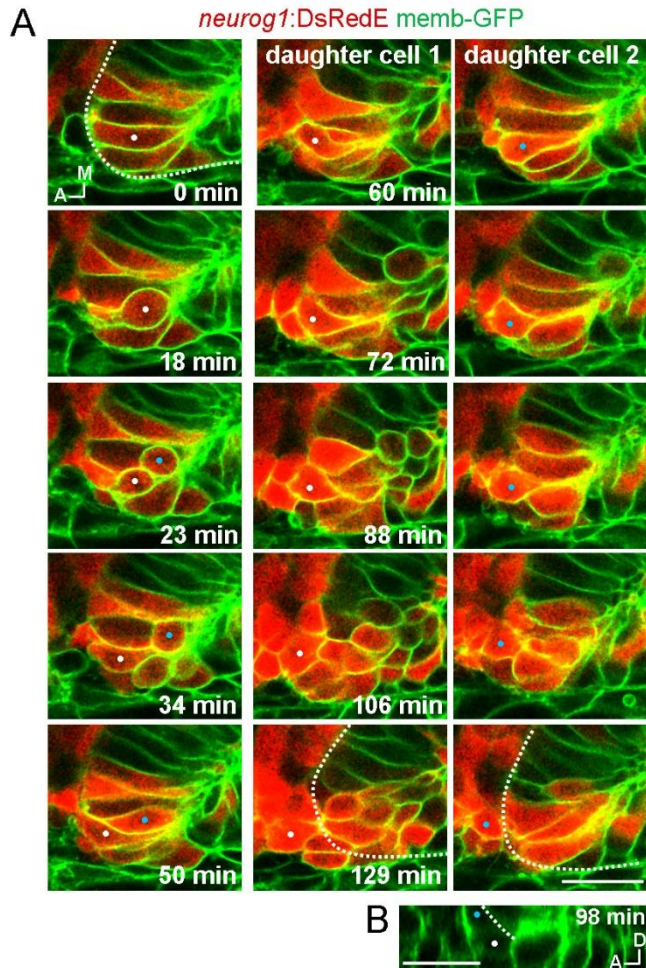
**Figure 27. Division of *neurog1* expressing cell.**

**(A)** Selected planes from a 3D time-lapse of a *neurog1*+ mitosis. White and blue dots track the daughter cells. Dashed lines indicate the approximated limit of the vesicle. Selected planes for each daughter cell are shown from 60 min onwards. At 129 min cells are delaminated. **(B)** Reslice of a frame at 98 min from the movie shown in (A) showing the z proximity between the tracked daughter cells during delamination (the red signal was removed for better visualization). Scale bars, 20 μm. *See also Figure S4 and Movies S10 and S11*.

## 2.5. Ingressing cells instruct neuronal specification

The incorporation of the pioneer cells and their rapid exit from the otic primordium led us to wonder about their role in the establishment of the NgD. These early-specified cells might contribute by their inclusion as specified cells or additionally play other roles. To address this question, we decided to remove these cells during their migration, before reaching the placode. We identified the position of the stream of the ingressing cells by the DsRedE signal (**Figure 28A**) and laser-ablated them unilaterally at 12.5 hpf (**Figure 28B**).
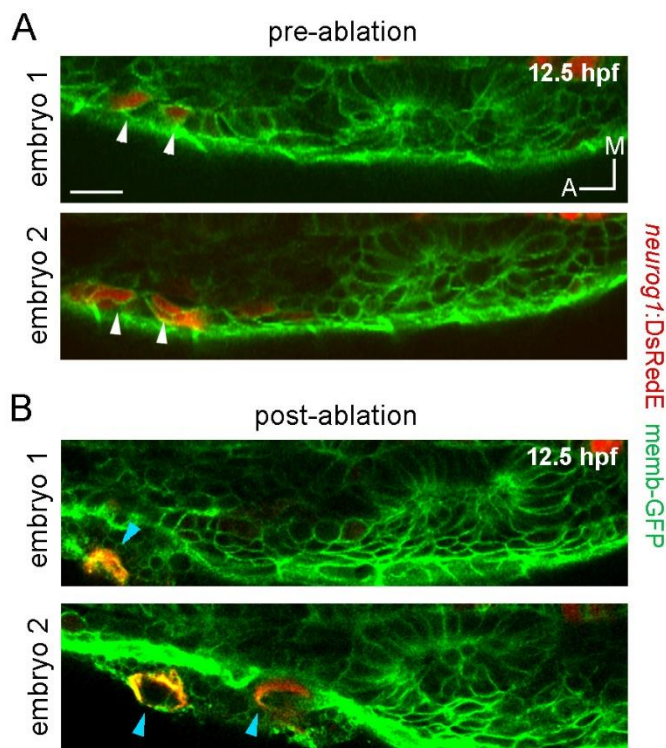


**Figure 28. Laser ablation of ingressing cells.**
**(A, B)** Laser ablation of *neurog1+* cells before ingression. Two different embryos are shown. Images of the otic primordium and its anterior region at 12.5 hpf just before **(A)** and after **(B)** laser-ablation. White arrowheads indicate *neurog1+* cells. Blue arrowheads localize the ablated region. Embryo 1 only received one

laser pulse and embryo 2 several laser pulses (only two are visible in this plane). The contrast of the red signal was increased to improve visualization. All embryos are TgBAC(*neurog1*:DsRedE)[n16] and membranes are stained with memb-GFP. Scale bar, 20 μm.

The effects on neuronal specification were examined in 3D in the otic vesicle at 18.5 hpf (**Figure 29A**; Movie S12 see Appendix 7.2), before delamination becomes significant. *neurog1* expression was analyzed by quantification of the $F_{cell}$ of cells belonging to the NgD (**Figure 29B**). Ablation of a limited number of cells led to a decrease in the global level of DsRedE expression (GLE, calculated as the sum of the $F_{cell}$ for all *neurog1*^{+} cells) in the vesicle of the ablated side, as compared to the vesicle of the contralateral not-ablated side from the embryo (**Figure 29A** and **Figure 30A**; non-ablated side: 1549±140.7, ablated side: 370±118 a.u). This effect was dependent on the number of laser pulses applied: when more cells were ablated, more severe was the specification phenotype observed (compare embryos 1 and 2 from **Figure 29B**; the embryo 2 received more laser pulses), despite the overall morphology of the NgD being unaffected. Analysis of specification at 21 hpf confirms that the effect of ablation persists and, thus, does not appear to represent a delay in neuronal specification (**Figure S5A-B**; Movie S12 see Appendix 7.1 and 7.2). Moreover, the effect is specific to otic *neurog1* expression, since DsRedE expression in the neural tube was not affected by ablation (**Figure S5C** see Appendix 7.1).
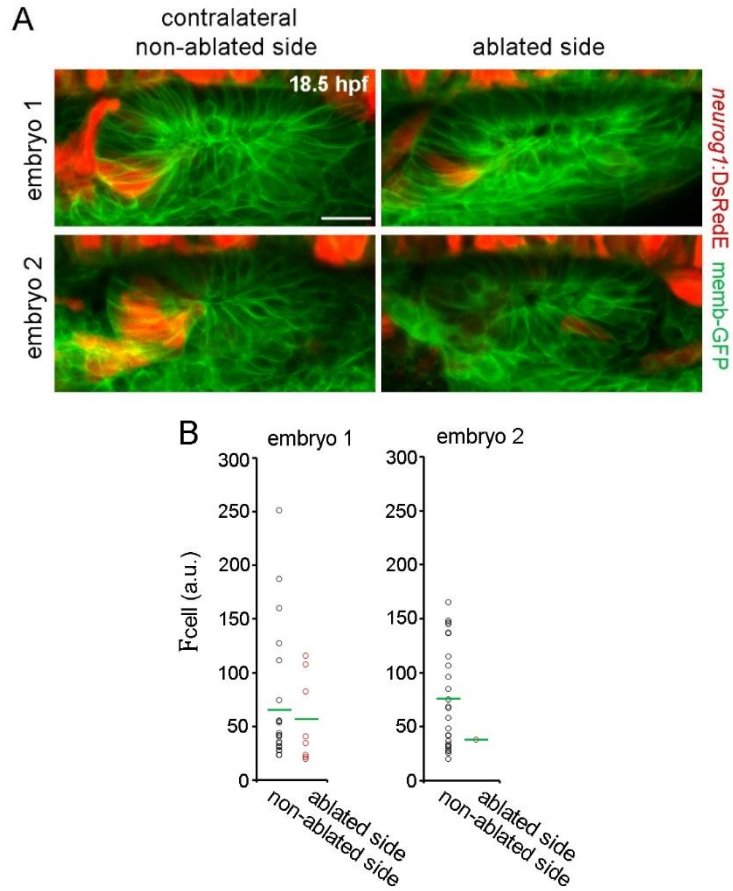
**Figure 29. Neuronal specification after ablation.**

**(A, B)** *neurog1* expression pattern inside the vesicle after ablation. **(A)** Average z-projections of embryos shown in (Figure 28) 5 hours after ablation (18.5 hpf). The ablated side and their contralateral non-ablated side of the same embryo are shown. **(B)** Quantification of $F_{cell}$ in each *neurog1*+ cell of the vesicles shown in (A). Each dot indicates one cell. Green lines indicate the mean of each condition. Scale bar, 20 μm. *See also Figure S5 and Movie S12*.

When comparing the number of *neurog1*+ cells (N*neurog1*+), we also found a reduction in the ablated side vesicle compared to the control vesicle (**Figure 30B**; non-ablated side: 24.5±1.4, ablated side: 8.2±2.6 cells). This result could be partially explained by the failure of the ablated

cells to ingress into the forming NgD. These results also indicate that when ablating the cells that will be part of the NgD, the cells now located in the same position do not change their fate and become neural specified, as expected if cell identity would be dictated by cell position. Interestingly, the number of cells eliminated by ablation (and the ones produced by their divisions) cannot account for the large decrease in the number of *neurog1*+ cells in the vesicles of the ablated side (**Figure 30B**). This suggests that ingressing cells play an instructive role on the specification of other cells of the NgD (i.e. local specification). To shed light on this possibility, we calculated the mean value for $F_{cell}$ ($\bar{F}_{cell}$) in vesicles from each experimental condition. This parameter was also reduced by the ablation (**Figure 30C**; non-ablated side: 63.6±5.7, ablated side: 44.2±5.2 a.u.), suggesting that the global reduction in fluorescence was not only caused by a decrease in the number of *neurog1*+ cells, but that the *neurog1* transcriptional activity inside these cells was also reduced. Accordingly, the number of *neurog1*+Hi cells (N*neurog1*+Hi) was also significantly lowered by ablation (**Figure 30D**; non-ablated side: 5.5±0.6, ablated side: 0.7±0.5 cells).
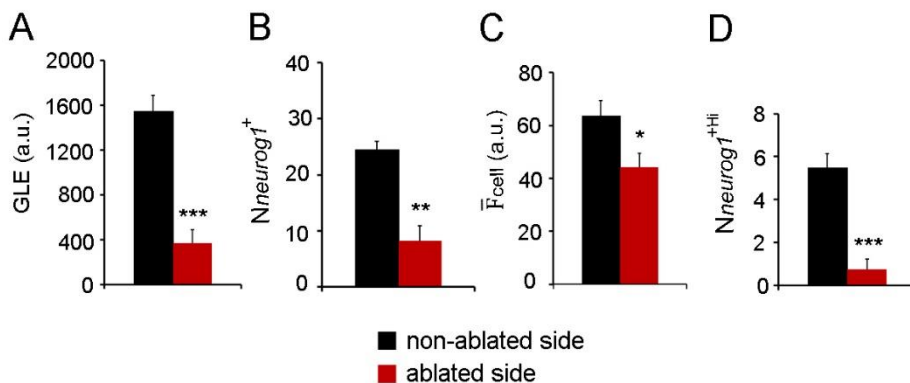


**Figure 30. Ingressing cells instruct local neuronal specification.**
**(A-D)** Parameters of neurogenic specification at the single cell level: GLE **(A)** N*neurog1*+ **(B)**, $\bar{F}_{cell}$ **(C)**, and N*neurog1*+Hi **(D)** are shown. Data are mean s.e.m. (n=4). t-test ***P<0.001, **P<0.005, *P<0.05.

However, it is possible that the *neurog1*[+Hi] cells at the time point analyzed are mainly ingressed cells, and thus by eliminating them, we decreased the $\bar{F}_{cell}$ in each vesicle by a relative increase in *neurog1*[+Low] cells. We discarded this possibility by backtracking cells identified as *neurog1*[+Hi] at 19 hpf, and observing that most of them are *neurog1*^{-} cells at 13 hpf and are located inside the epithelizing placode before ingression takes place, therefore belonging to the pool of cells specified locally (**Figure 31**).



*neurog1*:DsRedE  memb-GFP
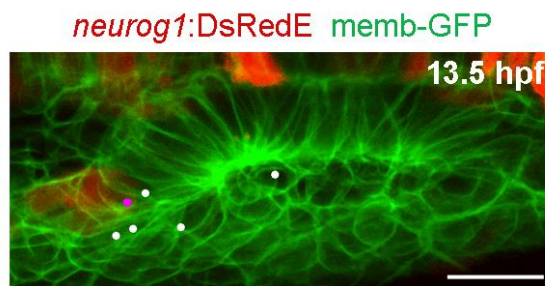
**Figure 31. *neurog1*[+Hi] cells are specified locally.**
Dots show the location at 13.5 hpf of backtracked cells corresponding to *neurog1*[+Hi] cells at 19 hpf. Pink dot: *neurog1*[+] ingressed cell. White dots: *neurog1*^{-} cells. The 3D reconstruction of the placode shown is representative of two different analyzed embryos. Scale bar, 20 μm.

Altogether, these results indicate that ingressing cells contribute to the NgD both through their incorporation as *neurog1*^{+} cells and by promoting *neurog1* expression non-autonomously in other cells of the domain.

## 2.6. FGF controls cell ingression

To understand how the specification processes identified above are promoted, we decided to explore the role of FGF signaling, a pathway reported to control both *neurog1* expression in the vesicle and the number of neurons in the SAG (Vemaraju et al., 2012; Wang et al., 2015). To this aim, embryos were incubated with the FGFRs inhibitor SU5402 from 11 hpf until 19 hpf, beginning the treatment after otic placode induction (**Figure 32A-B**). Analysis on neuronal specification indicated that SU5402 reduced the GLE (**Figure 32C**), in agreement with the previous ISH analysis of *neurog1* expression (Léger and Brand, 2002; Vemaraju et al., 2012). This reduction is caused not only by a decreased mean level of *neurog1* expression in each cell (**Figure 32B-C**), but also by a reduction in the number of *neurog1*^{+} cells, and particularly in the *neurog1*[+Hi] cells (**Figure 32C**).
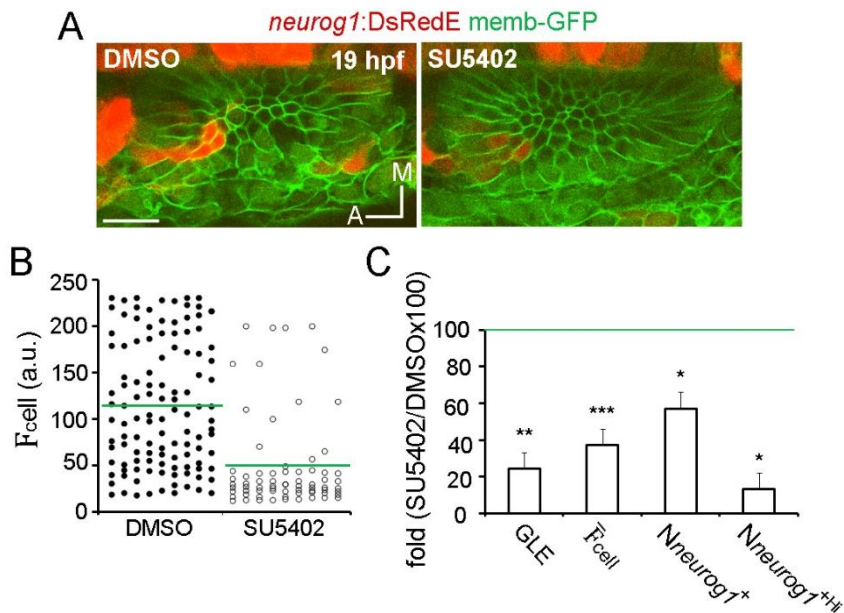


**Figure 32. FGF control of neurogenic specification**.
**(A-C)** *neurog1* expression pattern inside the vesicle at 19 hpf in embryos incubated in DMSO or SU5402. **(A)** Images of otic vesicles at 19 hpf incubated

from 11 hpf in DMSO or SU5402 (ventral planes). **(B)** Quantification of $F_{cell}$ for cells of vesicles from the groups shown in (A). Each dot indicates one cell. Green lines indicate the mean of each condition. n=5 for DMSO and n=6 for SU5402. **(C)** Parameters of neurogenic specification at the single cell level for the data shown in (B): GLE, $\bar{F}_{cell}$, N$neurog1^+$ and N$neurog1^{+Hi}$ are shown as fold change of SU5402/DMSOx100. Scale bar, 20 $\mu$m. Data are mean s.e.m. t-test ***P<0.001, **P<0.005, *P<0.05. Scale bars, 20 $\mu$m.

Considering that FGF signaling controls early stages of chick inner ear morphogenesis (Sai and Ladher, 2008), it is possible that the reduction in the number of specified cells by SU5402 be a consequence of a more general defect in the vesicle or the NgD. Therefore, we next evaluated the role of the FGF signaling over morphogenesis, using the same partition of a cuboid as above. We observed that SU5402 reduced the number of cells in the whole vesicle (**Figure 33A-B**), but the effect over the NgD was more pronounced. Similar changes in volume also occur (**Figure 33C**). Therefore, the cell densities in the neurogenic and non-neurogenic regions do not change significantly (**Figure 33D**). The preferential effect on the NgD is associated with the reduction of the protuberance of the vesicle (**Figure 33A**). Therefore, there is a global reduction of cells in the NgD and not only of *neurog1*+ cells.

We next evaluated if the reduction in the number of cells is due to a decreased proliferation after FGF signaling blockade. We compared the number of mitotic events by pH3 immunofluorescence between SU5402-treated and control embryos and found that FGF signaling indeed promotes proliferation during early otic development (**Figure 33E-F**). These results indicate that FGF signaling regulates the morphogenesis of the NgD, and suggest that reduction in the number of cells and loss of the protuberance when the pathway is blocked could be consequence of reduced proliferation.
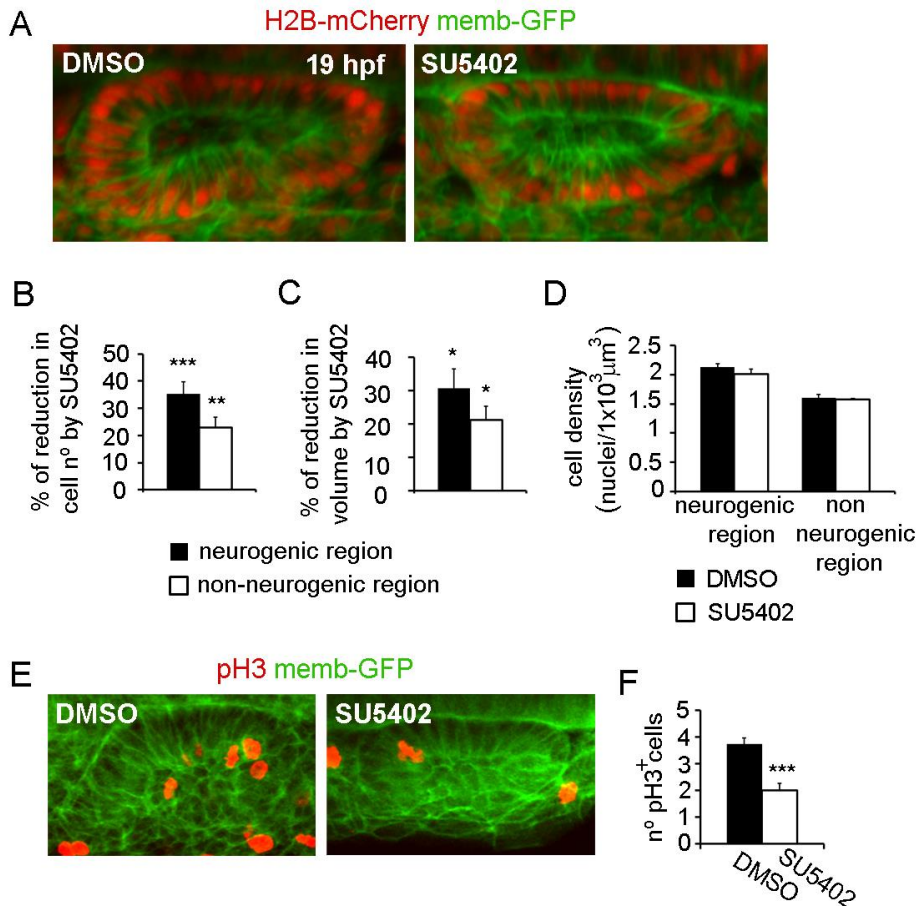
**Figure 33. FGF control of morphogenesis**.

**(A-D)** Quantitative analysis of morphogenesis at 19 hpf in embryos incubated in DMSO or SU5402. Membranes are stained with memb-GFP and nuclei with H2B-mCherry. **(A)** Images of otic vesicles at 19 hpf incubated from 11 hpf in DMSO or SU5402. z-projections are shown. **(B-D)** Morphometric analysis of embryos from the groups shown in (A) using the cuboid shown in Figure 21A. n=5 for DMSO and n=8 for SU5402. Quantification of the cell number **(B)**, volume **(C)** and cell density **(D)** for the indicated regions are shown and expressed as % of reduction produced by SU5402 (B, C). **(E, F)** Immunostaining of pH3 and GFP of 16 hpf embryos expressing memb-GFP and incubated in DSMO or Su5402 from 11 hpf. Data are mean s.e.m. t-test ***P<0.001, **P<0.005, *P<0.05.

In order to uncouple the possible effects of FGF signaling on cell proliferation and on cell specification, we decided to evaluate the relevance of proliferation for neural specification and NgD morphogenesis. We incubated the embryos from 13 to 19 hpf with a combination of aphidicolin and hydroxyurea (AH) as previously reported (shown to inhibit about 95% of the mitotic events (Hoijman et al., 2015)). Similar to the SU5402-treated embryos, AH reduced the GLE and the number of *neurog1*^{+} cells (**Figure 34A-C**). However, the mean *neurog1* expression levels in each cell did not change (**Figure 34C**), indicating that although proliferation is critical to determine the proper number of specified cells inside the domain, the level of *neurog1* expression in each specified cell is independent of the proliferative state of the vesicle. AH also reproduced the SU5402 reduction in the number of cells in the neurogenic and non-neurogenic regions (**Figure 34D-E**; and the preferential reduction in the neurogenic region). However, the volumes did not change significantly (**Figure 34F**), the protuberance remains (**Figure 34D**) and the density of cells decreases (**Figure 34G**; and reduces more in the neurogenic region). Thus, although proliferation is important for the increased cell density present in the neurogenic region, the formation of a protuberance does not rely exclusively on an increased cell number or proliferation rate but on an FGF-dependent morphogenetic event. These results also suggest that the FGF-dependent proliferation could regulate the number of specified cells, but the control by FGF signaling of the *neurog1* expression levels should operate by other mechanisms.
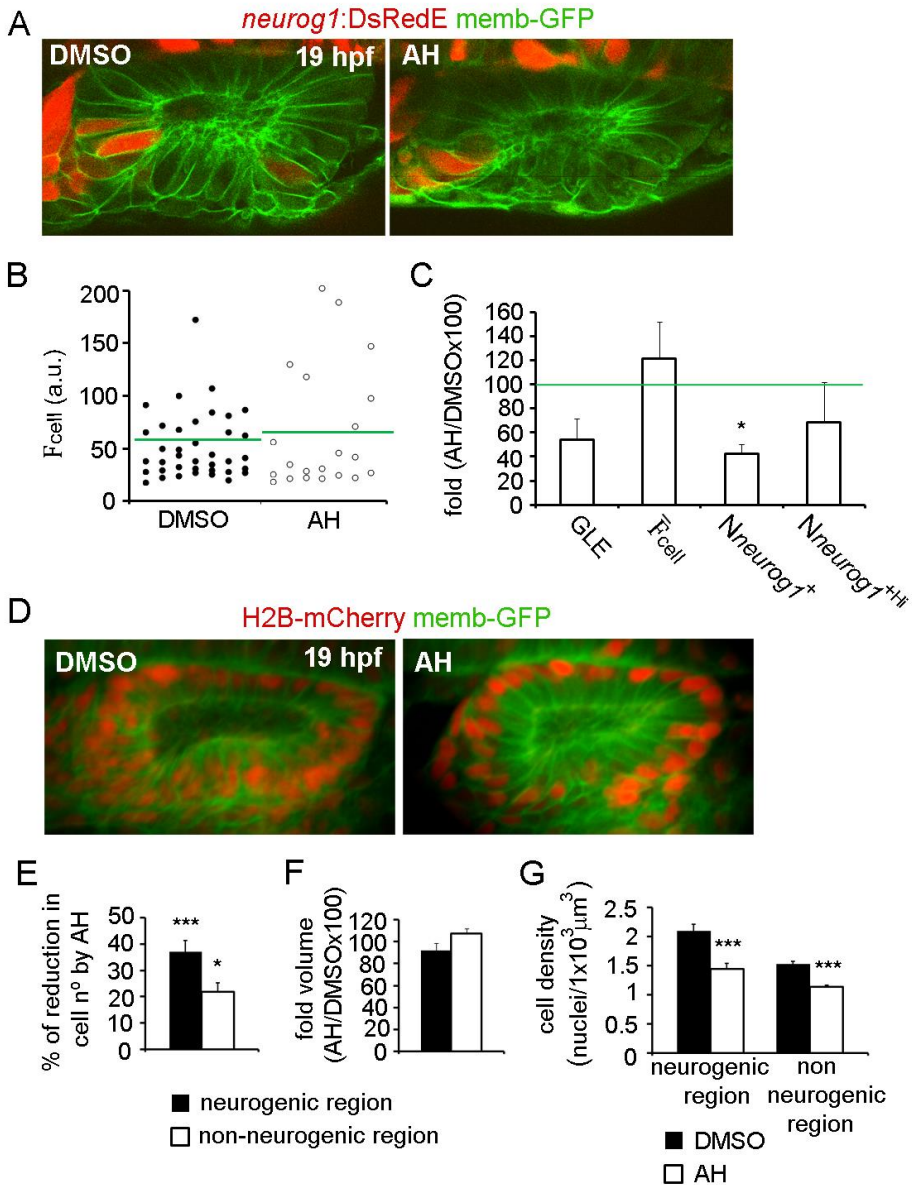
Figure 34. AH control of neurogenic specification and morphogenesis.
(A-C) *neurog1* expression pattern inside the vesicle at 19 hpf in embryos
incubated in DMSO or AH. (A) Images of otic vesicles at 19 hpf incubated from
13 hpf in DMSO or AH. (B) Quantification of $F_{cell}$ for cells of vesicles from the
groups shown in (A). Each dot indicates one cell. Green lines indicate the mean
of each condition. n=4 for DMSO and n=5 for AH. (C) Parameters of neurogenic

specification at the single cell level for the data shown in (B): GLE, $\bar{F}_{cell}$, N$neurog1^+$ and N$neurog1^{+Hi}$ are shown as fold change AH/DMSOx100. **(D-G)** Quantitative analysis of morphogenesis at 19 hpf in embryos incubated in DMSO or AH. Membranes are stained with memb-GFP and nuclei with H2B-mCherry. **(D)** Images of otic vesicles at 19 hpf incubated from 13 hpf in DMSO or AH. z-projections are shown. **(E-G)** Morphometric analysis of embryos from the groups shown in (D) using the cuboid shown in Figure 21A. n=6 for DMSO and n=7 for AH. Quantification of the cell number **(E)**, volume **(F)** and cell density **(G)** for the indicated regions are shown and expressed as % of reduction produced AH (N), or fold change AH/DMSOx100 (O). Data are mean s.e.m. t-test ***P<0.001, **P<0.005, *P<0.05.

Given that the phenotype from the FGF-signaling blockade is similar to the one resulting from cell ablation (reduction in the number of *neurog1*+ cells and particularly levels of *neurog1* expression); we asked if both ingressing cells and the FGF pathway could be part of the same specification pathway. We hypothesize that FGF signaling might be controlling the early cell ingression event since SU5402 has a strong effect over the number of SAG neurons when treatment is performed before 14 hpf (Wang et al., 2015). We tested this hypothesis blocking the FGF signaling from 11 hpf onwards and photoconverting at 13 hpf the nuclear staining of NLS-Eos in cells located anterior to the otic placode (**Figure 35A**, left panels). At 18 hpf, we quantified the number of cells with photoconverted nuclei inside the vesicle (**Figure 35A**, central panels) and, as shown in **Figure 35B**, SU5402 significantly reduced the number of ingressed cells (DMSO: 4.7±1.1, SU5402: 1.0±0.4 cells). These results suggest that FGF pathway is contributing to neuronal specification by promoting the ingression of the pioneer cells into the vesicle.

96
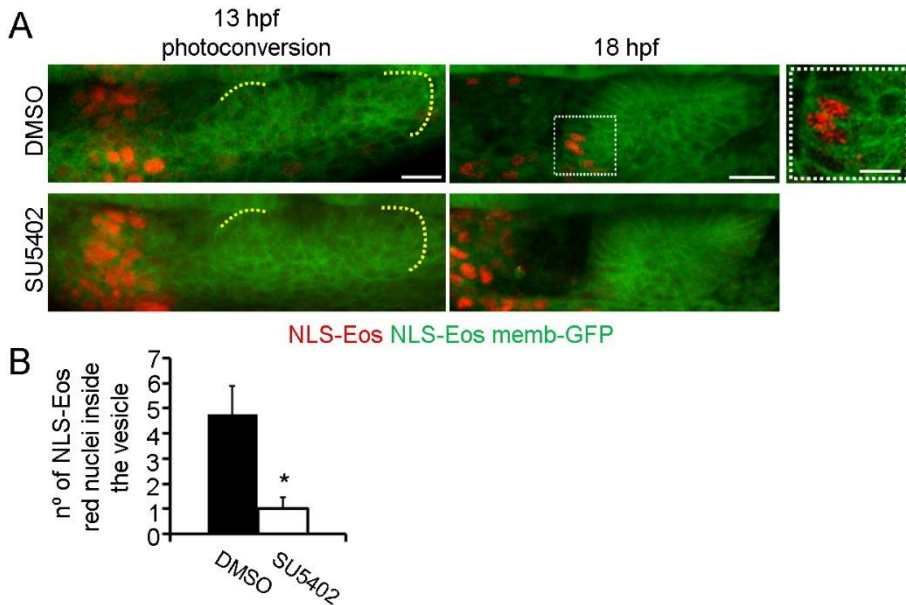
**Figure 35. FGF control of neurogenic specification.**

**(A)** Photoconversion of a region anterior to the placode of NLS-Eos stained nuclei at 13 hpf in embryos expressing memb-GFP and treated with DMSO or SU5402 from 11 hpf (z-projections). At 18 hpf photoconverted nuclei were observed in cells inside the vesicle in DMSO conditions. High magnification in the right (dotted square. Scale bar, 10 $\mu$m). Dotted yellow lines indicate the limits of the otic vesicle. **(B)** Quantification of the number of photoconverted nuclei inside the vesicle; n=6 for DMSO and n=7 for SU5402. Data are mean s.e.m. t-test ***P<0.001, **P<0.005, *P<0.05. Scale bars, 20 $\mu$m.

In conclusion, here we have analyzed the morphogenesis of the NgD taking into account the coordination between cell dynamics and cell specification. We determine that the NgD couples local cell specification, cell proliferation and, surprisingly, cell ingression. Therefore, we have identified a group of cells that specify outside the otic primordium and ingress into the prospective NgD of the otic vesicle subsequently instructing other cells from the domain to be specified. All this process is being controlled by FGF. Moreover, cells inside the domain divide, presenting symmetric and apical divisions with no specific order between *neurog1* expression and division. Finally, specified cells delaminate from the NgD and coalesce into the SAG (**Figure 36**).
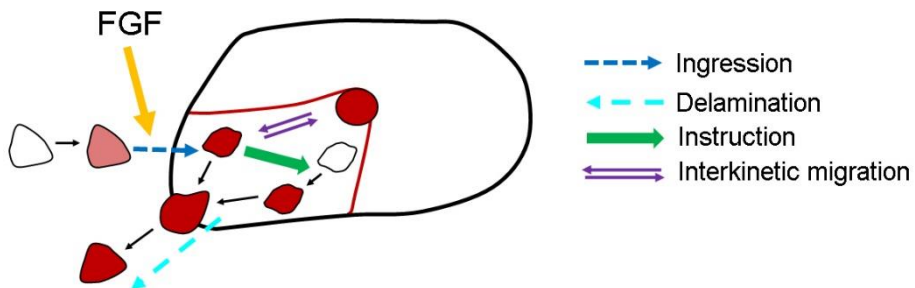


**Figure 36. FGF control of neurogenic specification.**
Scheme of cell dynamics playing a role in neuronal patterning of the inner ear.

## Author Contributions

EH and LF performed the experiments and analyzed the data. EH, LF and BA conceived the project and wrote the manuscript.

# Chapter 3: Cellular and molecular mechanisms of delamination

Otic neuroblasts are specified within the epithelium and to become neurons of the SAG, they undergo a delamination process in which they get out of the epithelium and acquire motility characteristics. Therefore, neuroblast delamination from the otic epithelium resembles an EMT process, in which turning an epithelial cell into a mesenchymal cell requires alterations in morphology, cellular architecture, adhesion, and migration capacity.

## Aims of Chapter 3:

1. To investigate the expression pattern of molecular markers of the developmental EMT process during neuroblast delamination.

2. To visualize the cellular behaviors during neuroblast delamination.

3. To investigate possible signaling pathways driving cell migration during delamination.

One of the most striking and evident morphogenetic event in the otic NgD is the loss of the neuronal specified cells by delamination. During this process, neuroblasts leave the epithelium of origin. Afterwards, they acquire migratory properties and remain in the adjacent mesenchyme forming the SAG. The mechanisms and molecular players involved in inner ear neuroblasts delamination and migration are poorly understood and in this Chapter we provide a description of the process in real time and identify possible molecules involved in it.

## 3.1. Cellular behaviors during delamination

When we focused specifically in the dynamics of the delamination process *in vivo*, we could see that the earliest morphological event during otic neuroblast delamination is a high basal protrusive activity. *neurog1* positive cells present blebs (asterisks) at their basal membrane during delamination (**Figure 37**; Movie S13 see Appendix 7.2). Blebs are hydrostatic pressure and cytoplasmic-flow propelled cellular protrusions that initiate either by local decrease in membrane-cortex attachment, or local rupture of the cortex itself (Paluch and Raz, 2013). By time lapse imaging, we could observe that the speed of bleb formation increases progressively. At the beginning, when the cell is still properly accommodated in the epithelium, blebs are observed every 4-6 minutes from the formation of one bleb to another (**Figure 37** first and second lines, Movie S13 see Appendix 7.2). By the time of cellular exit from the epithelium, bleb formation is more frequent (a new bleb can be observed after 1.5-3 minutes), and more than one bleb can be formed in the same cell (**Figure 37** third line; Movie S13 see Appendix 7.2). Moreover, blebs present a regular and highly dynamic life cycle. They extend and retract at high speed as seen in a movie at high temporal resolution (2sec 636ms) (**Figure 38A**; Movie S14 see Appendix 7.2). After several rounds of protrusive activity, exit of neuroblast from the

epithelium is observed (**Figure 37**, 90 min). In parallel, within the epithelium, delaminating cells suffer other shape changes at the apical side, a drastic cytoplasmic constriction is observed (**Figure 37, arrowheads**).
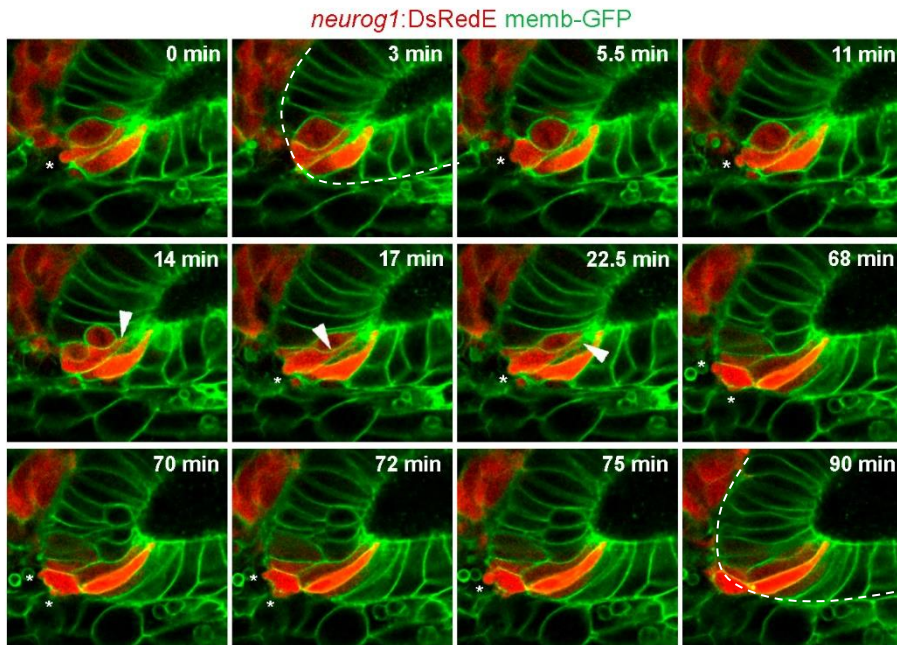


**Figure 37. Bleb formation in delaminating neuroblasts.**
Selected frames of a movie of an otic placode from a TgBAC(*neurog1*:DsRedE)[n16] embryo shown in coronal planes. Membranes are stained with memb-GFP. Blebs are indicated with an asterisk. Arrowheads indicate the apical side of the delaminating cell. Dashed lines indicate the limit of the otic vesicle. *See also Movie S13.*

Bleb formation has been proposed to be initiated due to an increase in the intracellular pressure, a reduction of the molecular links connecting the cortex to the membrane and/or rupture of the actin cortex at the region where the bleb forms (Charras et al., 2005; Paluch et al., 2005; Paluch and Raz, 2013). Furthermore, bleb formation was shown to be

dependent on the level of myosin contractility that could be regulated by an influx of $Ca^{2+}$ into the cell contributing to the separation of the plasma membrane from the cytoskeleton and protrusion formation (Blaser et al., 2006). Therefore, we wanted to check whether bleb formation in delaminating cells follows the same mechanisms previously described. To this aim we imaged bleb formation but this time focused on the myosin contraction and $Ca^{2+}$ levels.

The actomyosin cytoskeleton consists of networks of fiber-like actin filaments that are cross-linked by the molecular motor myosin II. Myosin II is a hexamer that consists of two myosin heavy chains (MHC), two regulatory myosin light chains (MLC), and two essential light chains (ELC). Phosphorylation of the MLC regulates the activity of myosin II, that generates contractile force by sliding the antiparallel actin filament arrays towards each other and promotes tissue surface tension (Yamada et al., 2005; Martin, 2010). Live imaging of myosin light chain GFP reporting natural myosin contractility observed through GFP fluorescence, indicates that myosin is recruited beneath the membrane (**Figure 38A** 1.60 sec) and behind the bleb during bleb retraction phase (**Figure 38A** from 1.20 to 1.90 sec; Movie S14 see Appendix 7.2). The first image shows myosin recruitment from the previous formed bleb (**Figure 38A** 0 sec). This recruitment could be important for the reestablishment of the membrane-cortex contacts.

Moreover, we monitored $Ca^{2+}$ accumulation during bleb formation. We injected embryos with mRNA encoding for the GCaMP3.1 biosensor. When $Ca^{2+}$ concentration increases, calcium binds to calmodulin resulting in a conformational change that leads to GFP fluorescence (Tian et al., 2009). We observe an increase in $Ca^{2+}$ concentration within the bleb when it is formed (**Figure 38B**; Movie S15 see Appendix 7.2).
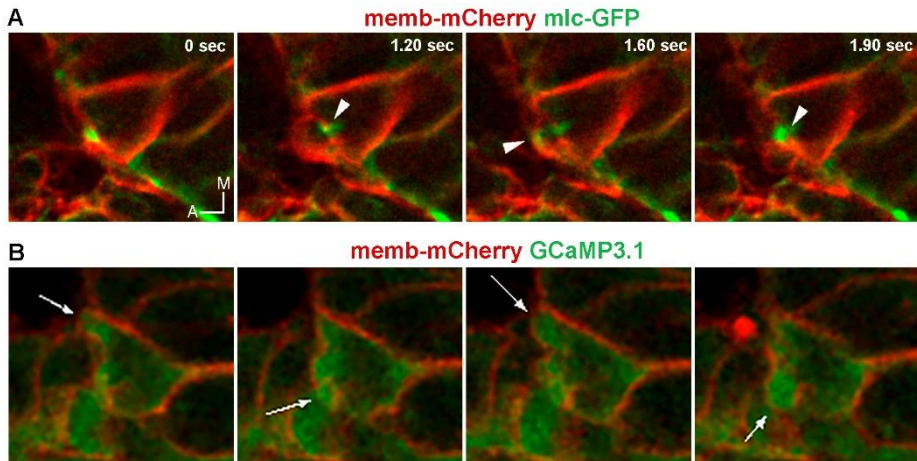
**Figure 38. Myosin recruitment and calcium accumulation in bleb formation.**

**(A)** Selected frames of a movie of a pre-delaminating cell from a Tg(b-actin:myl12.1-eGFP embryo shown in coronal planes. Images show a sequence of a bleb formation: initiation, growth and retraction. Membranes are stained with memb-mCherry. White arrowheads indicate myosin light chain recruitment. **(B)** Selected frames of a movie of a pre-delaminating cell from a wild-type embryo shown in coronal planes. Membranes are stained with memb-mCherry and changes in $Ca^{2+}$ concentration are visualized in green. White arrows indicate $Ca^{2+}$ accumulation during bleb formation. *See also Movies S14 and S15.*

For blebs to occur, most probably the integrity of the basal lamina must be lost. Therefore, we next aimed to determine the integrity of the basal lamina during neuroblast delamination process. In chick it was shown that cells from the otic epithelium displace the basal lamina during migration (Hemond and Morest, 1991). Moreover, in zebrafish it was already described that the basal surface of the otic epithelium becomes irregular during delamination (Haddon and Lewis, 1996), suggesting that the limits of the basal lamina could be broken.

Indeed, during otic neuroblast delamination we detect breaks in the basal lamina in transversal sections (**Figure 39**). Those breaks are detected in medial sections and, specifically, in the ventral part of the otic epithelium (**Figure 39B, E** arrowheads), being the posterior part of the vesicle completely intact (**Figure 39C, F**). Moreover, some cells also seem to delaminate from the anterior region at 22 hpf, but located more lateral, where laminin is also lost (**Figure 39A** arrowhead).
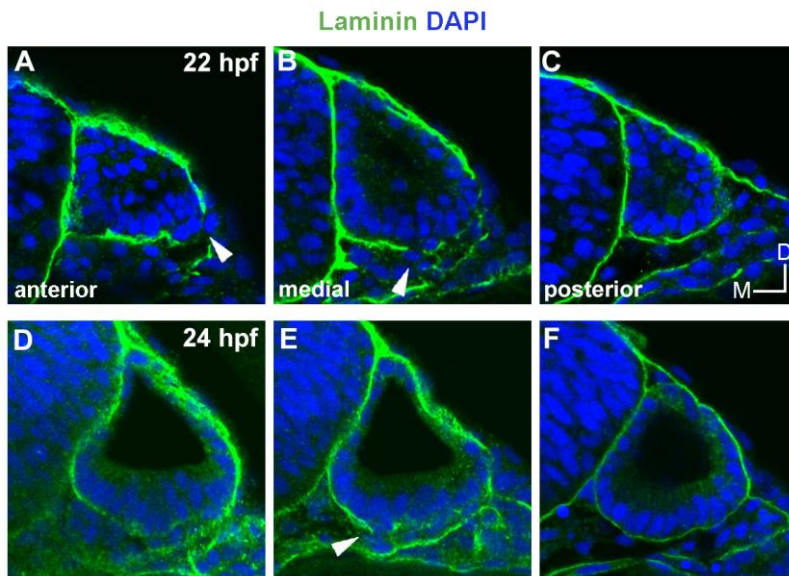


**Figure 39. Basal lamina breaks at the region of neuroblast delamination.** **(A-F)** Laminin staining at 22 hpf (A-C) and 24 hpf (D-F) in transversal sections. Nuclei are counterstained with DAPI. White arrowheads indicate breaks in the basal lamina.

## 3.2. Hallmarks of EMT induction are present during neuroblast delamination

The delamination process resembles an EMT event in which epithelial cells lose their characteristic polarity, disassemble cell-cell junctions and become more migratory. A switch in cell adhesion molecules, in which cells shift to express different isoforms of the cadherin transmembrane proteins, promotes the exit of cells from the epithelium. Cadherins, apart from their roles in cell adhesion can promote cell segregation from other epithelial cells during EMT and increase motility (Maeda et al., 2005; Wheelock et al., 2008). In NCC it has been shown that its delamination from the neural tube involves the downregulation of N-cadherin and Cadherin 6 as well as the *de novo* expression of type II cadherins, such as Cadherin 7 and 11 (Nakagawa and Takeichi, 1995, 1998; Vallin et al., 1998; Cheung and Briscoe, 2003; Cheung et al., 2005; Chalpe et al., 2010), suggesting a switch from strong classical cadherin cell adhesion in pre-migratory cells to a weaker type of adhesion in migratory cells. It has been described that *cadherin6* (*cdh6*) is expressed in zebrafish NCC promoting apical detachment and cell motility (Clay and Halloran, 2014). Therefore, we aimed to determine whether the EMT marker *chd6* is expressed in the zebrafish otic epithelium. We could see that *cdh6* is expressed in few cells located in position to delaminate and in neurons from the SAG (**Figure 40**). At 18 hpf, in flat-mount images *cdh6* is broadly expressed in cells located in the anteroventral region of the otic epithelium (**Figure 40A**). In transverse sections at 18 and 24 hpf, it is detected mainly in the SAG (**Figure 40B-E**) and in few cells located at the most anteroventral and medial parts of the otic vesicle (**Figure 40E** arrowhead).
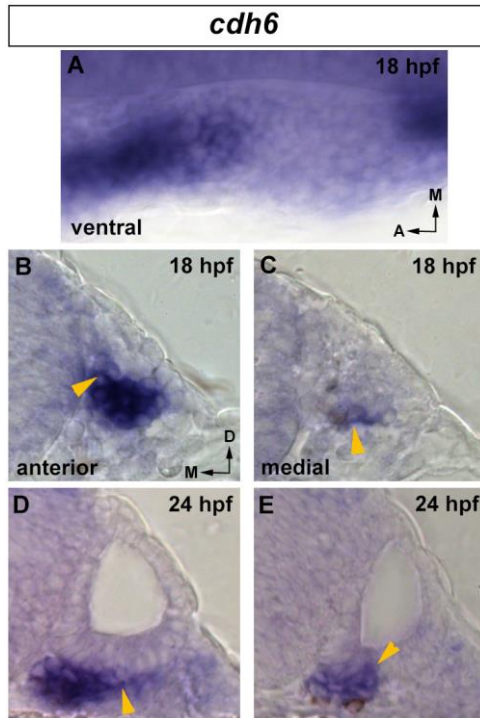
**Figure 40. *cdh6* is expressed in pre-delaminating cells in the otic vesicle and in the SAG.**
**(A)** Dorsal view of 18 hpf embryos stained by in situ hybridization for *cdh6* in a ventral plane. **(B-E)** Transversal sections, medial to left, dorsal to top of 18 hpf (B-C) and 24 hpf (D-E) embryos stained by in situ hybridization for *cdh6.* Orange arrowheads indicate *cdh6* expression in epithelial cells

Altogether, the results show that *cdh6* is expressed in pre-delaminating cells within the otic epithelium and in neurons from the SAG. Moreover, the basal lamina is broken at the region of neuroblast delamination.

## 3.3. The CXCL12-CXCR4 signaling pathway is expressed in the inner ear

Cell migration is key for cells to reach their final destination during development. Chemokines are vertebrate-specific proteins that function primarily in controlling directed cell movements forming gradients in the extracellular space perceived by specific transmembrane receptors (Bussmann and Raz, 2015). The best-characterized chemokines, that function during zebrafish embryonic development, are the homologs of the human homeostatic chemokine CXCL12 that bind to the receptor CXCR4. Cxcl12-Cxcr4 signaling interactions have already been described to be involved in single-cell migration of zebrafish PGC (Doitsidou et al., 2002; Blaser et al., 2006; Boldajipour et al., 2011) and in the collective cell migration of the zebrafish lateral line primordium (Dalle Nogare et al., 2014). Delaminated neuroblast leave the otic epithelium and migrate a short distance to coalesce into the SAG. Therefore, we wanted to determine whether chemokine-guided cell migration could be involved in cellular extrusion from the otic epithelium, and/or required for guiding cells through its way to the SAG. Therefore, we have analyzed the expression of the receptor *cxcr4a* and its ligand *cxcl12b* during the stages of neuroblasts delamination (**Figure 41**). We found that *cxcr4a* is expressed both, in the epithelial neuroblasts and in cells from the SAG (**Figure 41A-D**). At 22 hpf we can detect expression in some cells at the anteromedial region of the epithelium (**Figure 41A**, orange arrowhead), but it is mainly expressed in ventral planes in the anteromedial and anterolateral regions of the otic placode (**Figure 41B**). At 24 hpf *cxcr4* expression is mainly detected in ventral planes and restricted to the anterolateral region (**Figure 41C-D**, white arrowheads), and can also be detected in the posteromedial domain (**Figure 41D**, orange arrowhead). On the other hand, expression of the ligand *cxcl12b* at 24 hpf is detected in cells of the mesoderm underneath the otic vesicle

(**Figure 41E-F**, orange arrowheads). These expression patterns suggest that the ligand cxcl12b could be guiding the exit of neuroblasts from the otic epithelium through the cxrc4a receptor.
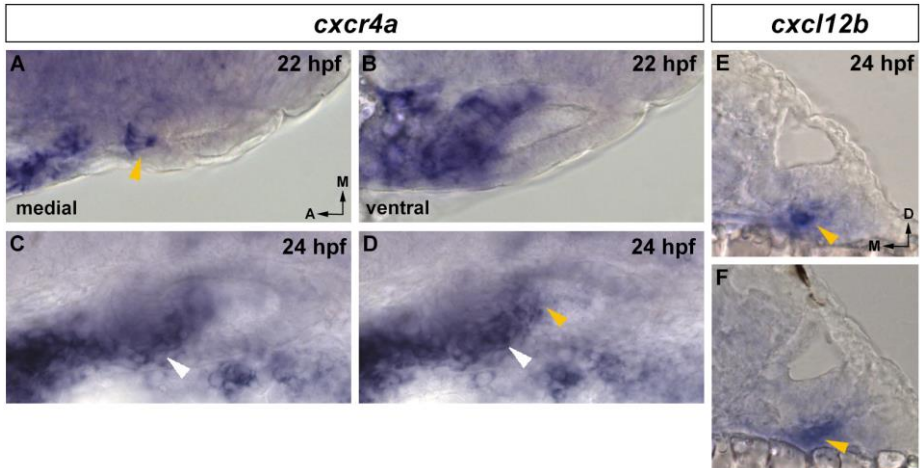


**Figure 41. Chemokine expression in the otic epithelium during neuroblast delamination.**

**(A-D)** Dorsal views of 22 hpf (A, B) and 24 hpf (C, D) embryos stained by in situ hybridization for *cxcr4a* in medial and ventral planes. **(E, F)** Transversal sections, medial to left, dorsal to top of 24 hpf embryos stained by in situ hybridization for *cxcl12b*. Orange and white arrowheads indicate chemokine expression.

In conclusion, here we have analyzed the dynamics of the delamination process, by which neuroblasts leave the otic epithelium and acquire migratory properties to coalesce into the SAG. We have identified bleb formation in pre-delaminating *neurog1* positive cells located at the anterolateral region of the otic vesicle. Bleb formation process is highly dynamic, they appear and retract at high speed, present high levels of free $Ca^{2+}$ and activation of myosin contraction occurs during its retraction. We also suggest a possible role of chemokine signaling in

mediating the exit of neuroblast from the epithelium and/or in guiding its migration through the SAG. Finally, we also show that cdh6 could also be involved in the neuroblasts de-epithelialization, thus following the same mechanisms as an EMT process.

# 3. DISCUSSION

112

# Chapter 1: Identification of the role of *her4* in inner ear development and its relationship with proneural genes and Notch signaling

During inner ear development the establishment and formation of the sensory and neurogenic domains is key for proper function of the organ. Therefore, a tight regulation and spatiotemporal control of the development of neurosensory elements is required. In the zebrafish inner ear *atoh1* is expressed in the sensory precursors that will generate HCs and *neurog1* expression appears few hours later in the first neuronal specified cells in the anterior domain and subsequently expands to more medial positions (Haddon et al., 1998a; Ma et al., 1998; Andermann et al., 2002; Millimaki et al., 2007; Radosevic et al., 2011, 2014). These proneural genes are initially expressed in equivalent groups of cells and through Notch-mediated lateral inhibition the initial pattern is refined and proneural gene expression is restricted to single cells that enter a differentiation pathway (Artavanis-Tsakonas and Simpson, 1991; Campuzano and Modolell, 1992; Jarman et al., 1993; Ma et al., 1996).

In Chapter 1, we have explored the role of *her4*, a zebrafish orthologue of mammalian *Hes5*, in inner ear development and its relationship with proneural genes and Notch signaling. We have shown that zebrafish *her4* is expressed in the neurogenic and sensory domains and requires *neurog1* and *atoh1b* for its expression, respectively. Moreover, *her4* in the neurogenic domain is dependent on Notch, while initial broad induction of *her4* in the presumptive sensory domain does not require Notch but *atoh1b*. However, later on Notch restricts *her4* expression to the future sensory maculae. Furthermore, we show that *her4* mediates lateral inhibition during neurogenesis, but not during sensorigenesis.

## Role and regulation of *her4* in the neurogenic domain

In the neurogenic domain *her4* and *neurog1* expressions are spatially correlated, with a temporal delay between *neurog1* induction and *her4*, suggesting an intermediate step. Moreover, *her4* expression was lost from the neurogenic domain in both Notch (*mib*^{-/-}) and *neurog1* mutants, suggesting a role of *her4* during neuronal fate selection. The fact that in the neurogenic domain *her4* expression depends on Notch, positions Notch as the intermediary pathway that activates *her4* downstream of *neurog1*. Moreover, depletion of *her4* leads to an increase in the population of neurons. This is similar to what was previously reported for *her4* role in primary neurogenesis (Takke et al., 1999). Moreover, this result is in accordance with the negative autoregulation of *Neurog1* through Notch-mediated lateral inhibition in mouse (Raft et al., 2007). Neither the loss of function of *her4* nor *Hes5* has already been analyzed directly in inner ear neurogenesis (all studies being focused on HC development (Zine et al., 2001)). The data demonstrate for the first time that in the inner ear, as in the CNS (Yeo et al., 2007), *her4* participates in Notch-mediated lateral inhibition to control the final number of neuronal cells.


## Role and regulation of *her4* in the sensory domain

In the sensory domain, *her4* is regulated differently. In the presumptive sensory territory *her4* expression is highly dynamic and identical to *atoh1b*. It initially encompasses a broad medial territory of the otic placode to progressively restrict to the future anterior and posterior maculae. Our initial hypothesis was that *her4* expression in the CMD would depend on Notch, and repress *atoh1b*. Therefore, since the expression pattern of *her4* is the same as the one of *atoh1b*, we expected that *her4* would be activated by Notch a little bit earlier (ISH times are not always extremely precise) than *atoh1b* and thus repress *atoh1b* expression in the CMD and segregate the prosensory domain in

114

two patches. However, initial *her4* expression requires *atoh1b* and Fgf signaling but not Notch, indicating that it cannot be assumed that *her4* is always regulated by Notch. Nonetheless, in an intermediate developmental period, Notch regulates *her4* expression in the CMD. However, it is a negative but not positive regulation. Our work thus shows that *her4* is not the downstream target of Notch to repress *atoh1b* expression in the CMD. *her6*, another member of her repressors, cannot perform this role since is not expressed in the CMD at 12.5-13 hpf (**Figure S1,** see Appendix 7.1). Thus, it still remains elusive how Notch represses *atoh1b* in the CMD to obtain two segregated the sensory patches.

Notch, in addition to *her4*, also down-regulates *atoh1b* in the CMD (Millimaki et al., 2007). Since initial *her4* expression depends on *atoh1b*, we propose that the effect of Notch on *her4* is most probably mediated by *atoh1b*. However, we cannot exclude that Notch inhibits *her4* directly in the CMD in parallel to *atoh1b*. At later stages, *her4* persists at the sensory maculae requiring Notch-activity. Interestingly, by 16 hpf, *her4* expression levels appear higher than *atoh1b*, suggesting that from this period onwards, *her4* expression can be maintained independently of *atoh1b*. This coincides with the period of *atoh1a* activation and probably also Notch pathway. Thus, we propose that by 16 hpf, *her4* regulation changes from a direct regulation by the proneural *atoh1b* to a regulation by *atoh1a* and Notch.

The complex spatiotemporal regulation of *her4* expression suggests multiple cis-regulatory regions controlling *her4* transcription. Yet no data exists on the regulatory regions of this locus. The promoter of mouse *Hes5* has been characterized (Takebayashi et al., 1995) and, in chick, labels cells responding to Notch and undergoing lateral inhibition during HC formation (Chrysostomou et al., 2012). Here we show evidences for a Notch independent regulation of *her4* in the sensory domain, not been

115

described yet in chick and mouse. This might be due to a lack of data at early developmental times or to a divergence in the regulatory mechanisms from anamniote to amniote animals.

The role of Notch in HC development has been widely studied. The best known role of Notch in HC development is in the process of lateral inhibition, in which cells activated by Notch activate target genes and suppress HC fate versus SC fate (Haddon et al., 1998b; Lanford et al., 1999; Kiernan et al., 2005a; Brooker et al., 2006; Takebayashi et al., 2007). In agreement with a putative role of *her4* downstream of Notch activity during sensorigenesis, we expected to observe an increase in the number of HC after *her4* knockdown. Indeed, this is what was shown for its mouse orthologue Hes5, in which null mutant mice for *Hes5* show supernumerary HC (Zine et al., 2001). However, we failed to observe increased numbers of *atoh1b* and *atoh1a* expressing cells. This is not due to inefficacy of *her4*-MO since it was tested in Tg(*her4*:EGFP)[y83] embryos and also it resulted in expansion of *deltaB* expression. One of the most plausible explanations is that, contrary to what happens in the neurogenic domain, other *her* genes compensate for *her4* loss in the sensory domain. *her6*, a *Hes1* orthologue, is expressed exclusively in the sensory domain already from 12.5 hpf (**Figure S1,** see Appendix 7.1) and could act redundantly with *her4*. The presence of *her6* in the sensory patches but not in neurogenic domain could explain why depletion of *her4* has a stronger effect in the latter. This is in agreement with data in mouse, where Hes and Hey genes cooperate in HC development and a graded increase in HC number was related to a reduction in Hes/Hey dosage, being the highest increase in compound mutants for *Hes1*, *Hes5* and *Hey1* (Tateya et al., 2011). Moreover, in zebrafish it has already been proposed that *her4* and *her6* work in concert to maintain the cyclic gene expression coordination among adjacent cells during paraxial mesoderm somitogenesis (Pasini et al.,

116

2004). Therefore, to explore the possibility that *her6* acts, in cooperation with *her4,* as a Notch effector during inner ear sensory development, we should knock down her6 activity through morpholino injection.

## Mutual regulation between sensory and neurogenic development

In chick, the transcription of *atoh1* lags by almost 2 days the expression of *neurog1* in the anteroventral domain of the otic placode (Alsina et al., 2004; Pujades et al., 2006). Therefore, the specification of otic neurons, as judged by the induction of *neurog1,* precedes HC specification. Moreover, genetic fate mapping indicated that the region of embryonic HCs was neurogenic at prior stages and that HCs from the sensory maculae of the utricle and saccule derive from the *neurog1*-positive domain in mice (Raft et al., 2007). In chick, a clonal relation between sensory neurons and utricular epithelial cells was also found (Satoh and Fekete, 2005). Together with a clonal relationship between neurons and HCs, mutual antagonism between *atoh1* and *neurog1* has been shown (Matei et al., 2005; Raft et al., 2007; Jahan et al., 2012). In *Neurog1*^{-/-} mouse embryos expansion of HCs in the future utricle was observed, conversely increased number of neuronal cells was detected in *Atoh1* mutants (Raft et al., 2007).

We show that zebrafish *atoh1b* and *atoh1a* are induced before *neurog1*. Whether this discrepancy has any functional relevance is still not known. Disruption of *neurog1* by MO injection caused an expansion of HCs from the posterior macula (Sapede et al., 2012). This was further confirmed in the present study, since *neurog1* mutants also display an increase on the expression of *her4* only in the posterior macula.

However, we also explored *neurog1* expression after blockade of *atoh1b*, as the first proneural gene defining the prosensory domain. Our

data suggests that loss of *atoh1b* proneural activity does not modify *neurog1* expression neither in the neurogenic domain nor in the sensory domain, suggesting that *neurog1* expression and the definition of the neurogenic domain is not influenced by *atoh1b* proneural gene. Moreover, since two *atoh1* genes are present in zebrafish, further work deleting both *atoh1b* and *atoh1a* genes should provide better insights into proneural cross-regulation between sensory and neurogenic fates.

## Chapter 2: Pioneer *neurog1* expressing cells ingress in the otic primordium and instruct neuronal specification

During inner ear development, cell fate specification and morphogenesis are coupled for the generation specific cell types at precise positions. Several groups, including ours, have performed rigorous studies on inner ear regionalization and patterning. However, these results are based in the analysis of the development of otic domains as static tissues restricted by regional gene expression and with little dynamical information. The second Chapter of this thesis focuses on the construction of the NgD by combining live-imaging, cell tracking and quantitative gene expression analysis and represents a step forward from the analysis performed in Chapter 1.

We have identified a new group of cells that act as pioneers of the otic neurogenic domain. These cells have two essential roles: they constitute the first specified cells of the domain and promote specification of resident cells of the vesicle, thus spreading the neural commitment (**Figure 36**). To our knowledge, this is the first example of neuronal progenitors instructing specification of other progenitors. In the mammal developing brain, neurons of the cortical plate migrate to invade the dorsal telencephalon and are able to control the timing of progenitor neurogenesis (Teissier et al., 2012).

Our analysis challenges the view that otic neuronal specification takes place in a static tissue. Indeed, our work shows that elaborate cell behaviors underlie development of the NgD, including intra-organ cell movements, delamination, cell divisions and importantly, cell ingression (**Figure 36**). We propose that the domain of the vesicle expressing

*neurog1* is maintained over time by a sustained turnover of cells added by local specification and proliferation, and leaving the domain by delamination.

Ingression of progenitors to the otic placode could also be relevant for sequential stages of their own differentiation, in a similar way that migration is important for maturation of either immature neurons in the mouse cortex (Ayala et al., 2007), or progenitors of the *Drosophila* optic lobe (Apitz and Salecker, 2015).

Our data indicate that the SAG integrates neuronal cells from at least two different origins: the ingressing cells and the ones specified locally. Different neuronal populations have been already identified in the SAG, including vestibular and auditory neurons (Torres and Giraldez, 1998; Bell et al., 2008). Whether the different populations of progenitor giving rise to the NgD will differentiate into different functionally subgroups of neurons inside the ganglion still needs to be addressed.

## Pioneer cells and positional information

The otic neurogenic domain emerges in a defined ventroanterolateral position due to the dialogue of several signaling pathways that regionalize the otic placode (Fekete and Wu, 2002; Abelló and Alsina, 2007; Maier et al., 2014; Raft and Groves, 2014). In light of this, within the otic placode the fate of each cell would be dictated by its position in the tissue (Brigande et al., 2000a; Bok et al., 2005, 2007; Whitfield and Hammond, 2007) upon the influence of the extrinsic signals. However, we observe that ingressing cells are specified in movement and prior to their incorporation to the anterolateral domain of the otic epithelium. Moreover, when ingressing cells are laser ablated, the cells in the otic vesicle located in the position of the ingressed cells (i.e. receiving the same putative diffusing morphogens) do not seem to adopt a neurogenic fate. This suggests that secreted factors establish a region

120

competent for neurogenic specification, to which the ingressing cells (and probably other mechanisms) provide instructive signals to induce *neurog1* expression. In agreement with this possibility, Tbx1, the main transcription factor involved in otic neurogenic regionalization, is a repressor of *neurog1* expression. Tbx1 is excluded from the anterior part of the vesicle, making the region competent to be induced by neurogenic signals (Raft et al., 2004; Bok et al., 2011; Radosevic et al., 2011). Thus, in addition to the reported role of cell movements on the spatial delimitation of different domains of the neural tube (Xiong et al., 2013; Kicheva et al., 2014), we propose that coordination between cell movement and cell communication contributes to the neuronal pattern of the otic vesicle.

## Signals for ingression and instruction

In embryos mutant for FGF3, FGF8 and FGF10, and embryos in which FGF signaling has been temporally blocked, distinct phases of otic neural development are impaired (Pirvola et al., 2000; Léger and Brand, 2002; Alvarez et al., 2003; Wright and Mansour, 2003b; Alsina et al., 2004; Zelarayan et al., 2007; Vemaraju et al., 2012). Our work indicates that FGF signaling regulates the ingression of the pioneer cells into the neurogenic domain, suggesting that some of the previously reported effects on *neurog1* expression could be due to this novel role. The FGF signaling is known to control cell behavior in other organs, such as the epithelialization and cell migration during kidney tubulogenesis and lateral line development (Aman and Piotrowski, 2008; Atsuta and Takahashi, 2015). Thus, FGF signaling in the otic placode could either delay the anterior folding of the otic placode (**Figure S3**) or stimulate cell migration, allowing cell ingression.

A central question that emerges from our analysis is how ingressing cells regulate *neurog1* expression in their NgD neighbors. The Notch

pathway could participate in this process. However, since Notch activation reduces by lateral inhibition the number of specified neuronal cells (Haddon et al., 1998a; Abelló et al., 2007) and ingression enhances it, the instructive signal should inhibit Notch activity. A putative signal provided by the ingressing cells could be an FGF. The expression pattern of FGF10a suggests that is expressed in the pioneer cells (McCarroll and Nechiporuk, 2013). This would imply the secretion of a molecule from a mobile source (instead of a fixed location described for morphogens).

## Divisions in the neurogenic domain are symmetric and apical

Our 4D analysis allowed us to address for first time the mode of division in the otic NgD. We found that in all cases (divisions from *neurog1*⁻ or *neurog1*⁺ cells) both daughter cells acquire a neuronal fate. During the time frame analyzed, no divisions were found where one daughter cell remained as a *neurog1*⁻ progenitor while the other activates the proneural expression, as has been described in the neural tube (Wilcock et al., 2007; Das and Storey, 2012; Taverna et al., 2014). However, we cannot discard, that asymmetric division occur at later times or at very low frequency.

Studies on fixed chick otic vesicles described the presence of mitosis in the basal side of the epithelium in addition to the luminal ones (Alvarez et al., 1989). Such mitoses were termed "basal divisions" similar to the ones taking place in the retina in which mitotic cells are no longer polarized apically and in contact to the ventricular membrane (Weber et al., 2014). In our study, we also observed non-luminal mitoses, but they remain in contact with a Pard3 scaffold keeping their apical polarity.

## Morphogenesis of the neurogenic domain

Our analysis uncovered how the composition of the domain is regulated by cell ingression, not only by adding previously specified cells, but also by promoting local *neurog1* expression. On the contrary, the size of the specified region does not seem to be regulated by cell ingression, as occurs when delamination is inhibited by the absence of NeuroD (a regional specification-dependent exit of progenitors), leading to an accumulation of cells in the region (Liu et al., 2000). Similarly, the size of neural tube domains is influenced by regional differentiation-dependent exit of progenitors (Kicheva et al., 2014).

We show that proliferation controls the number of specified cells within the domain and its size, that is reduced in proportion with the size of the whole otic vesicle. Therefore, the reduction of the protuberance observed after FGF signaling blockage suggests that it could be an FGF-dependent morphogenetic event. Moreover, in zebrafish otic vesicle, it has already been described that later in development FGF could regulate the balance between specification and neuronal maturation and maintenance of an appropriate number of mature neurons (Vemaraju et al., 2012).

## Spatiotemporal dynamics of proneural expression

Neural specification usually occurs in epithelialized tissues. However, we observed activation of *neurog1* expression in the pioneer cells before epithelialization, suggesting that stable cell-cell contacts would be dispensable to initiate proneural expression. Similarly, in mouse *neurog2* is expressed in migrating sensory neuron precursors (Marmigère and Ernfors, 2007), although its expression begins before exiting the epithelium and migration (Zirlinger et al., 2002).

We were able to visualize for first time the transit of an otic neuronal progenitor from *neurog1* expression to delamination. Analysis of *neurog1* expression levels suggests that delamination occurs once a given threshold of proneural expression is reached; probably associated to *neurod* induction.

The otic placode and other cranial placodes originate from a large common pre-placodal region (PPR) adjacent to the neural plate (Bailey and Streit, 2006). Precursors from the PPR segregate and coalesce into individual cranial placodes that progressively acquire specific identities (Streit, 2002; Bhat and Riley, 2011; McCarroll et al., 2012; Breau and Schneider-Maunoury, 2014; Saint-Jeannet and Moody, 2014). Our data revealed that otic *neurog1* is expressed before of what it was conceived by ISH analysis and outside the placode by a group of cells that ingress during morphogenesis. This suggests that neural specification might precede the acquisition of a defined placodal identity. Thus, we propose that some PPR precursors might already be neural committed and that their subsequent allocation into the placodes (by random or directed movements) provides them one or another placodal identity. Further work in this direction might shed light into this hypothesis.

In conclusion, our study indicates that cell movements underlie an instruction essential for otic neuronal specification, a crucial step in neurogenesis. Unravelling the complex mechanisms that determine the number of neurons incorporated in a forming ganglion could help to understand anomalies associated, as auditory neuropathies.

# Chapter 3: Cellular and molecular mechanisms of delamination

In this Chapter we provide a preliminary analysis of the delamination process of otic neuroblasts at cellular and molecular levels.

## Bleb formation during neuroblast delamination

Several studies have focused on the dynamics and mechanisms of bleb formation, but these were done either in culture cells, *in vivo*-individual migrating cells or in 3D matrices, and none were done in a whole 3D epithelium from an organ structure (Cunningham, 1995; Charras et al., 2005, 2008; Even-Ram and Yamada, 2005; Tournaviti et al., 2007; Ruprecht et al., 2015). Here we show *in vivo* neuroblasts delamination from the otic vesicle. Cells in the otic epithelium are highly compacted and present rounded morphology bleb protrusions at their basal side during delamination. We see that during blebbing, the membrane detaches from the cortex and expands. After expansion, the cortex myosin reassembles under the membrane and leads to bleb retraction. Therefore, during otic neuroblast delamination, actomysosin contractility is generated to retract the bleb as seen in other systems (Cunningham, 1995; Charras et al., 2006; Sheetz et al., 2006). Moreover, blebs could represent an efficient mean to explore extracellular environment or break the basal lamina, being a possible mechanism for cell delamination.

Mechanisms operating at the apical side of a blebbing cell during its delamination are still elusive. We could only detect a possible constriction and elongation of the apical side. In chick and mouse neural tube, mechanism for de-epithelialization and lose of apical contact in neuronal precursors have been described (Borrell et al., 2012; Rousso

et al., 2012; Das and Storey, 2014). Some of these mechanisms are based either in the apical detachment through the repression of the expression of a key component of adherens junctions (Rousso et al., 2012) or in the abscission of the apical endfoot from the apical belt of adherens junctions (Das and Storey, 2014). These processes are regulated by proneural genes expressed in the differentiating neurogenic cells and, similar to an EMT, involve the downregulation of cadherins and other factors which allows the migration of cells basally and its delamination from the ventricular surface. In this way, cells lose their apical polarity and ciliary proteins, which contributes to their subsequent cell cycle exit and differentiation (Alexandre et al., 2010; Rousso et al., 2012; Das and Storey, 2014). Moreover, in zebrafish retina it has been shown that inhibition of N-cadherin mediated adhesion is required to promote apical process detachment (Wong et al., 2012). Cells in the otic epithelium are densely packed and it is difficult to see what happens at the single-cell level. Thus, similarly to some of these studies, we should analyze specifically whether apical determinants and membrane integrity are affected during delamination performing mosaic stainings.

## Hallmarks of EMT are present during neuroblasts delamination

During NCC migration from the neural tube, it is suggested that the regulation of the expression of cadherins is essential for their dispersion (Thiery et al., 1982; Akitaya and Bronner-Fraser, 1992; Nakagawa and Takeichi, 1998). Here we have analyzed the expression of *cdh6* during otic neuroblasts delamination and we suggest that its function could be associated with the exit of neuroblasts from the epithelium. However, the role of cdh6 in cell delamination is unclear, since it has been suggested to either suppress EMT by cell adhesion or promote it by

126

mediating pro-EMT signals. For example, in chick neural tube, Cdh6B is transiently expressed at the premigratory phase and its downregulation leads to premature NCCs migration (Coles et al., 2007). On the contrary, in zebrafish hindbrain, premigratory NCCs lose N-Cadherin and upregulate cdh6 prior to EMT which promotes apical detachment (Clay and Halloran, 2014). Therefore, it is not clear whether cdh6 expression that we observe in the pre-delaminating cells of the otic epithelium is necessary for delamination, or whether it is being downregulated in order to allow cellular exit. In mouse otic epithelium, it has been suggested that the expression of classical cadherins is increased in migrating neuroblasts compared with the otic epithelium. Moreover, neuroblasts retained the ability to segregate from the epithelium but remained compacted immediately adjacent to the originating tissue, suggesting an important role of cell-cell interactions (Davies, 2011). It is worth mentioning that Cdh6 has also been suggested to determine where subcellular forces of actomyosin are generated during EMT. Cdh6 is enriched in apical regions promoting apical NCCs detachment and it is required for apical F-actin accumulation. However, it is suggested that Cdh6 does not regulate blebbing (Clay and Halloran, 2014).

It is also known that cells need to break the basal lamina to successfully delaminate (Cheung et al., 2005). Actually, this is what we see during neuroblast delamination. Moreover, the break in the basal lamina seems to coincide with the region of delamination. This breakage, could be mediated by other factors such as Snail which is known contribute to basal lamina degradation by activating metalloproteases and by repressing laminin expression (Jordà et al., 2005; Haraguchi et al., 2008). Moreover, Snail factors have already been described to be expressed in the otic epithelium (Thisse et al., 1995; Léger and Brand, 2002; Zecca et al., 2015).

## Mechanisms of cell motility

After delamination, cells acquire migratory properties in order to migrate to the SAG. It was suggested that zebrafish PGCs exclusively use blebs during migration and that the chemokine SDF-1 ligand promotes bleb like protrusions through the local increase of intracellular calcium and subsequent actomyosin contractions at the cellular leading edge (Blaser et al., 2006). This is in concordance with our results showing *cxcl12b* and *cxcr4a* expression during otic neuroblast delamination. Interestingly, in zebrafish, these genes have been duplicated in the course of the whole-genome duplication giving rise to the two paralogs of the ligand, cxcl12a and cxcl12b and two paralogs of the receptor, cxcr4a and cxcr4b. They were identified to be essential for PGCs and lateral line migration (David et al., 2002; Doitsidou et al., 2002; Knaut et al., 2003). In zebrafish cxcl12a-cxcr4b and cxcl12b-cxcr4a interactions have been shown. Moreover, the PGCs that express cxcr4b and therefore being exposed to both ligands, ignore the ligand cxcl12b and only cxcl12a guides the cells towards their target (Boldajipour et al., 2011). Also, in the zebrafish posterior lateral line primordium collective cell migration is guided through cxcl12a ligand depending on cxcr4b receptor (Dalle Nogare et al., 2014). Here, we present expression data on the pair cxcr4a-cxcl12b but we should investigate in more detail the expression patterns of the other pair, cxcl12a-cxcr4b.

Finally, it is worth noting that there are different modes of EMT processes. In contrast to the complete EMT in which all epithelial cells undergo the process simultaneously causing a complete dislocation of the epithelial structure and formation of a single mesenchyme, otic neuroblasts seem to undergo a mechanism similar to a partial and progressive EMT process. A small number of epithelial cells undergo EMT individually and separately over time such that the epithelial structure is maintained intact during the whole process (Duband, 2010).

## General overview and future directions

The developmental patterning mechanisms that underlie the formation of the otic sensory and neurogenic domains are complex and highly coordinated. Although a great number of studies describe the signals and transcription factors involved in cell fate decisions and neurosensory identity, morphogenetic movements should be explored in-depth. High resolution microscopy techniques allowed us to visualize in ever-greater detail at single-cell level otic neurogenic specification and the formation of the NgD through visualization of *neurog1* expression dynamics *in vivo*. The creation of the NgD, required for cells to acquire neuronal identity, occurs concomitantly with a regional morphogenetic process. Therefore, further steps into that issue, and developing specific markers for otic morphogenesis and patterning, would allow us to fully integrate cell specification with cell behaviors dictating otic morphogenesis at different developmental stages. The generation of zebrafish transgenic lines reporting the activity of patterning signaling pathways such as FGF coupled with proneural gene expression could help to determine the effect of morphogenesis on cell specification. Moreover, new microscopy techniques such as light sheet imaging would allow us to analyze global cell dynamics in the inner ear allowing the imaging of large fields of cells, at high speed, and for long time periods. Therefore, we could analyze how the NgD evolves and its morphogenetic characteristics al late developmental stages.

Understanding the relationships between the structural variations and cellular adaptations in tissue growth and development regulated by gene expression during inner ear morphogenesis could be relevant for the generation of inner ear sensory epithelia in 3D cultures. To date, *in vitro* generation of whole inner ear organoids from embryonic stem-cells has been achieved (Koehler and Hashino, 2014; Liu et al., 2016). These

organoids are composed by inner ear sensory epithelia containing HCs displaying some functional properties of native vestibular HCs, and being innervated by sensory-like neurons. However, some of the morphological transitions that take place during *in vivo* inner ear development are difficult to achieve. Therefore, unveiling the mechanisms regulating the dynamic variations in the cellular differentiation process and the structural specializations will represent a breakthrough in the developmental biology field.

We have also shown that the delamination process seems to molecularly fit in a developmental EMT. At cellular level, high spatio-temporal resolution live imaging provides important detailed snapshots of the delamination process visualizing protein localization during bleb formation, and provides us with better insights into how cells coordinate membrane protrusions at their leading edge. On the other hand, the mechanics of cellular exit from the epithelium and relevance of the loss of the apical contact for EMT are still elusive. Therefore, we should analyze cell behaviors during delamination at single-cell level performing mosaic staining of cell membrane and apical determinants. Taking into account that the EMT process is also used by cancer cells to disseminate and colonize distant parts of the organism, and cell migration is central to many chronic human diseases, including cancer, cardiovascular disease and chronic inflammation, new insights into the crucial molecules and cellular processes required for cell protrusion and migration during development will be important in designing therapies to counter these diseases.

Finally, coupling the great advances in the generation of new microscopy techniques and the great visualization allowed by the zebrafish inner ear, we can achieve a high real time resolution of the dynamics of cell rearrangements, cell adhesion contacts and cell

migration, reinforcing the significant advantages of the inner ear as a model for the future goals of developmental biology.

132

# 4. CONCLUSIONS

## Chapter 1

1. *her4* is expressed in both the sensory and neurogenic domains, with a dynamic expression pattern spatiotemporally correlated with the expression of proneural genes *atoh1b* and *neurog1*.

2. In the sensory domain, *her4* regulation undergoes a switch from an initial induction independent of Notch activity to a later Notch-dependent maintenance in the future sensory maculae.

3. Initial broad induction of *her4* in the sensory domain requires *atoh1b* and Fgf signaling, while in the neurogenic domain *her4* expression is dependent on Notch signaling downstream of *neurog1*.

4. *her4* does not act as the downstream target of Notch to repress *atoh1b* expression in the CMD.

5. Depletion of *atoh1b* does not affect neither *her4* nor *neurog1* expression in the neurogenic domain.

6. neurog1, in addition to regulate *her4* expression in the neurogenic domain, seems to influence the development of the posterior macula.

7. her4 has no effect on the expression of HC specification markers *atoh1b* and *atoh1a*. However, through Notch-mediated later inhibition, *her4* regulates neuronal specification.

# Chapter 2

1. During neuronal specification stages the NgD has an asymmetric morphology presenting particular features; a protuberance at the anterolateral region, high number of cells, high cell density and an increased proliferation rate compared with other domains of the otic vesicle.

2. A group of pioneer cells specified anterior to the otic primordium, migrate and ingress into the epithelializing otic placode, contributing to the NgD.

3. Ingressed cells instruct local cell specification within the NgD non cell-autonomously.

4. *neurog1* positive cells are also added to the NgD through local specification and cell division.

5. All divisions in the NgD are symmetric and apical, and there is no preferential order between *neurog1* activation and cell division.

6. FGF controls the size of the NgD by increasing the number of cells, and also its morphology through a FGF specific morphogenetic event uncoupled of proliferation.

7. *neurog1* expression levels require FGF signaling which promotes pioneer cell ingression, but are independent of cell proliferation.

8. Cells delaminate relative to *neurog1* expression levels and not to the time elapsed from the beginning of *neurog1* expression.

## Chapter 3

1. Otic delamination seems to molecularly fit into a typical developmental EMT.

2. *cdh6* is expressed in epithelial pre-delaminating cells and in the SAG.

3. The basal lamina is disrupted at the region of delamination.

4. Pre-delaminating epithelial cells display blebs at their basal side.

5. Blebs are formed during delamination and present local myosin light chain recruitment and $Ca^{2+}$ accumulation.

6. Expression of the chemokine receptor cxcr4a is present in delaminating neuroblasts and the ligand cxcl12b in adjacent tissues.

138

# 5. MATERIALS AND METHODS

## Zebrafish strains and maintenance

All the experiments performed for this thesis were done using zebrafish embryos and larvae obtained by pair mating of adult fish in the PRBB zebrafish facility by standard methods. The zebrafish protocols followed the guidelines and were approved by the IACUC, Comité Ético de Experimentación Animal-Parc de Recerca Biomèdica de Barcelona (CEEA-PRBB). Strains were maintained individually as inbred lines. In addition to wild-type (AB), the following zebrafish mutant and transgenic lines of either sex were used:

**mib**[ta52b] is a mutant line presenting a point mutation that results in aminoacid substitution eliminating the catalytic activity of the Notch E3 ubiquitin ligase necessary for Delta endocytosis (Itoh et al., 2003).

**neurog1**[hi1059] is a *neurog1* mutant line obtained by retroviral insertional mutagenesis (Golling et al., 2002).

**Tg(*her4*:EGFP)**[y83] is a stable reporter line where a 3.4 kb 5'-flanking region of *her4* DNA containing 22 bp of 5' UTR sequence is controlling EGFP expression (Yeo et al., 2007).

**TgBAC(*neurog1*:*DsRedE*)**[nl6] is a BAC reporter line that expresses the fluorescent protein DsRed-Express upon activation of the *neurog1* promoter (Drerup and Nechiporuk, 2013).

**Tg(*neurod:eGFP*)** is a BAC reporter line that contains 67 kb of sequence upstream and 89 kb downstream of *neurod* and an enhanced GFP gene positioned at an endogenous start site (Obholzer et al., 2008).

**Tg(*actb1:Lifeact-GFP*)** is a transgenic line expressing Lifeact-GFP (Behrndt et al., 2012).

**Tg(β-actin:myl12.1-eGFP)** is a transgenic line expressing Myosin light-chain GFP (Behrndt et al., 2012).

**Tg(*Xla.Eef1a1:H2B-Venus*)** is a transgenic line to track nuclei (Recher et al., 2013).

Homozygous mutant *mib*<sup>ta52b</sup> and *neurog1*<sup>hi1059</sup> embryos were obtained by pairwise mating of heterozygous adult carriers and descendant embryos were genotyped after *in situ* hybridization.

Embryos were developed in an incubator at 28.5ºC in system water containing methylene blue and staged after counting somite number. Embryonic stages are given as hours post-fertilization (hpf) at 28.5ºC (Kimmel et al., 1995).

## Whole mount in situ hybridization

Antisense RNA probe synthesis was done by *in vitro* transcription of linearized DNA vectors or PCR amplification products. In the first case, vectors carried the sequence of interest, flanked by T3, T7 or SP6 polymerases sequence. The following probes were used: *atoh1b* and *atoh1a* (Millimaki et al., 2007), *neurog1* (Itoh and Chitnis, 2001), *her4* (Gajewski et al., 2006), *deltaB* (Haddon et al., 1998b), *cdh6* (Liu et al., 2006), *cxcr4a* and *cxcl12b* (Cha et al., 2012).

<u>DNA linearization and purification</u>

1 µg of plasmid DNA was incubated at 37ºC with the specific restriction enzyme (**Table 1**) in the final volume of 20 µl. After 2h, the enzymatic reaction was stopped by adding 1 µl of proteinase K (10 mg/ml) and 1 µl of SDS 10%, and incubating the reaction at 37ºC 30 min. Then, the linearized plasmid was purified adding 80 µl of H2O, 11 µl of 3M Na Acetate, 278 µl of 100% ethanol, incubating at -20ºC for 1h and, finally, centrifuging 30 min at 13000 rpm at 4ºC. The pellet was next washed with 500 µl of 70% ethanol and centrifuged 10 min at 13000 at 4ºC. Once dry, the linearized plasmid was resuspended in 20 µl of $H_2O$.

The restriction enzymes and polymerases used to synthesize each probes are listed below:

| Probe | Restriction enzyme/RNA polymerase |
|---|---|
| *atoh1a* | HindIII /T7 |
| *atoh1b* | BamHI/T7 |
| *her4* | XhoI/T3 |
| *neurog1* | XhoI/T7 |
| *deltaB* | EcoRI/T7 |
| *cdh6* | BamHI/T7 |
| *cxcr4a* | NotI/Sp6 |
| *cxcl12b* | NcoI/Sp6 |

**Table 1.** Restriction enzymes and RNA polymerases used for the generation of riboprobes for *in situ* hybridization.

On the other hand, *her6* probe was generated by PCR amplification from 48 hpf embryos cDNA, adding T7 polymerase binding side at 5' of the reverse primer and following RNA transcription.

cDNA library generation specific PCR amplification

Total RNA isolation was done using Trizol (Invitrogen) extraction protocol. Reverse transcription of obtained RNA was performed using SuperScript III Reverse Trascriptase Kit from Invitrogen. To selectively amplify *her6* gene the Expand High Fidelity PLUS PCR system (Roche) and the following primers were used:

her6-FW: 5'- AACACAGATCCCACCGTTCT-3'

her6-RV-T7: 5'-TTGTAATACGACTCACTATAGGCAAACGGAGTCTG ACGTGAC-3'

Once prepared the mix as described in the manufacturer datasheet, the following cycler program was used:

| 94ºC | 2 min | |
|------|-------|-----|
| 94ºC | 30 sec | |
| 55ºC | 30 sec | 30x |
| 68ºC | 3 min | |
| 68ºC | 7 min | |
| 4ºC | hold | |

In order to verify the PCR product, 1 µl of the reaction was run on 1% agarose gel/1xTBE.

RNA probe transcription

For the generation of antisense probes, linearized DNA or PCR products were incubated 37ºC with the specific RNA polymerase (**Table 1**) and digoxigenin-labeled nucleotides (DIG RNA labeling mix (Roche)) in a final volume of 20 µl. After 2h, riboprobes were purified adding 30 µl of $H_2O$, 300 µl of cold 100% ethanol, 10 µl of 4M LiCl, incubating the reaction 30 min at -20ºC and centrifuging for 30 min at 13000 rpm at 4ºC. The pellet was then washed with 500 µl of cold 70% ethanol and centrifuged 10 min at 13000 rpm at 4ºC. Once dry, the RNA probes were resuspended in 20 µl of $H_2O$ and 1µl was run in a 1% agarose gel/1xTBE to verify the transcription.

Whole-mount *in situ* hybridization (ISH) in zebrafish larvae

Embryos were isolated at desired developmental stages as described by (Kimmel et al., 1995). Dechorionated zebrafish embryos were fixed in 4% paraformaldehyde (PFA) overnight at 4ºC and dehydrated in methanol series, rehydrated again and permeabilized with 10 mg/ml proteinase K (Sigma) at RT for 5-10 min depending on their stage. DIG-labeled probes were hybridized overnight at 70ºC, detected using anti-DIG-AP antibody at 1:2000 dilution (Roche) and developed with

NBT/BCIP (Roche) according to (Thisse et al., 2004). After *in situ* hybridization, larvae were post-fixed overnight in 4% PFA and used for imaging either mounted in 100% glycerol or in sections. In the second case, larvae were incubated 1h in 15% sucrose (in PBS) then in 7.5% gelatin/15% sucrose and placed in a cryomold in the desired orientation. Blocks were frozen in 2-Methylbutane (Sigma-Aldrich) for tissue preservation and cryosectioned at 20 µm on a Leica CM 1510-1 cryostat. Sections were collected on Superfrost slides and mounted with mowiol.

## ISH image acquisition

Pictures were acquired in a Leica DRM microscope or in Leica MZFLIII stereomicroscope using a Leica DFC300 FX camera and the Leica IM50 software. Adobe Photoshop 7.0.1 software was used for photograph editing.

## Antisense morpholinos (MO)

MOs were obtained from Gene Tools. Embryos were injected at 1-cell stage. The *her4*-MO (So et al., 2009) was designed to block the translation of *her4* mRNA transcript with sequence: 5'-ATT GCT GTG TGT CTT GTG TTC AGT T-3'. *her4*-MO was injected at concentration 0.025 mM and its efficiency was assessed by the specific loss of GFP signal from the Tg(*her4*:EGFP)[y83] transgenic line (Yeo et al., 2007). The *atoh1b*-MO (Millimaki et al., 2007) was injected at concentration 5 µg/µl and its sequence is 5'-TCA TTG CTT GTG TAG AAA TGC ATA T-3'.

## mRNA Microinjection

To label cellular and subcellular structures, mRNA encoding for the following fusion proteins were injected at 1-cell stage after being synthesized with the SP6 mMessenger mMachine kit (Ambion): H2B-mCherry or H2B-GFP (100-150 pg) (Olivier et al., 2010), NLS-Eos (100-150 pg) (Sapede et al., 2012), Pard3-GFP (50-75 pg) (Buckley et al.,

145

2013), Lyn-EGFP (membrane-GFP (100-150 pg)) (Köster and Fraser, 2001), membrane-mCherry (100-150 pg) (Megason, 2009) and GCaMP3.1 (50-75 pg) (Sieger et al., 2012).

## Drug treatments

For the *her4* regulation experiment, dechorionated zebrafish embryos were incubated with 50 µM SU5402 (Merk Millipore 572630). Incubations were done at 28.5ºC, starting at 10 hpf until the sacrification of the animals at 16 hpf.

For the morphogenesis and specification analysis, dechorionated embryos were treated with SU5402 25 µM (Merk Millipore 572630) or aphidicolin 300 µM (Merck Millipore) in combination with hydroxyurea 100 mM (Sigma) added to the embryo medium.

For control treatments, embryos were incubated in an equivalent concentration of dimethyl sulfoxide (DMSO, Sigma).

## Live imaging and image processing

Live embryos were embedded in low melting point agarose at 1% in embryo medium including tricaine (150mg l$^{-1}$) for dorsal confocal imaging using a 20x (0.8 NA) glycerol-immersion lens. Imaging was done using a SP5 Leica confocal microscope in a chamber heated at 28.5°C. z-stacks 20 to 80 $\mu$m thick spanning a portion or the entire otic vesicle (a z-plane imaged every 0.5-2 $\mu$m) were taken every 1 to 3 minutes for 2-12 hours. For myosin and Ca$^{2+}$ imaging images were taken every 2 to 4 seconds. Raw data were processed, analyzed and quantified with FIJI software (Schindelin et al., 2012). For visualization purposes, the images were despeckled. For quantifications of *neurog1* expression, images were not modified. Movies were assembled selecting a plane from every z-stack at every time point to better visualize the phenotype (or track a cell) or shown as 3D reconstructions. A representative movie from at least three different embryos is shown.

Images in figures are either shown as confocal coronal sections, 3D reconstructions or average z-projections of z-stacks. To track the trajectory of individual cells, 3D movies were analyzed using the MtrackJ, Manual tracking plugins of ImageJ (Meijering et al., 2012), and temporal color code applied to generate a single image of the tracks.

## Morphometric and proliferation analysis

To perform quantifications in different regions of the otic vesicle, we live imaged a z-stack and built a rectangular cuboid defined by external vertices of the organ. The cuboid was divided in 8 equally sized regions, and quantifications were performed inside each region. Before quantification the z-stacks were aligned in 3D to correct for variability in orientations during mounting, in order to guarantee the coronal sectioning of the vesicle. For volume calculation the x-y area of the tissue in each plane of the z-stack was measured and then multiplied by the z spacing every plane (the volume of the lumen was subtracted). The number of cells in each region was determined manually by counting H2B-mCherry stained nuclei on z-stacks, using the Cell counter plugging of ImageJ (Kurt De Vos, University of Sheffield). 3D visualization of Lyn-GFP plasma membrane staining helped the identification of each single cell. To quantify the number of cell divisions in the otic epithelium in a period of time, high temporal resolution videos (1 min frequency) in 3D of H2B-GFP stained nuclei were analyzed manually to detect every chromosome segregation event. The number of divisions in each region of the vesicle was determined building a cuboid as described above for each time point. Proliferation levels in fixed tissue were analyzed by pH3 immunostaining as describe below.

## Two photon laser ablation

To ablate a group of cells, a two-photon laser beam from a Leica SP5 microscope was applied over one side of the embryos mounted in agarose (the contralateral side was maintained intact as a control). The cells to ablate were identified by single photon confocal imaging recognizing the DsRedE fluorescence in cells anterior to the otic vesicle. Right after ablation, imaging of the vesicle was performed to confirm the damage caused (dead cells were clearly visualized). 2-3 cells died on each ablation pulse. Several sequential pulses at different location were applied to kill an increased number of cells. No damage outside the ablated region was observed. Ablated embryos were maintained mounted at 28ºC until the moment in which specification analysis was performed (see below).

## Photoconversion experiments

To detect ingression of cells into the placode, photoconversion of NLS-Eos expressing nuclei was performed with UV light ($\lambda$ = 405 nm, using a 20x objective in a Leica SP5 system) on 13 hpf mounted embryos. A 3D ROI of cells about 25 $\mu$m apart from the anterior limit of the epithelializing placode was photoconverted. Photoconversion was checked by confocal imaging right after UV illumination. The embryos were then removed from the agarose and incubated in embryo medium until 20 hpf to check for cell ingression by 3D imaging. When blockade of FGFR was performed, embryos were dechorionated at 11 hpf, incubated with SU5402 or DMSO in embryo medium until 13 hpf, mounted in agarose including SU5402 or DMSO, photoconverted, imaged, unmounted, and incubated in presence of the drugs in solution until 19 hpf to check for cell ingression by 3D imaging. In some cases, the TgBAC(*neurog1*:*DsRedE*)[nl6] line was used.

## Specification analysis

To analyze specification phenotypes z-stacks were acquired with fixed settings (laser power and detector gain) between different experimental groups (or vesicles in the case of ablations). The settings were adjusted to detect a range of increased or decreased fluorescence levels without saturation or lack of signal. DsRedE fluorescence was quantified in single planes using imageJ. A small region of a few pixels was created and a mean fluorescence level in each cell ($F_{cell}$) was calculated by averaging 3 quantifications in different x, y and z positions of the cytosol (the background was deducted from each measurement). To consider a cell positive for DsRedE expression, a threshold was defined empirically for each set of experiments, as the minimum level at which DsRedE expression in different z planes was unambiguously detected (to avoid mistakes produced by fluorescence coming from cells located at other z positions). We then calculated the mean $F_{cell}$ in each vesicle ($\bar{F}_{cell}$), the number of *neurog1*^{+} positive cells, and the GLE as the sum of the $F_{cell}$ for all the *neurog1*^{+} cells in a vesicle. *neurog1*[+Hi] cells were defined as the ones that have fluorescent level higher than 1.5x $\bar{F}_{cell}$ of the control (DMSO or non-ablated side) vesicles. Dynamic quantifications were performed by sequentially measuring fluorescence at consecutive times of a video in the same cell. The mean rate of increase in fluorescence was calculated as $\frac{\Delta F}{\Delta t}$. The same single cell fluorescence quantifications were performed in the neuroepithelial cells of the hindbrain, in a region adjacent to the otic vesicle.

## Laminin and pH3 immunostaining

Dechorionated zebrafish embryos were fixed in 4% PFA overnight at 4ºC and immunostaining was performed either in whole-mount or in cryostat sections. Embryos for sections were cryoprotected in 15% sucrose and embedded in 7.5% gelatine/15% sucrose. Blocks were frozen in 2-Methylbutane (Sigma) for tissue preservation and

cryosectioned at 14 $\mu$m on a Leica CM 1950 cryostat. After washing in 0.1% PBT, and blocking in 0.1% PBT, 2% Bovine Serum Albumin (BSA), and 10% normal goat serum (NGS) for 1h at RT, embryos were incubated overnight at 4ºC in blocking solution with the appropriate primary antibody: rabbit anti-Laminin (Sigma, 1:200) and rabbit anti-pH3 (Merck Millipore 06-570; 1:500). After extensive washing in 0.1% PBT, donkey anti-rabbit Alexa-488 (Thermo fisher scientific A21206; 1:400) and goat anti-rabbit Alexa-594 (Thermo fisher scientific A11037; 1:400) were incubated overnight at 4°C in blocking solution. Sections were counterstained with 1 $\mu$g/ml DAPI, mounted in Mowiol (Sigma-Aldrich) and imaged in a Leica SP5 confocal microscope.

## Statistics

All statistical comparisons are indicated in figure legends; including one sample and unpaired t-test performed using GraphPad.

# 6. BIBLIOGRAPHY

Abelló G, Alsina B (2007) Establishment of a proneural field in the inner ear. Int J Dev Biol 51:483–493.

Abelló G, Khatri S, Giráldez F, Alsina B (2007) Early regionalization of the otic placode and its regulation by the Notch signaling pathway. Mech Dev 124:631–645.

Abelló G, Khatri S, Radosevic M, Scotting PJ, Giráldez F, Alsina B (2010) Independent regulation of Sox3 and Lmx1b by FGF and BMP signaling influences the neurogenic and non-neurogenic domains in the chick otic placode. Dev Biol 339:166–178.

Acloque H, Thiery JP, Nieto MA (2008) The physiology and pathology of the EMT. Meeting on the epithelial-mesenchymal transition. EMBO Rep 9:322–326.

Adam J, Myat A, Le Roux I, Eddison M, Henrique D, Ish-Horowicz D, Lewis J (1998) Cell fate choices and the expression of Notch, Delta and Serrate homologues in the chick inner ear: parallels with Drosophila sense-organ development. Development 125:4645–4654.

Adamska M, Herbrand H, Adamski M, Krüger M, Braun T, Bober E (2001) FGFs control the patterning of the inner ear but are not able to induce the full ear program. Mech Dev 109:303–313.

Adolf B, Bellipanni G, Huber V, Bally-Cuif L (2004) atoh1.2 and beta3.1 are two new bHLH-encoding genes expressed in selective precursor cells of the zebrafish anterior hindbrain. Gene Expr Patterns 5:35–41.

Ahlstrom JD, Erickson CA (2009) The neural crest epithelial-mesenchymal transition in 4D: a "tail" of multiple non-obligatory cellular mechanisms. Development 136:1801–1812.

Akitaya T, Bronner-Fraser M (1992) Expression of cell adhesion molecules during initiation and cessation of neural crest cell migration. Dev Dyn 194:12–20.

Alexandre P, Reugels AM, Barker D, Blanc E, Clarke JDW (2010) Neurons derive from the more apical daughter in asymmetric divisions in the zebrafish neural tube. Nat Neurosci 13:673–679.

Alsina B, Abello G, Ulloa E, Henrique D, Pujades C, Giraldez F (2004) FGF signaling is required for determination of otic neuroblasts in the chick embryo. Dev Biol 267:119–134.

Alsina B, Giraldez F, Pujades C (2009) Patterning and cell fate in ear development. Int J Dev Biol 53:1503–1513.

Alsina B, Giraldez F, Varela-Nieto I (2003) Growth factors and early development of otic neurons: interactions between intrinsic and extrinsic signals. Curr Top Dev Biol 57:177–206.

Alsina B, Whitfield TT (in press, 2016) Sculpting the labyrinth: morphogenesis of the developing inner ear. Semin Cell Dev Biol.

Alvarez IS, Martin-Partido G, Rodriguez-Gallardo L, Gonzalez-Ramos C, Navascues J (1989) Cell proliferation during early development of the chick embryo otic anlage: quantitative comparison of migratory and nonmigratory regions of the otic epithelium. J Comp Neurol 290:278–288.

Alvarez Y, Alonso MT, Vendrell V, Zelarayan LC, Chamero P, Theil T, Bosl MR, Kato S, Maconochie M, Riethmacher D, Schimmang T (2003) Requirements for FGF3 and FGF10 during inner ear formation. Development 130:6329–6338.

Aman A, Piotrowski T (2008) Wnt/Beta-Catenin and Fgf Signaling Control Collective Cell Migration by Restricting Chemokine Receptor Expression. Dev Cell 15:749–761.

Andermann P, Ungos J, Raible DW (2002) Neurogenin1 defines zebrafish cranial sensory ganglia precursors. Dev Biol 251:45–58.

Apitz H, Salecker I (2015) A region-specific neurogenesis mode requires migratory progenitors in the Drosophila visual system. Nat Neurosci 18:46–55.

Artavanis-tsakonas S, Rand MD, Lake RJ (1999) Notch Signaling: Cell Fate Control and Signal Integration in Development. 284:770–777.

Artavanis-Tsakonas S, Simpson P (1991) Choosing a cell fate: a view from the Notch locus. Trends Genet 7:403–408.

154

Atsuta Y, Takahashi Y (2015) FGF8 coordinates tissue elongation and cell epithelialization during early kidney tubulogenesis. Development 142:2329–2337.

Ayala R, Shu T, Tsai LH (2007) Trekking across the Brain: The Journey of Neuronal Migration. Cell 128:29–43.

Bae YK, Shimizu T, Hibi M (2005) Patterning of proneuronal and inter-proneuronal domains by hairy- and enhancer of split-related genes in zebrafish neuroectoderm. Development 132:1375–1385.

Bailey AP, Bhattacharyya S, Bronner-Fraser M, Streit A (2006) Lens Specification Is the Ground State of All Sensory Placodes, from which FGF Promotes Olfactory Identity. Dev Cell 11:505–517.

Bailey AP, Streit A (2006) Sensory Organs: Making and Breaking the Pre-Placodal Region. Curr Top Dev Biol 72:167–204.

Baird RA, Burton MD, Lysakowski A, Fashena DS, Naeger RA (2000) Hair cell recovery in mitotically blocked cultures of the bullfrog saccule. Proc Natl Acad Sci U S A 97:11722–11729.

Baker C V, Bronner-Fraser M (2001) Vertebrate cranial placodes I. Embryonic induction. Dev Biol 232:1–61.

Baker CVH, Bronner-Fraser M (1997) The origins of the neural crest. Part II: An evolutionary perspective. Mech Dev 69:13–29.

Baker NE, Yu SY (1997) Proneural function of neurogenic genes in the developing Drosophila eye. Curr Biol 7:122–132.

Batlle E, Sancho E, Francí C, Domínguez D, Monfar M, Baulida J, García De Herreros A (2000) The transcription factor snail is a repressor of E-cadherin gene expression in epithelial tumour cells. Nat Cell Biol 2:84–89.

Baum B, Settleman J, Quinlan MP (2008) Transitions between epithelial and mesenchymal states in development and disease. Semin Cell Dev Biol 19:294–308.

Baye LM, Link BA (2008) Nuclear migration during retinal development. Brain Res 1192:29–36.

Behrndt M, Roensch J, Grill SW, Heisenberg C (2012) Forces driving epithelial spreading in zebrafish gastrulation. 257:10–14.

Bell D, Streit A, Gorospe I, Varela-Nieto I, Alsina B, Giraldez F (2008) Spatial and temporal segregation of auditory and vestibular neurons in the otic placode. Dev Biol 322:109–120.

Bénazéraf B (2011) A random cell motility gradient downstrem of FGF controls elongation of an amniote embryo. 466:248–252.

Bermingham NA, Hassan BA, Price SD, Vollrath MA, Ben-Arie N, Eatock RA, Bellen HJ, Lysakowski A, Zoghbi HY (1999) Math1: An Essential Gene for the Generation of Inner Ear Hair Cells. Science (80- ) 284:1837–1841.

Bertrand N, Castro DS, Guillemot F (2002) Proneural genes and the specification of neural cell types. Nat Rev Neurosci 3:517–530.

Betizeau M, Cortay V, Patti D, Pfister S, Gautier E, Bellemin-Ménard A, Afanassieff M, Huissoud C, Douglas RJ, Kennedy H, Dehay C (2013) Precursor Diversity and Complexity of Lineage Relationships in the Outer Subventricular Zone of the Primate. Neuron 80:442–457.

Bever MM, Fekete DM (2002) Atlas of the developing inner ear in zebrafish. Dev Dyn 223:536–543.

Bevis BJ, Glick BS (2002) Rapidly maturing variants of the Discosoma red fluorescent protein (DsRed). Nat Biotechnol 20:83–87.

Bhat N, Riley BB (2011) Integrin-a5 coordinates assembly of posterior cranial placodes in zebrafish and enhances Fgf-dependent regulation of otic/epibranchial cells. PLoS One 6.

Bhattacharyya S, Bailey AP, Bronner-Fraser M, Streit A (2004) Segregation of lens and olfactory precursors from a common territory: Cell sorting and reciprocity of Dlx5 and Pax6 expression. Dev Biol 271:403–414.

Blaser H, Reichman-Fried M, Castanon I, Dumstrei K, Marlow F, Kawakami K, Solnica-Krezel L, Heisenberg CP, Raz E (2006) Migration of Zebrafish Primordial Germ Cells: A Role for Myosin Contraction and Cytoplasmic Flow. Dev Cell 11:613–627.

Bok J, Bronner-Fraser M, Wu DK (2005) Role of the hindbrain in dorsoventral but not anteroposterior axial specification of the inner ear. Development 132:2115–2124.

Bok J, Chang W, Wu DK (2007) Patterning and morphogenesis of the vertebrate inner ear. Int J Dev Biol 51:521–533.

Bok J, Raft S, Kong KA, Koo SK, Drager UC, Wu DK (2011) Transient retinoic acid signaling confers anterior-posterior polarity to the inner ear. Proc Natl Acad Sci U S A 108:161–166.

Boldajipour B, Doitsidou M, Tarbashevich K, Laguri C, Yu SR, Ries J, Dumstrei K, Thelen S, Dörries J, Messerschmidt E-M, Thelen M, Schwille P, Brand M, Lortat-Jacob H, Raz E (2011) Cxcl12 evolution--subfunctionalization of a ligand through altered interaction with the chemokine receptor. Development 138:2909–2914.

Bolós V, Peinado H, Pérez-Moreno M a, Fraga MF, Esteller M, Cano A (2003) The transcription factor Slug represses E-cadherin expression and induces epithelial to mesenchymal transitions: a comparison with Snail and E47 repressors. J Cell Sci 116:499–511.

Borrell V, Cárdenas A, Ciceri G, Galcerán J, Flames N, Pla R, Nóbrega-Pereira S, García-Frigola C, Peregr??n S, Zhao Z, Ma L, Tessier-Lavigne M, Marín O (2012) Slit/Robo Signaling Modulates the Proliferation of Central Nervous System Progenitors. Neuron 76:338–352.

Brabletz T (2012) EMT and MET in Metastasis: Where Are the Cancer Stem Cells? Cancer Cell 22:699–701.

Brand M, Heisenberg CP, Jiang YJ, Beuchle D, Lun K, Furutani-Seiki M, Granato M, Haffter P, Hammerschmidt M, Kane D a, Kelsh RN, Mullins MC, Odenthal J, van Eeden FJ, Nüsslein-Volhard C (1996) Mutations in zebrafish genes affecting the formation of the boundary between midbrain and hindbrain. Development 123:179–190.

Breau MA, Schneider-Maunoury S (2014) Mechanisms of cranial placode assembly. Int J Dev Biol 58:9–19.

Brigande J V, Iten LE, Fekete DM (2000a) A fate map of chick otic cup closure reveals lineage boundaries in the dorsal otocyst. Dev Biol 227:256–270.

Brigande J V, Kiernan A, Gao X, Iten LE, Fekete DM (2000b) Molecular genetics of pattern formation in the inner ear: do compartment boundaries play a role? Proc Natl Acad Sci U S A 97:11700–11706.

Brooker R, Hozumi K, Lewis J (2006) Notch ligands with contrasting functions: Jagged1 and Delta1 in the mouse inner ear. Development 133:1277–1286.

Brown ST, Wang J, Groves AK (2005) Dlx gene expression during chick inner ear development. J Comp Neurol 483:48–65.

Brumwell CL, Hossain W a, Morest DK, Bernd P (2000) Role for basic fibroblast growth factor (FGF-2) in tyrosine kinase (TrkB) expression in the early development and innervation of the auditory receptor: in vitro and in situ studies. Exp Neurol 162:121–145.

Brunet JF, Ghysen A (1999) Deconstructing cell determination: proneural genes and neuronal identity. Bioessays 21:313–318.

Bryant J, Goodyear RJ, Richardson GP (2002) Sensory organ development in the inner ear: molecular and cellular mechanisms. Br Med Bull 63:39–57.

Buckley CE, Ren X, Ward LC, Girdler GC, Araya C, Green MJ, Clark BS, Link B a, Clarke JDW (2013) Mirror-symmetric microtubule assembly and cell interactions drive lumen formation in the zebrafish neural rod. EMBO J 32:30–44.

Bultje RS, Castaneda-Castellanos DR, Jan LY, Jan YN, Kriegstein AR, Shi SH (2009) Mammalian Par3 Regulates Progenitor Cell Asymmetric Division via Notch Signaling in the Developing Neocortex. Neuron 63:189–202.

Burighel P, Caicci F, Manni L (2011) Hair cells in non-vertebrate models: Lower chordates and molluscs. Hear Res 273:14–24.

Burighel P, Caicci F, Zaniolo G, Gasparini F, Degasperi V, Manni L (2008) Does hair cell differentiation predate the vertebrate appearance? Brain Res Bull 75:331–334.

Burighel P, Lane NJ, Fabio G, Stefano T, Zaniolo G, Candia Carnevali MD, Manni L (2003) Novel, secondary sensory cell organ in ascidians:

158

In search of the ancestor of the vertebrate lateral line. J Comp Neurol 461:236–249.

Bussmann J, Raz E (2015) Chemokine-guided cell migration and motility in zebrafish development. EMBO J 34:1309–1318.

Cai T, Seymour ML, Zhang H, Pereira F a., Groves AK (2013) Conditional deletion of Atoh1 reveals distinct critical periods for survival and function of hair cells in the organ of Corti. J Neurosci 33:10110–10122.

Campuzano S, Modolell J (1992) Patterning of the Drosophila nervous system: the achaete-scute gene complex. Trends Genet 8:202–208.

Cano A, Pérez-Moreno MA, Rodrigo I, Locascio A, Blanco MJ, del Barrio MG, Portillo F, Nieto MA (2000) The transcription factor snail controls epithelial-mesenchymal transitions by repressing E-cadherin expression. Nat Cell Biol 2:76–83.

Carney PR, Couve E (1989) Cell polarity changes and migration during early development of the avian peripheral auditory system. Anat Rec 225:156–164.

Cau E, Casarosa S, Guillemot F (2002) Mash1 and Ngn1 control distinct steps of determination and differentiation in the olfactory sensory neuron lineage. Development 129:1871–1880.

Cau E, Gradwohl G, Fode C, Guillemot F (1997) Mash1 activates a cascade of bHLH regulators in olfactory neuron progenitors. Development 124:1611–1621.

Cayouette M, Whitmore A V, Jeffery G, Raff M (2001) Asymmetric segregation of Numb in retinal development and the influence of the pigmented epithelium. J Neurosci 21:5643–5651.

Cha YR, Fujita M, Butler M, Isogai S, Kochhan E, Siekmann AF, Weinstein BM (2012) Chemokine signaling directs trunk lymphatic network formation along the preexisting blood vasculature. Dev Cell 22:824–836.

Chalpe AJ, Prasad M, Henke AJ, Paulson AF (2010) Regulation of cadherin expression in the chicken neural crest by the Wnt/β-catenin signaling pathway. Cell Adhes Migr 4:431–438.

Charras G, Yarrow J, Horton M, Mahadevan L, Mitchison T (2005) Non-equilibration of hydrostatic pressure in blebbing cells. Nature 435:365–369.

Charras GT, Coughlin M, Mitchison TJ, Mahadevan L (2008) Life and times of a cellular bleb. Biophys J 94:1836–1853.

Charras GT, Hu CK, Coughlin M, Mitchison TJ (2006) Reassembly of contractile actin cortex in cell blebs. J Cell Biol 175:477–490.

Chen H, Thiagalingam A, Chopra H, Borges MW, Feder JN, Nelkin BD, Baylin SB, Ball DW (1997) Conservation of the Drosophila lateral inhibition pathway in human lung cancer: a hairy-related protein (HES-1) directly represses achaete-scute homolog-1 expression. Proc Natl Acad Sci U S A 94:5355–5360.

Chenn A, McConnell SK (1995) Cleavage orientation and the asymmetric inheritance of notch1 immunoreactivity in mammalian neurogenesis. Cell 82:631–641.

Cheung M, Briscoe J (2003) Neural crest development is regulated by the transcription factor Sox9. Development 130:5681–5693.

Cheung M, Chaboissier MC, Mynett A, Hirst E, Schedl A, Briscoe J (2005) The transcriptional control of trunk neural crest induction, survival, and delamination. Dev Cell 8:179–192.

Chitnis AB (1995) The role of Notch in lateral inhibition and cell fate specification. Mol Cell Neurosci 6:311–321.

Chrysostomou E, Gale JE, Daudet N (2012) Delta-like 1 and lateral inhibition during hair cell formation in the chicken inner ear: evidence against cis-inhibition. Development 139:3764–3774.

Clay MR, Halloran MC (2014) Cadherin 6 promotes neural crest cell detachment via F-actin regulation and influences active Rho distribution during epithelial-to-mesenchymal transition. Development 141:2506–2515.

Cole LK, Le Roux I, Nunes F, Laufer E, Lewis J, Wu DK (2000) Sensory organ generation in the chicken inner ear: Contributions of bone morphogenetic protein 4, Serrate1, and lunatic fringe. J Comp Neurol 424:509–520.

Coles EG, Taneyhill LA, Bronner-Fraser M (2007) A critical role for Cadherin6B in regulating avian neural crest emigration. Dev Biol 312:533–544.

Corwin JT, Cotanche DA (1988) Regeneration of sensory hair cells after acoustic trauma. Science 240:1772–1774.

Costa MR, Wen G, Lepier A, Schroeder T, Götz M (2008) Par-complex proteins promote proliferative progenitor divisions in the developing mouse cerebral cortex. Development 135:11–22.

Cunningham CC (1995) Actin polymerization and intracellular solvent flow in cell surfase blebbing. JCell Biol 129(6):1589–1599.

D'Amico-Martel A, Noden DM (1983) Contributions of placodal and neural crest cells to avian cranial peripheral ganglia. Am J Anat 166:445–468.

Dalle Nogare D, Somers K, Rao S, Matsuda M, Reichman-Fried M, Raz E, Chitnis AB (2014) Leading and trailing cells cooperate in collective migration of the zebrafish Posterior Lateral Line primordium. Development 141:3188–3196.

Das RM, Storey KG (2012) Mitotic spindle orientation can direct cell fate and bias Notch activity in chick neural tube. EMBO Rep 13:448–454.

Das RM, Storey KG (2014) Apical abscission alters cell polarity and dismantles the primary cilium during neurogenesis. Science 343:200–204.

Das T, Payer B, Cayouette M, Harris WA (2003) In vivo time-lapse imaging of cell divisions during neurogenesis in the developing zebrafish retina. Neuron 37:597–609.

Daudet N, Ariza-McNaughton L, Lewis J (2007) Notch signalling is needed to maintain, but not to initiate, the formation of prosensory patches in the chick inner ear. Development 134:2369–2378.

David NB, Sapède D, Saint-Etienne L, Thisse C, Thisse B, Dambly-Chaudière C, Rosa FM, Ghysen A (2002) Molecular basis of cell migration in the fish lateral line: role of the chemokine receptor CXCR4 and of its ligand, SDF1. Proc Natl Acad Sci U S A 99:16297–16302.

David R, Ahrens K, Wedlich D, Schlosser G (2001) Xenopus Eya1 demarcates all neurogenic placodes as well as migrating hypaxial muscle precursors. Mech Dev 103:189–192.

Davies D (2011) Cell-extracellular matrix versus cell-cell interactions during the development of the cochlear-vestibular ganglion. J Neurosci Res 89:1375–1387.

Davis RL, Turner DL (2001) Vertebrate hairy and Enhancer of split related proteins: transcriptional repressors regulating cellular differentiation and embryonic patterning. Oncogene 20:8342–8357.

Doe CQ, Bowerman B (2001) Asymmetric cell division: Fly neuroblast meets worm zygote. Curr Opin Cell Biol 13:68–75.

Doitsidou M, Reichman-Fried M, Stebler J, Köprunner M, Dörries J, Meyer D, Esguerra C V., Leung T, Raz E (2002) Guidance of primordial germ cell migration by the chemokine SDF-1. Cell 111:647–659.

Dong Z, Yang N, Yeo SY, Chitnis A, Guo S (2012) Intralineage Directional Notch Signaling Regulates Self-Renewal and Differentiation of Asymmetrically Dividing Radial Glia. Neuron 74:65–78.

Drerup CM, Nechiporuk A V. (2013) JNK-Interacting Protein 3 Mediates the Retrograde Transport of Activated c-Jun N-Terminal Kinase and Lysosomes. PLoS Genet 9.

Duband JL (2010) Diversity in the molecular and cellular strategies of epithelium-to- mesenchyme transitions: Insights from the neural crest. Cell Adhes Migr 4:458–482.

Erkman L, McEvilly RJ, Luo L, Ryan AK, Hooshmand F, O'Connell SM, Keithley EM, Rapaport DH, Ryan AF, Rosenfeld MG (1996) Role of transcription factors Brn-3.1 and Brn-3.2 in auditory and visual system development. Nature 381:603–606.

Esteve P, Bovolenta P (1999) cSix4, a member of the six gene family of transcription factors, is expressed during placode and somite development. Mech Dev 85:161–165.

Even-Ram S, Yamada KM (2005) Cell migration in 3D matrix. Curr Opin Cell Biol 17:524–532.

Farah MH, Olson JM, Sucic HB, Hume RI, Tapscott SJ, Turner DL (2000) Generation of neurons by transient expression of neural bHLH proteins in mammalian cells. Development 127:693–702.

Fekete DM (2000) Ear rings: FGF3 involvement comes full circle. Trends Neurosci 23:332.

Fekete DM, Wu DK (2002) Revisiting cell fate specification in the inner ear. Curr Opin Neurobiol 12:35–42.

Fietz SA, Huttner WB (2011) Cortical progenitor expansion, self-renewal and neurogenesis-a polarized perspective. Curr Opin Neurobiol 21:23–35.

Fischer A, Gessler M (2007) Delta-Notch-and then? Protein interactions and proposed modes of repression by Hes and Hey bHLH factors. Nucleic Acids Res 35:4583–4596.

Fode C, Gradwohl G, Morin X, Dierich A, LeMeur M, Goridis C, Guillemot F (1998) The bHLH protein NEUROGENIN 2 is a determination factor for epibranchial placode-derived sensory neurons. Neuron 20:483–494.

Freter S, Muta Y, Mak S-S, Rinkwitz S, Ladher RK (2008) Progressive restriction of otic fate: the role of FGF and Wnt in resolving inner ear potential. Development 135:3415–3424.

Friedman RA, Makmura L, Biesiada E, Wang X, Keithley EM (2005) Eya1 acts upstream of Tbx1, Neurogenin1, NeuroD and the neurotrophins BDNF and NT-3 during inner ear development. Mech Dev 122:625–634.

Fritzsch B, Beisel KW, Jones K, Farias I, Maklad A, Lee J, Reichardt LF (2002) Development and evolution of inner ear sensory epithelia and their innervation. J Neurobiol 53:143–156.

Gajewski M, Elmasri H, Girschick M, Sieger D, Winkler C (2006) Comparative analysis of her genes during fish somitogenesis suggests a mouse/chick-like mode of oscillation in medaka. Dev Genes Evol 216:315–332.

Gallagher BC, Henry JJ, Grainger RM (1996) Inductive processes leading to inner ear formation during Xenopus development. Dev Biol 175:95–107.

Garcia-Bellido A (1979) Genetic Analysis of the Achaete-Scute System of DROSOPHILA MELANOGASTER. Genetics 91:491–520.

Ghysen A, Dambly-Chaudière C (1988) From DNA to form: the achaete-scute complex. Genes Dev 2:495–501.

Golling G, Amsterdam A, Sun Z, Antonelli M, Maldonado E, Chen W, Burgess S, Haldi M, Artzt K, Farrington S, Lin SY, Nissen RM, Hopkins N (2002) Insertional mutagenesis in zebrafish rapidly identifies genes essential for early vertebrate development. Nat Genet 31:135–140.

Götz M, Huttner WB (2005) The cell biology of neurogenesis. Nat Rev Mol Cell Biol 6:777–788.

Goudarzi M, Banisch TU, Mobin MB, Maghelli N, Tarbashevich K, Strate I, van den Berg J, Blaser H, Bandemer S, Paluch E, Bakkers J, Tolić-Nørrelykke IM, Raz E (2012) Identification and Regulation of a Molecular Module for Bleb-Based Cell Motility. Dev Cell 23:210–218.

Graham A, Begbie J (2000) Neurogenic placodes: A common front. Trends Neurosci 23:313–316.

Graham A, Blentic A, Duque S, Begbie J (2007) Delamination of cells from neurogenic placodes does not involve an epithelial-to-mesenchymal transition. Development 134:4141–4145.

Greenwald I, Rubin GM (1992) Making a difference: the role of cell-cell interactions in establishing separate identities for equivalent cells. Cell 68:271–281.

Grosse AS, Pressprich MF, Curley LB, Hamilton KL, Margolis B, Hildebrand JD, Gumucio DL (2011) Cell dynamics in fetal intestinal epithelium: implications for intestinal growth and morphogenesis. Development 138:4423–4432.

Groves AK, Bronner-Fraser M (2000) Competence, specification and commitment in otic placode induction. Development 127:3489–3499.

Groves AK, Fekete DM (2012) Shaping sound in space: the regulation of inner ear patterning. Development 139:826–826.

Guillemot F (1999) Vertebrate bHLH genes and the determination of neuronal fates. Exp Cell Res 253:357–364.

Gurdon JB (1987) Embryonic induction -- molecular prospects. Development 99:285–306.

Guth PS, Perin P, Norris CH, Valli P (1998) The vestibular hair cells: post-transductional signal processing. Prog Neurobiol 54:193–247.

Haddon C, Jiang YJ, Smithers L, Lewis J (1998a) Delta-Notch signalling and the patterning of sensory cell differentiation in the zebrafish ear: evidence from the mind bomb mutant. Development 125:4637–4644.

Haddon C, Lewis J (1996) Early ear development in the embryo of the zebrafish, Danio rerio. J Comp Neurol 365:113–128.

Haddon C, Mowbray C, Whitfield T, Jones D, Gschmeissner S, Lewis J (1999) Hair cells without supporting cells: further studies in the ear of the zebrafish mind bomb mutant. J Neurocytol 28:837–850.

Haddon C, Smithers L, Schneider-Maunoury S, Coche T, Henrique D, Lewis J (1998b) Multiple delta genes and lateral inhibition in zebrafish primary neurogenesis. Development 125:359–370.

Hammond KL, Whitfield TT (2011) Fgf and Hh signalling act on a symmetrical pre-pattern to specify anterior and posterior identity in the zebrafish otic placode and vesicle. Development 138:3977–3987.

Hans S, Christison J, Liu D, Westerfield M (2007) Fgf-dependent otic induction requires competence provided by Foxi1 and Dlx3b. BMC Dev Biol 7:5.

Hans S, Liu D, Westerfield M (2004) Pax8 and Pax2a function synergistically in otic specification, downstream of the Foxi1 and Dlx3b transcription factors. Development 131:5091–5102.

Hansen D V, Lui JH, Parker PRL, Kriegstein AR (2010) Neurogenic radial glia in the outer subventricular zone of human neocortex. Nature 464:554–561.

Haraguchi M, Okubo T, Miyashita Y, Miyamoto Y, Hayashi M, Crotti TN, McHugh KP, Ozawa M (2008) Snail regulates cell-matrix adhesion by regulation of the expression of integrins and basement membrane proteins. J Biol Chem 283:23514–23523.

Hartenstein V, Stollewerk A (2015) The evolution of early neurogenesis. Dev Cell 32:390–407.

Hartman BH, Basak O, Nelson BR, Taylor V, Bermingham-Mcdonogh O, Reh TA (2009) Hes5 expression in the postnatal and adult mouse inner ear and the drug-damaged cochlea. JARO - J Assoc Res Otolaryngol 10:321–340.

Hassan BA, Bellen HJ (2000) Doing the MATH: Is the mouse a good model for fly development? Genes Dev 14:1852–1865.

Hay ED (1995) An overview of epithelio-mesenchymal transformation. Acta Anat (Basel) 154:8–20.

Hay ED (2005) The mesenchymal cell, its role in the embryo, and the remarkable signaling mechanisms that create it. Dev Dyn 233:706–720.

Hemond SG, Morest DK (1991) Ganglion formation from the otic placode and the otic crest in the chick embryo: mitosis, migration, and the basal lamina. Anat Embryol (Berl) 184:1–13.

Hoijman E, Rubbini D, Colombelli J, Alsina B (2015) Mitotic cell rounding and epithelial thinning regulate lumen growth and shape. Nat Commun 6:7355.

Hossain WA, Zhou X, Rutledge A, Baier C, Morest DK (1996) Basic fibroblast growth factor affects neuronal migration and differentiation in normotypic cell cultures from the cochleovestibular ganglion of the chick embryo. Exp Neurol 138:121–143.

Hudspeth AJ (1989) How the ear's works work. Nature 341:397–404.

Huttner WB, Kosodo Y (2005) Symmetric versus asymmetric cell division during neurogenesis in the developing vertebrate central nervous system. Curr Opin Cell Biol 17:648–657.

Inoue A, Takahashi M, Hatta K, Hotta Y, Okamoto H (1994) Developmental regulation of islet-1 mRNA expression during neuronal differentiation in embryonic zebrafish. Dev Dyn 199:1–11.

Ip YT, Gridley T (2002) Cell movements during gastrulation: Snail dependent and independent pathways. Curr Opin Genet Dev 12:423–429.

Itoh M, Chitnis AB (2001) Expression of proneural and neurogenic genes in the zebrafish lateral line primordium correlates with selection of hair cell fate in neuromasts. Mech Dev 102:263–266.

Itoh M, Kim CH, Palardy G, Oda T, Jiang YJ, Maust D, Yeo SY, Lorick K, Wright GJ, Ariza-McNaughton L, Weissman AM, Lewis J, Chandrasekharappa SC, Chitnis AB (2003) Mind bomb is a ubiquitin ligase that is essential for efficient activation of Notch signaling by Delta. Dev Cell 4:67–82.

Itoh Y, Tyssowski K, Gotoh Y (2013) Transcriptional coupling of neuronal fate commitment and the onset of migration. Curr Opin Neurobiol 23:957–964.

Jacobson A (1966) Inductive Processes in Embryonic Development. Science 152:25–34.

Jacobson AG (1963) The determination and positioning of the nose, lens and ear. II. The role of the endoderm. J Exp Zool 154:285–291.

Jacobson AG, Sater AK (1988) Features of embryonic induction. Development 104:341–359.

Jahan I, Pan N, Kersigo J, Calisto LE, Morris KA, Kopecky B, Duncan JS, Beisel KW, Fritzsch B (2012) Expression of Neurog1 instead of Atoh1 can partially rescue organ of Corti cell survival. PLoS One 7:e30853.

Jan YN, Jan LY (1994) Genetic control of cell fate specification in Drosophila peripheral nervous system. Annu Rev Genet 28:373–393.

Jarman AP, Grau Y, Jan LY, Jan YN (1993) atonal is a proneural gene that directs chordotonal organ formation in the Drosophila peripheral nervous system. Cell 73:1307–1321.

Jarman AP, Sun Y, Jan LY, Jan YN (1995) Role of the proneural gene, atonal, in formation of Drosophila chordotonal organs and photoreceptors. Development 121:2019–2030.

Jarriault S, Brou C, Logeat F, Schroeter EH, Kopan R, Israel A (1995) Signalling downstream of activated mammalian Notch. Nature 377:355–358.

Jarriault S, Le Bail O, Hirsinger E, Pourquié O, Logeat F, Strong CF, Brou C, Seidah NG, Israël A (1998) Delta-1 Activation of Notch-1 Signaling Results in HES-1 Transactivation. Mol Cell Biol 18:7423–7431.

Jayasena CS, Ohyama T, Segil N, Groves AK (2008) Notch signaling augments the canonical Wnt pathway to specify the size of the otic placode. Development 135:2251–2261.

Jimenez F, Modolell J (1993) Neural fate specification in Drosophila. Curr Opin Genet Dev 3:626–632.

Johansson CB, Momma S, Clarke DL, Risling M, Lendahl U, Frisén J (1999) Identification of a neural stem cell in the adult mammalian central nervous system. Cell 96:25–34.

Jordà M, Olmeda D, Vinyals A, Valero E, Cubillo E, Llorens A, Cano A, Fabra A (2005) Upregulation of MMP-9 in MDCK epithelial cell line in response to expression of the Snail transcription factor. J Cell Sci 118:3371–3385.

Kageyama R, Nakanishi S (1997) Helix-loop-helix factors in growth and differentiation of the vertebrate nervous system. Curr Opin Genet Dev 7:659–665.

Kageyama R, Ohtsuka T, Hatakeyama J, Ohsawa R (2005) Roles of bHLH genes in neural stem cell differentiation. Exp Cell Res 306:343–348.

Kalluri R, Weinberg R a (2009) Review series The basics of epithelial-mesenchymal transition. J Clin Invest 119:1420–1428.

Kantarci H, Edlund RK, Groves AK, Riley BB (2015) Tfap2a Promotes Specification and Maturation of Neurons in the Inner Ear through Modulation of Bmp, Fgf and Notch Signaling. PLoS Genet 11:1–23.

Karpinski BA, A Bryan C, Paronett EM, Baker JL, Fernandez A, Horvath A, Maynard TM, Moody SA, LaMantia A-S (2016) A cellular and molecular mosaic establishes growth and differentiation states for cranial sensory neurons. Dev Biol 415:228–241.

Kawaguchi D, Furutachi S, Kawai H, Hozumi K, Gotoh Y (2013) Dll1 maintains quiescence of adult neural stem cells and segregates asymmetrically during mitosis. Nat Commun 4:1880.

Keller R, Davidson LA, Shook DR (2003) How we are shaped: The biomechanics of gastrulation. Differentiation 71:171–205.

Khatri SB, Edlund RK, Groves AK (2014) Foxi3 is necessary for the induction of the chick otic placode in response to FGF signaling. Dev Biol 391:158–169.

Kicheva A, Bollenbach T, Ribeiro A, Valle HP, Lovell-Badge R, Episkopou V, Briscoe J (2014) Coordination of progenitor specification and growth in mouse and chick spinal cord. Science 345:1254927.

Kiernan AE, Cordes R, Kopan R, Gossler A, Gridley T (2005a) The Notch ligands DLL1 and JAG2 act synergistically to regulate hair cell development in the mammalian inner ear. Development 132:4353–4362.

Kiernan AE, Pelling AL, Leung KKH, Tang ASP, Bell DM, Tease C, Lovell-Badge R, Steel KP, Cheah KSE (2005b) Sox2 is required for sensory organ development in the mammalian inner ear. Nature 434:1031–1035.

Kiernan AE, Xu J, Gridley T (2006) The notch ligand JAG1 is required for sensory progenitor development in the mammalian inner ear. PLoS Genet 2:27–38.

Kim WY, Fritzsch B, Serls A, Bakel LA, Huang EJ, Reichardt LF, Barth DS, Lee JE (2001) NeuroD-null mice are deaf due to a severe loss of the inner ear sensory neurons during. Development 128:417–426.

Kimmel CB, Ballard WW, Kimmel SR, Ullmann B, Schilling TF (1995) Stages of embryonic development of the zebrafish. Dev Dyn 10:253–310.

Kintner C (2002) Neurogenesis in Embryos and in Adult Neural Stem Cells. J Neurosci 22:639–643.

Knaut H, Werz C, Geisler R, Nüsslein-Volhard C (2003) A zebrafish homologue of the chemokine receptor Cxcr4 is a germ-cell guidance receptor. Nature 421:279–282.

Knoblich JA (2010) Asymmetric cell division: recent developments and their implications for tumour biology. Nat Rev Mol Cell Biol 11:849–860.

Kobayashi M, Osanai H, Kawakami K, Yamamoto M (2000) Expression of three zebrafish Six4 genes in the cranial sensory placodes and the developing somites. Mech Dev 98:151–155.

Koehler KR, Hashino E (2014) 3D mouse embryonic stem cell culture for generating inner ear organoids. Nat Protoc 9:1229–1244.

Korzh V, Sleptsova I, Liao J, He J, Gong Z (1998) Expression of zebrafish bHLH genes ngn1 and nrd defines distinct stages of neural differentiation. Dev Dyn 213:92–104.

Kosodo Y, Röper K, Haubensak W, Marzesco A-M, Corbeil D, Huttner WB (2004) Asymmetric distribution of the apical plasma membrane during neurogenic divisions of mammalian neuroepithelial cells. EMBO J 23:2314–2324.

Köster RW, Fraser SE (2001) Tracing transgene expression in living zebrafish embryos. Dev Biol 233:329–346.

Kozlowski DJ, Murakami T, Ho RK, Weinberg ES (1997) Regional cell movement and tissue patterning in the zebrafish embryo revealed by fate mapping with caged fluorescein. Biochem Cell Biol 75:551–562.

Kriegstein AR, Götz M (2003) Radial glia diversity: A matter of cell fate. Glia 43:37–43.

Kroehne V, Freudenreich D, Hans S, Kaslin J, Brand M (2011) Regeneration of the adult zebrafish brain from neurogenic radial glia-type progenitors. Development 138:4831–4841.

Kulesa PM, Gammill LS (2010) Neural crest migration: Patterns, phases and signals. Dev Biol 344:566–568.

LaBonne C, Bronner-Fraser M (1998) Neural crest induction in Xenopus: evidence for a two-signal model. Development 125:2403–2414.

Ladher RK, Anakwe KU, Gurney AL, Schoenwolf GC, Francis-West PH (2000) Identification of synergistic signals initiating inner ear development. Science 290:1965–1967.

Ladher RK, O'Neill P, Begbie J (2010) From shared lineage to distinct functions: the development of the inner ear and epibranchial placodes. Development 137:1777–1785.

Ladher RK, Wright TJ, Moon AM, Mansour SL, Schoenwolf GC (2005) FGF8 initiates inner ear induction in chick and mouse. Genes Dev 19:603–613.

Lamouille S, Xu J, Derynck R (2014) Molecular mechanisms of epithelial-mesenchymal transition. Natl Rev Mol Cell Biol 15:178–196.

Lancaster MA, Knoblich JA (2012) Spindle orientation in mammalian cerebral cortical development. Curr Opin Neurobiol 22:737–746.

Lanford PJ, Lan Y, Jiang R, Lindsell C, Weinmaster G, Gridley T, Kelley MW (1999) Notch signalling pathway mediates hair cell development in mammalian cochlea. Nat Genet 21:289–292.

Lassiter RNT, Stark MR, Zhao T, Zhou CJ (2014) Signaling mechanisms controlling cranial placode neurogenesis and delamination. Dev Biol 389:39–49.

Lee J, Hollenberg S, Snider L, Turner D, Lipnick N, Weintraub H (1995) Conversion of Xenopus ectoderm into neurons by NeuroD, a basic helix-loop-helix protein. Science (80- ) 268:836–844.

Lee JE (1997) Basic helix-loop-helix genes in neural development. Curr Opin Neurobiol 7:13–20.

Lee J-Y, Goldstein B (2003) Mechanisms of cell positioning during C. elegans gastrulation. Development 130:307–320.

Léger S, Brand M (2002) Fgf8 and Fgf3 are required for zebrafish ear placode induction, maintenance and inner ear patterning. Mech Dev 119:91–108.

Leon Y, Vazquez E, Sanz C, Vega JA, Mato JM, Giraldez F, Represa J, Varela-Nieto I (1995) Insulin-like growth factor-I regulates cell proliferation in the developing inner ear, activating glycosyl-phosphatidylinositol hydrolysis and Fos expression. Endocrinology 136:3494–3503.

Leung L, Klopper A V., Grill SW, Harris W a., Norden C (2012) Apical migration of nuclei during G2 is a prerequisite for all nuclear motion in zebrafish neuroepithelia. Development 138:5003–5013.

Lewis ER, Narins PM (1999) The Acoustic Periphery of Amphibians: Anatomy and Physiology. In: Comparative Hearing: Fish and Amphibians (Fay RR, Popper AN, eds), pp 101–154. New York, NY: Springer New York.

Lewis J (1998) Notch signalling and the control of cell fate choices in vertebrates. Semin Cell Dev Biol 9:583–589.

Li H, Liu H, Sage C, Huang M, Chen ZY, Heller S (2004) Islet-1 expression in the developing chicken inner ear. J Comp Neurol 477:1–10.

Li R (2013) The art of choreographing asymmetric cell division. Dev Cell 25:439–450.

Li R, Gundersen GG (2008) Beyond polymer polarity: how the cytoskeleton builds a polarized cell. Nat Rev Mol Cell Biol 9:860–873.

Liem KF, Tremml G, Roelink H, Jessell TM (1995) Dorsal differentiation of neural plate cells induced by BMP-mediated signals from epidermal ectoderm. Cell 82:969–979.

Litsiou A, Hanson S, Streit A (2005) A balance of FGF, BMP and WNT signalling positions the future placode territory in the head. Development 132:4051–4062.

Liu D, Chu H, Maves L, Yan Y-L, Morcos P a, Postlethwait JH, Westerfield M (2003) Fgf3 and Fgf8 dependent and independent transcription factors are required for otic placode specification. Development 130:2213–2224.

Liu JP, Jessell TM (1998) A role for rhoB in the delamination of neural crest cells from the dorsal neural tube. Development 125:5055–5067.

Liu M, Pereira FA, Price SD, Chu MJ, Shope C, Himes D, Eatock RA, Brownell WE, Lysakowski A, Tsai MJ (2000) Essential role of BETA2/NeuroD1 in development of the vestibular and auditory systems. Genes Dev 14:2839–2854.

Liu Q, Liu B, Wilson AL, Rostedt J (2006) Cadherin-6 Message Expression in the Nervous System of Developing Zebrafish. Dev Dyn 235:272–278.

Liu X-P, Koehler KR, Mikosz AM, Hashino E, Holt JR (2016) Functional development of mechanosensitive hair cells in stem cell-derived organoids parallels native vestibular hair cells. Nat Commun 7:11508.

Lombardo A, Isaacs H V, Slack JM (1998) Expression and functions of FGF-3 in Xenopus development. Int J Dev Biol 42:1101–1107.

Lopez-Bendito G, Sánchez-Alcaniz JA, Pla R, Borrell V, Picó E, Valdeolmillos M, Marin O (2008) Chemokine signaling controls intracortical migration and final distribution of GABAergic interneurons. J Neurosci 28:1613–1624.

López-Nouoa JM, Nieto MA (2009) Inflammation and EMT: An alliance towards organ fibrosis and cancer progression. EMBO Mol Med 1:303–314.

Lu B, Jan L, Jan Y (2000) Control of cell divisions in the nervous system: Symmetry and Asymmetry. Annu Rev Neurosci 23:531–556.

Ma Q, Anderson DJ, Fritzsch B (2000) Neurogenin 1 null mutant ears develop fewer, morphologically normal hair cells in smaller sensory epithelia devoid of innervation. J Assoc Res Otolaryngol 1:129–143.

Ma Q, Chen Z, del Barco Barrantes I, de la Pompa JL, Anderson DJ (1998) Neurogenin1 is Essential for the Determination of Neuronal Precursors for Proximal Cranial Sensory Ganglia. Neuron 20:469–482.

Ma Q, Kintner C, Anderson DJ (1996) Identification of neurogenin, a vertebrate neuronal determination gene. Cell 87:43–52.

Ma Q, Sommer L, Cserjesi P, Anderson DJ (1997) Mash1 and neurogenin1 expression patterns define complementary domains of neuroepithelium in the developing CNS and are correlated with regions expressing notch ligands. J Neurosci 17:3644–3652.

Macara IG, Mili S (2008) Polarity and Differential Inheritance-Universal Attributes of Life? Cell 135:801–812.

Maeda M, Johnson KR, Wheelock MJ (2005) Cadherin switching: essential for behavioral but not morphological changes during an epithelium-to-mesenchyme transition. J Cell Sci 118:873–887.

Mahmood R, Mason IJ, Morriss-Kay GM (1996) Expression of Fgf-3 in relation to hindbrain segmentation, otic pit position and pharyngeal arch morphology in normal and retinoic acid-exposed mouse embryos. Anat Embryol (Berl) 194:13–22.

Maier EC, Saxena A, Alsina B, Bronner ME, Whitfield TT (2014) Sensational placodes: Neurogenesis in the otic and olfactory systems. Dev Biol 389:50–67.

Maier EC, Whitfield TT (2014) RA and FGF Signalling Are Required in the Zebrafish Otic Vesicle to Pattern and Maintain Ventral Otic Identities. PLoS Genet 10.

Mansour SL (1994) Targeted disruption of int-2 (fgf-3) causes developmental defects in the tail and inner ear. Mol Reprod Dev 39:62–68.

Mansour SL, Goddard JM, Capecchi MR (1993) Mice homozygous for a targeted disruption of the proto-oncogene int-2 have developmental defects in the tail and inner ear. Development 117:13–28.

Marmigère F, Ernfors P (2007) Specification and connectivity of neuronal subtypes in the sensory lineage. Nat Rev Neurosci 8:114–127.

Maroon H, Walshe J, Mahmood R, Kiefer P, Dickson C, Mason I (2002) Fgf3 and Fgf8 are required together for formation of the otic placode and vesicle. Development 129:2099–2108.

Martin AC (2010) Pulsation and stabilization: Contractile forces that underlie morphogenesis. Dev Biol 341:114–125.

Martin AC, Goldstein B (2014) Apical constriction: themes and variations on a cellular mechanism driving morphogenesis. Development 141:1987–1998.

Martin K, Groves AK (2006) Competence of cranial ectoderm to respond to Fgf signaling suggests a two-step model of otic placode induction. Development 133:877–887.

Matei V, Pauley S, Kaing S, Rowitch D, Beisel KW, Morris K, Feng F, Jones K, Lee J, Fritzsch B (2005) Smaller inner ear sensory epithelia in Neurog 1 null mice are related to earlier hair cell cycle exit. Dev Dyn 234:633–650.

McCarroll MN, Lewis ZR, Culbertson MD, Martin BL, Kimelman D, Nechiporuk AV (2012) Graded levels of Pax2a and Pax8 regulate cell differentiation during sensory placode formation. Development 139:2740–2750.

McCarroll MN, Nechiporuk AV (2013) Fgf3 and Fgf10a work in concert to promote maturation of the epibranchial placodes in Zebrafish. PLoS One 8:1–13.

McKay IJ, Lewis J, Lumsden A (1996) The role of FGF-3 in early inner ear development: an analysis in normal and kreisler mutant mice. Dev Biol 174:370–378.

McLarren KW, Litsiou A, Streit A (2003) DLX5 positions the neural crest and preplacode region at the border of the neural plate. Dev Biol 259:34–47.

Megason SG (2009) In toto imaging of embryogenesis with confocal time-lapse microscopy. Methods Mol Biol 546:317–332.

Meijering E, Dzyubachyk O, Smal I (2012) Methods for cell and particle tracking. Methods Enzymol 504:183–200.

Meyen D, Tarbashevich K, Banisch TU, Wittwer C, Reichman-Fried M, Maugis B, Grimaldi C, Messerschmidt EM, Raz E (2015) Dynamic filopodia are required for chemokine-dependent intracellular polarization during guided cell migration in vivo. Elife 2015:1–25.

Millimaki BB, Sweet EM, Dhason MS, Riley BB (2007) Zebrafish atoh1 genes: classic proneural activity in the inner ear and regulation by Fgf and Notch. Development 134:295–305.

Miyata T (2008) Development of three-dimensional architecture of the neuroepithelium: role of pseudostratification and cellular "community". Dev Growth Differ 50 Suppl 1:S105–S112.

Miyata T, Kawaguchi A, Saito K, Kawano M, Muto T, Ogawa M (2004) Asymmetric production of surface-dividing and non-surface-dividing cortical progenitor cells. Development 131:3133.

Mohamed OA, Clarke HJ, Dufort D (2004) Beta-Catenin Signaling Marks the Prospective Site of Primitive Streak Formation in the Mouse Embryo. Dev Dyn 231:416–424.

Müller M, v Weizsäcker E, Campos-Ortega J a (1996) Expression domains of a zebrafish homologue of the Drosophila pair-rule gene hairy correspond to primordia of alternating somites. Development 122:2071–2078.

Murre C, Schonleber P, Cabrera C V, Buskin JN, Hauschka S, Lassar AB, Weintraub H, Baltimore D (1989) Interactions between Heterologous Helix-Loop-Helix Proteins Generate Complexes That Bind Specifically to a Common DNA Sequence. 58:537–544.

Nakagawa S, Takeichi M (1995) Neural crest cell-cell adhesion controlled by sequential and subpopulation-specific expression of novel cadherins. Development 121:1321–1332.

Nakagawa S, Takeichi M (1998) Neural crest emigration from the neural tube depends on regulated cadherin expression. Development 125:2963–2971.

Neave B, Holder N, Patient R (1997) A graded response to BMP-4 spatially coordinates patterning of the mesoderm and ectoderm in the zebrafish. Mech Dev 62:183–195.

Nechiporuk A, Linbo T, Poss KD, Raible DW (2006) Specification of epibranchial placodes in zebrafish. Development 134:611–623.

Neves J, Kamaid A, Alsina B, Giraldez F (2007) Differential expression of Sox2 and Sox3 in neuronal and sensory progenitors of the developing inner ear of the chick. J Comp Neurol 503:487–500.

Neves J, Parada C, Chamizo M, Giraldez F (2011) Jagged 1 regulates the restriction of Sox2 expression in the developing chicken inner ear: a mechanism for sensory organ specification. Development 138:735–744.

Nguyen L, Besson A, Roberts JM, Guillemot F (2006) Coupling cell cycle exit, neuronal differentiation and migration in cortical neurogenesis. Cell Cycle 5:2314–2318.

Nguyen VH, Schmid B, Trout J, Connors S a, Ekker M, Mullins MC (1998) Ventral and lateral regions of the zebrafish gastrula, including the neural crest progenitors, are established by a bmp2b/swirl pathway of genes. Dev Biol 199:93–110.

Nichols DH, Pauley S, Jahan I, Beisel KW, Millen KJ, Fritzsch B (2008) Lmx1a is required for segregation of sensory epithelia and normal ear histogenesis and morphogenesis. Cell Tissue Res 334:339–358.

Nieto MA (2009) Epithelial-Mesenchymal Transitions in development and disease: Old views and new perspectives. Int J Dev Biol 53:1541–1547.

Nieto MA (2011) The ins and outs of the epithelial to mesenchymal transition in health and disease. Annu Rev Cell Dev Biol 27:347–376.

Nieto MA (2013) Epithelial plasticity: a common theme in embryonic and cancer cells. Science 342:1234850.

Nieto MA, Cano A (2012) The epithelial-mesenchymal transition under control: Global programs to regulate epithelial plasticity. Semin Cancer Biol 22:361–368.

Nieto MA, Sargent MG, Wilkinson DG, Cooke J (1994) Control of cell behavior during vertebrate development by slug, a zinc-finger gene. Science 264:835–839.

Niwa N, Hiromi Y, Okabe M (2004) A conserved developmental program for sensory organ formation in Drosophila melanogaster. Nat Genet 36:293–297.

Noctor SC, Martínez-Cerdeño V, Ivic L, Kriegstein AR (2004) Cortical neurons arise in symmetric and asymmetric division zones and migrate through specific phases. Nat Neurosci 7:136–144.

Norden C, Young S, Link BA, Harris WA (2009) Actomyosin Is the Main Driver of Interkinetic Nuclear Migration in the Retina. Cell 138:1195–1208.

Obholzer N, Wolfson S, Trapani JG, Mo W, Nechiporuk A, Busch-Nentwich E, Seiler C, Sidi S, Söllner C, Duncan RN, Boehland A, Nicolson T (2008) Vesicular glutamate transporter 3 is required for synaptic transmission in zebrafish hair cells. J Neurosci 28:2110–2118.

Oda H, Tsukita S, Takeichi M (1998) Dynamic behavior of the cadherin-based cell-cell adhesion system during Drosophila gastrulation. Dev Biol 203:435–450.

Ohnuma SI, Philpott A, Harris WA (2001) Cell cycle and cell fate in the nervous system. Curr Opin Neurobiol 11:66–73.

Ohsako S, Hyer J, Panganiban G, Oliver I, Caudy M (1994) hairy function as a DNA-binding helix- loop-helix repressor of Drosophila sensory organ formation. Genes Dev:2743–2755.

Ohtsuka T, Ishibashi M, Gradwohl G, Nakanishi S, Guillemot F, Kageyama R (1999) Hes1 and Hes5 as notch effectors in mammalian neuronal differentiation. EMBO J 18:2196–2207.

Ohyama T, Groves AK (2004a) Expression of mouse foxi class genes in early craniofacial development. Dev Dyn 231:640–646.

Ohyama T, Groves AK (2004b) Generation of Pax2-Cre Mice by Modification of a Pax2 Bacterial Artificial Chromosome. Genesis 38:195–199.

Ohyama T, Groves AK, Martin K (2007) The first steps towards hearing: Mechanisms of otic placode induction. Int J Dev Biol 51:463–472.

Ohyama T, Mohamed O a, Taketo MM, Dufort D, Groves AK (2006) Wnt signals mediate a fate decision between otic placode and epidermis. Development 133:865–875.

Olivier N, Luengo-oroz M a, Duloquin L, Faure E, Savy T, Veilleux I, Solinas X, Débarre D, Bourgine P, Santos A, Peyriéras N, Beaurepaire E (2010) Cell lineage reconstruction of early zebrafish embryo using label-free nonlinear microscopy. Science 329:967–971.

Paluch E, Piel M, Prost J, Bornens M, Sykes C (2005) Cortical actomyosin breakage triggers shape oscillations in cells and cell fragments. Biophys J 89:724–733.

Paluch EK, Raz E (2013) The role and regulation of blebs in cell migration. Curr Opin Cell Biol 25:582–590.

Paridaen JT, Huttner WB (2014) Neurogenesis during development of the vertebrate central nervous system. EMBO Rep 15:351–364.

Parks AL, Huppert SS, Muskavitch MAT (1997) The dynamics of neurogenic signalling underlying bristle development in Drosophila melanogaster. Mech Dev 63:61–74.

Pasini A, Jiang YJ, Wilkinson DG (2004) Two zebrafish Notch-dependent hairy/Enhancer-of-split-related genes, her6 and her4, are required to maintain the coordination of cyclic gene expression in the presomitic mesoderm. Development 131:1529–1541.

Pearson BJ, Doe CQ (2004) Specification of Temporal Identity in the Developing Nervous System. Annu Rev Cell Dev Biol 20:619–647.

Peinado H, Olmeda D, Cano A (2007) Snail, Zeb and bHLH factors in tumour progression: an alliance against the epithelial phenotype? Nat Rev Cancer 7:415–428.

Peinado H, Portillo F, Cano A (2004) Transcriptional regulation of cadherins during development and carcinogenesis. Int J Dev Biol 48:365–375.

Petrie RJ, Yamada KM (2015) Fibroblasts Lead the Way: A Unified View of 3D Cell Motility. Trends Cell Biol 25:666–674.

Peyre E, Morin X (2012) An oblique view on the role of spindle orientation in vertebrate neurogenesis. Dev Growth Differ 54:287–305.

Pfeffer PL, Gerster T, Lun K, Brand M, Busslinger M (1998) Characterization of three novel members of the zebrafish Pax2/5/8 family: dependency of Pax5 and Pax8 expression on the Pax2.1 (noi) function. Development 125:3063–3074.

Phillips BT, Bolding K, Riley BB (2001) Zebrafish fgf3 and fgf8 encode redundant functions required for otic placode induction. Dev Biol 235:351–365.

Phillips BT, Storch EM, Lekven AC, Riley BB (2004) A direct role for Fgf but not Wnt in otic placode induction. Development 131:923–931.

Pieper M, Eagleson GW, Wosniok W, Schlosser G (2011) Origin and segregation of cranial placodes in Xenopus laevis. Dev Biol 360:257–275.

Pirvola U, Spencer-Dene B, Xing-Qun L, Kettunen P, Thesleff I, Fritzsch B, Dickson C, Ylikoski J (2000) FGF/FGFR-2(IIIb) signaling is essential for inner ear morphogenesis. J Neurosci 20:6125–6134.

Pujades C, Kamaid A, Alsina B, Giraldez F (2006) BMP-signaling regulates the generation of hair-cells. Dev Biol 292:55–67.

Radde-Gallwitz K, Pan L, Gan L, Lin X, Segil N, Chen P (2004) Expression of Islet1 marks the sensory and neuronal lineages in the mammalian inner ear. J Comp Neurol 477:412–421.

Radosevic M, Fargas L, Alsina B (2014) The role of her4 in inner ear development and its relationship with proneural genes and Notch signalling. PLoS One 9.

Radosevic M, Robert-Moreno A, Coolen M, Bally-Cuif L, Alsina B (2011) Her9 represses neurogenic fate downstream of Tbx1 and retinoic acid signaling in the inner ear. Development 138:397–408.

Raft S, Groves AK (2014) Segregating neural and mechanosensory fates in the developing ear: patterning, signaling, and transcriptional control. Cell Tissue Res:315–332.

Raft S, Koundakjian EJ, Quinones H, Jayasena CS, Goodrich L V, Johnson JE, Segil N, Groves AK (2007) Cross-regulation of Ngn1 and Math1 coordinates the production of neurons and sensory hair cells during inner ear development. Development 134:4405–4415.

Raft S, Nowotschin S, Liao J, Morrow BE (2004) Suppression of neural fate and control of inner ear morphogenesis by Tbx1. Development 131:1801–1812.

Recher G, Jouralet J, Brombin A, Heuzé A, Mugniery E, Hermel J, Desnoulez S, Savy T, Herbomel P, Bourrat F, Peyriéras N, Jamen F, Joly J-S (2013) Zebrafish midbrain slow-amplifying progenitors exhibit high levels of transcripts for nucleotide and ribosome biogenesis. Development 140:4860–4869.

Reillo I, Borrell V (2012) Germinal zones in the developing cerebral cortex of ferret: Ontogeny, cell cycle kinetics, and diversity of progenitors. Cereb Cortex 22:2039–2054.

Represa J, Leon Y, Miner C, Giraldez F (1991) The int-2 proto-oncogene is responsible for induction of the inner ear. Nature 353:561–563.

Riley BB, Chiang M, Farmer L, Heck R (1999) The deltaA gene of zebrafish mediates lateral inhibition of hair cells in the inner ear and is regulated by pax2.1. Development 126:5669–5678.

Roszko I, Afonso C, Henrique D, Mathis L (2006) Key role played by RhoA in the balance between planar and apico-basal cell divisions in the chick neuroepithelium. Dev Biol 298:212–224.

Rousso DL, Pearson CA, Gaber ZB, Miquelajauregui A, Li S, Portera-Cailliau C, Morrisey EE, Novitch BG (2012) Foxp-Mediated Suppression of N-Cadherin Regulates Neuroepithelial Character and Progenitor Maintenance in the CNS. Neuron 74:314–330.

Roussos ET, Condeelis JS, Patsialou A (2011) Chemotaxis in cancer. Nat Rev Cancer 11:573–587.

Roztocil T, Matter-Sadzinski L, Alliod C, Ballivet M, Matter JM (1997) NeuroM, a neural helix-loop-helix transcription factor, defines a new transition stage in neurogenesis. Development 124:3263–3272.

Rubbini D, Robert-Moreno À, Hoijman E, Alsina B (2015) Retinoic Acid Signaling Mediates Hair Cell Regeneration by Repressing p27kip and sox2 in Supporting Cells. J Neurosci 35:15752–15766.

Ruprecht V, Wieser S, Callan-Jones A, Smutny M, Morita H, Sako K, Barone V, Ritsch-Marte M, Sixt M, Voituriez R, Heisenberg C-P (2015) Cortical contractility triggers a stochastic switch to fast amoeboid cell motility. Cell 160:673–685.

Sai X, Ladher RK (2008) FGF Signaling Regulates Cytoskeletal Remodeling during Epithelial Morphogenesis. Curr Biol 18:976–981.

Saint-Jeannet JP, Moody SA (2014) Establishing the pre-placodal region and breaking it into placodes with distinct identities. Dev Biol 389:13–27.

Sampath K, Stuart GW (1996) Developmental expression of class III and IV POU domain genes in the zebrafish. Biochem Biophys Res Commun 219:565–571.

Sánchez-Alcañiz JA, Haege S, Mueller W, Pla R, Mackay F, Schulz S, López-Bendito G, Stumm R, Marín O (2011) Cxcr7 Controls Neuronal Migration by Regulating Chemokine Responsiveness. Neuron 69:77–90.

Sanchez-Calderon H, Milo M, Leon Y, Varela-Nieto I (2007) A network of growth and transcription factors controls neuronal differentation and survival in the developing ear. Int J Dev Biol 51:557–570.

Sapede D, Dyballa S, Pujades C (2012) Cell lineage analysis reveals three different progenitor pools for neurosensory elements in the otic vesicle. J Neurosci 32:16424–16434.

Satoh T, Fekete DM (2005) Clonal analysis of the relationships between mechanosensory cells and the neurons that innervate them in the chicken ear. Development 132:1687–1697.

Sauer ME, Walker BE (1959) Radioautographic study of interkinetic nuclear migration in the neural tube. Proc Soc Exp Biol Med 101:557–560.

Savagner P, Yamada KM, Thiery JP (1997) The Zinc-Finger Protein Slug Causes DesmosomeDissociation, an Initial and Necessary Step forGrowth Factor–induced Epithelial–Mesenchymal Transition. 137:1–17.

Schimmang T (2007) Expression and functions of FGF ligands during early otic development. Int J Dev Biol 51:473–481.

Schindelin J, Arganda-Carreras I, Frise E, Kaynig V, Longair M, Pietzsch T, Preibisch S, Rueden C, Saalfeld S, Schmid B, Tinevez J-Y, White DJ,

Hartenstein V, Eliceiri K, Tomancak P, Cardona A (2012) Fiji: an open-source platform for biological-image analysis. Nat Methods 9:676–682.

Schlosser G (2006) Induction and specification of cranial placodes. Dev Biol 294:303–351.

Schlosser G (2010) Making senses development of vertebrate cranial placodes. Int Rev Cell Mol Biol 283:129–234.

Schlosser G, Ahrens K (2004) Molecular anatomy of placode development in Xenopus laevis. Dev Biol 271:439–466.

Schlosser G, Kintner C, Northcutt RG (1999) Loss of ectodermal competence for lateral line placode formation in the direct developing frog Eleutherodactylus coqui. Dev Biol 213:354–369.

Schlosser G, Northcutt RG (2000) Development of neurogenic placodes in Xenopus laevis. J Comp Neurol 418:121–146.

Scholpp S, Delogu A, Gilthorpe J, Peukert D, Schindler S, Lumsden A (2009) Her6 regulates the neurogenetic gradient and neuronal identity in the thalamus. Proc Natl Acad Sci U S A 106:19895–19900.

Shailam R, Lanford PJ, Dolinsky CM, Norton CR, Gridley T, Kelley MW (1999) Expression of proneural and neurogenic genes in the embryonic mammalian vestibular system. J Neurocytol 28:809–819.

Sheetz MP, Sable JE, Döbereiner H-G (2006) Continuous Membrane-Cytoskeleton Adhesion Requires Continuous Accommodation To Lipid and Cytoskeleton Dynamics. Annu Rev Biophys Biomol Struct 35:417–434.

Shitamukai A, Konno D, Matsuzaki F (2011) Oblique Radial Glial Divisions in the Developing Mouse Neocortex Induce Self-Renewing Progenitors outside the Germinal Zone That Resemble Primate Outer Subventricular Zone Progenitors. J Neurosci 31:3683–3695.

Shitamukai A, Matsuzaki F (2012) Control of asymmetric cell division of mammalian neural progenitors. Dev Growth Differ 54:277–286.

Shook D, Keller R (2003) Mechanisms, mechanics and function of epithelial-mesenchymal transitions in early development. Mech Dev 120:1351–1383.

Sieger D, Moritz C, Ziegenhals T, Prykhozhij S, Peri F (2012) Long-Range Ca2+ Waves Transmit Brain-Damage Signals to Microglia. Dev Cell 22:1138–1148.

Silva AO, Ercole CE, McLoon SC (2002) Plane of cell cleavage and numb distribution during cell division relative to cell differentiation in the developing retina. J Neurosci 22:7518–7525.

Skeath JB, Carroll SB (1994) The achaete-scute complex: generation of cellular pattern and fate within the Drosophila nervous system. FASEB J 8:714–721.

So JH, Chun HS, Bae YK, Kim HS, Park YM, Huh TL, Chitnis AB, Kim CH, Yeo SY (2009) Her4 is necessary for establishing peripheral projections of the trigeminal ganglia in zebrafish. Biochem Biophys Res Commun 379:22–26.

Solomon KS, Kudoh T, Dawid IB, Fritz A (2003) Zebrafish foxi1 mediates otic placode formation and jaw development. Development 130:929–940.

Solomon KS, Kwak SJ, Fritz A (2004) Genetic interactions underlying otic placode induction and formation. Dev Dyn 230:419–433.

Sommer L, Ma Q, Anderson DJ (1996) neurogenins, a novel family of atonal-related bHLH transcription factors, are putative mammalian neuronal determination genes that reveal progenitor cell heterogeneity in the developing CNS and PNS. Mol Cell Neurosci 8:221–241.

Spear PC, Erickson CA (2012) Interkinetic nuclear migration: A mysterious process in search of a function. Dev Growth Differ 54:306–316.

Stone JS, Rubel EW (1999) Delta1 expression during avian hair cell regeneration. Development 126:961–973.

Streit A (2002) Extensive cell movements accompany formation of the otic placode. Dev Biol 249:237–254.

Streit A (2004) Early development of the cranial sensory nervous system: From a common field to individual placodes. Dev Biol 276:1–15.

Streit A, Berliner AJ, Papanayotou C, Sirulnik A, Stern CD (2000) Initiation of neural induction by FGF signalling before gastrulation. Nature 406:74–78.

Streit A, Stern CD (1999) Establishment and maintenance of the border of the neural plate in the chick: Involvement of FGF and BMP activity. Mech Dev 82:51–66.

Swanson GJ, Howard M, Lewis J (1990) Epithelial autonomy in the development of the inner ear of a bird embryo. Dev Biol 137:243–257.

Sweet EM, Vemaraju S, Riley BB (2011) Sox2 and Fgf interact with Atoh1 to promote sensory competence throughout the zebrafish inner ear. Dev Biol 358:113–121.

Takebayashi K, Akazawa C, Nakanishi S, Kageyama R (1995) Structure and promoter analysis of the gene encoding the mouse helix-loop-helix factor HES-5. Identification of the neural precursor cell-specific promoter element. J Biol Chem 270:1342–1349.

Takebayashi S, Yamamoto N, Yabe D, Fukuda H, Kojima K, Ito J, Honjo T (2007) Multiple roles of Notch signaling in cochlear development. Dev Biol 307:165–178.

Takke C, Dornseifer P, v Weizsacker E, Campos-Ortega JA (1999) her4, a zebrafish homologue of the Drosophila neurogenic gene E(spl), is a target of NOTCH signalling. Development 126:1811–1821.

Tateya T, Imayoshi I, Tateya I, Ito J, Kageyama R (2011) Cooperative functions of Hes/Hey genes in auditory hair cell and supporting cell development. Dev Biol 352:329–340.

Taverna E, Götz M, Huttner WB (2014) The cell biology of neurogenesis: toward an understanding of the development and evolution of the neocortex.

Taverna E, Huttner WB (2010) Neural progenitor nuclei IN motion. Neuron 67:906–914.

Teissier A, Waclaw RR, Griveau A, Campbell K, Pierani A (2012) Tangentially migrating transient glutamatergic neurons control neurogenesis and maintenance of cerebral cortical progenitor pools. Cereb Cortex 22:403–416.

Theveneau E, Marchant L, Kuriyama S, Gull M, Moepps B, Parsons M, Mayor R (2010) Collective chemotaxis requires contact-dependent cell polarity. Dev Cell 19:39–53.

Theveneau E, Mayor R (2012) Neural crest delamination and migration: From epithelium-to-mesenchyme transition to collective cell migration. Dev Biol 366:34–54.

Theveneau E, Steventon B, Scarpa E, Garcia S, Trepat X, Streit A, Mayor R (2013) Chase-and-run between adjacent cell populations promotes directional collective migration. Nat Cell Biol 15:763–772.

Thiery JP, Acloque H, Huang RYJ, Nieto MA (2009) Epithelial-Mesenchymal Transitions in Development and Disease. Cell 139:871–890.

Thiery JP, Duband JL, Rutishauser U, Edelman GM (1982) Cell adhesion molecules in early chicken embryogenesis. Proc Natl Acad Sci U S A 79:6737–6741.

Thiery JP, Sleeman JP (2006) Complex networks orchestrate epithelial-mesenchymal transitions. Nat Rev Mol Cell Biol 7:131–142.

Thisse B, Heyer V, Lux A, Alunni V, Degrave A, Seiliez I, Kirchner J, Parkhill JP, Thisse C (2004) Spatial and temporal expression of the zebrafish genome by large-scale in situ hybridization screening. Methods Cell Biol 77:505–519.

Thisse C, Thisse B, Postlethwait JH (1995) Expression of snail2, a second member of the zebrafish snail family, in cephalic mesendoderm and presumptive neural crest of wild-type and spadetail mutant embryos. Dev Biol 172:86–99.

Tian L, Hires SA, Mao T, Huber D, Chiappe ME, Chalasani SH, Petreanu L, Akerboom J, McKinney SA, Schreiter ER, Bargmann CI, Jayaraman V, Svoboda K, Looger LL (2009) Imaging neural activity in worms, flies and mice with improved GCaMP calcium indicators. Nat Methods 6:875–881.

Torres M, Giraldez F (1998) The development of the vertebrate inner ear. Mech Dev 71:5–21.

Tournaviti S, Hannemann S, Terjung S, Kitzing TM, Stegmayer C, Ritzerfeld J, Walther P, Grosse R, Nickel W, Fackler OT (2007) SH4-domain-induced plasma membrane dynamization promotes bleb-associated cell motility. J Cell Sci 120:3820–3829.

Vallin J, Girault JM, Thiery JP, Broders F (1998) Xenopus cadherin-11 is expressed in different populations of migrating neural crest cells. Mech Dev 75:171–174.

Van Doren M, Bailey AM, Esnayra J, Ede K, Posakony JW (1994) Negative regulation of proneural gene activity: Hairy is a direct transcriptional repressor of achaete. Genes Dev 8:2729–2742.

Vannier C, Mock K, Brabletz T, Driever W (2013) Zeb1 regulates E-cadherin and Epcam (epithelial cell adhesion molecule) expression to control cell behavior in early zebrafish development. J Biol Chem 288:18643–18659.

Vemaraju S, Kantarci H, Padanad MS, Riley BB (2012) A spatial and temporal gradient of Fgf differentially regulates distinct stages of neural development in the zebrafish inner ear. PLoS Genet 8(11):e1003068.

Vendrell V, Carnicero E, Giraldez F, Alonso MT, Schimmang T (2000) Induction of inner ear fate by FGF3. Development 127:2011–2019.

Villares R, Cabrera C V. (1987) The achaete-scute gene complex of D. melanogaster: Conserved Domains in a subset of genes required for neurogenesis and their homology to myc. Cell 50:415–424.

Vitelli F, Viola A, Morishima M, Pramparo T, Baldini A, Lindsay E (2003) TBX1 is required for inner ear morphogenesis. Hum Mol Genet 12:2041–2048.

Waddington CH (1937) The determination of the auditory placode in the chick. JExpBiol 14:232–239.

Wakamatsu Y, Maynard TM, Jones SU, Weston JA (1999) NUMB localizes in the basal cortex of mitotic avian neuroepithelial cells and modulates neuronal differentiation by binding to NOTCH-1. Neuron 23:71–81.

Wang C, Li S, Januschke J, Rossi F, Izumi Y, Garcia-Alvarez G, Gwee SSL, Soon SB, Sidhu HK, Yu F, Matsuzaki F, Gonzalez C, Wang H (2011a) An Ana2/Ctp/mud complex regulates spindle orientation in Drosophila neuroblasts. Dev Cell 21:520–533.

Wang J, Wu Y, Zhao F, Wu Y, Dong W, Zhao J, Zhu Z, Liu D (2015) Fgf-Signaling-Dependent Sox9a and Atoh1a Regulate Otic Neural Development in Zebrafish. J Neurosci 35:234–244.

Wang Y, Li G, Stanco A, Long JE, Crawford D, Potter GB, Pleasure SJ, Behrens T, Rubenstein JLR (2011b) CXCR4 and CXCR7 Have Distinct Functions in Regulating Interneuron Migration. Neuron 69:61–76.

Weber IP, Ramos AP, Strzyz PJ, Leung LC, Young S, Norden C (2014) Mitotic Position and Morphology of Committed Precursor Cells in the Zebrafish Retina Adapt to Architectural Changes upon Tissue Maturation. Cell Rep 7:386–397.

Westerman BA, Murre C, Oudejans CBM (2003) The cellular Pax-Hox-Helix connection. Biochim Biophys Acta - Gene Struct Expr 1629:1–7.

Wheelock MJ, Shintani Y, Maeda M, Fukumoto Y, Johnson KR (2008) Cadherin switching. J Cell Sci 121:727–735.

Whitfield TT (2002) Zebrafish as a model for hearing and deafness. J Neurobiol 53:157–171.

Whitfield TT, Granato M, van Eeden FJ, Schach U, Brand M, Furutani-Seiki M, Haffter P, Hammerschmidt M, Heisenberg CP, Jiang YJ, Kane DA, Kelsh RN, Mullins MC, Odenthal J, Nusslein-Volhard C (1996) Mutations affecting development of the zebrafish inner ear and lateral line. Development 123:241–254.

Whitfield TT, Hammond KL (2007) Axial patterning in the developing vertebrate inner ear. Int J Dev Biol 51:507–520.

Whitfield TT, Riley BB, Chiang M-YY, Phillips B (2002) Development of the zebrafish inner ear. Dev Dyn 223:427–458.

Whitlock KE, Westerfield M (2000) The olfactory placodes of the zebrafish form by convergence of cellular fields at the edge of the neural plate. Development 127:3645–3653.

Wilcock AC, Swedlow JR, Storey KG (2007) Mitotic spindle orientation distinguishes stem cell and terminal modes of neuron production in the early spinal cord. Development 134:1943–1954.

Wildner H, Müller T, Cho S-H, Bröhl D, Cepko CL, Guillemot F, Birchmeier C (2006) dILA neurons in the dorsal spinal cord are the product of terminal and non-terminal asymmetric progenitor cell divisions, and require Mash1 for their development. Development 133:2105–2113.

Wilkinson DG, Peters G, Dickson C, McMahon AP (1988) Expression of the FGF-related proto-oncogene int-2 during gastrulation and neurulation in the mouse. EMBO J 7:691–695.

Williams JA, Holder N (2000) Cell turnover in neuromasts of zebrafish larvae. Hear Res 143:171–181.

Woda JM, Pastagia J, Mercola M, Artinger KB (2003) Dlx proteins position the neural plate border and determine adjacent cell fates. Development 130:331–342.

Wong GKW, Baudet M-L, Norden C, Leung L, Harris W a. (2012) Slit1b-Robo3 Signaling and N-Cadherin Regulate Apical Process Retraction in Developing Retinal Ganglion Cells. J Neurosci 32:223–228.

Woods C, Montcouquiol M, Kelley MW (2004) Math1 regulates development of the sensory epithelium in the mammalian cochlea. Nat Neurosci 7:1310–1318.

Woods CG, Bond J, Enard W (2005) Autosomal recessive primary microcephaly (MCPH): a review of clinical, molecular, and evolutionary findings. Am J Hum Genet 76:717–728.

Wright TJ, Mansour SL (2003a) Fgf3 and Fgf10 are required for mouse otic placode induction. Development 130:3379–3390.

Wright TJ, Mansour SL (2003b) FGF signaling in ear development and innervation. Curr Top Dev Biol 57:225–259.

Wu DK, Nunes FD, Choo D (1998) Axial specification for sensory organs versus non-sensory structures of the chicken inner ear. Development 125:11–20.

Wu DK, Oh SH (1996) Sensory organ generation in the chick inner ear. J Neurosci 16:6454–6462.

Xiang M, Gan L, Li D, Chen ZY, Zhou L, O'Malley BW, Klein W, Nathans J (1997) Essential role of POU-domain factor Brn-3c in auditory and vestibular hair cell development. Proc Natl Acad Sci U S A 94:9445–9450.

Xiang M, Gao WQ, Hasson T, Shin JJ (1998) Requirement for Brn-3c in maturation and survival, but not in fate determination of inner ear hair cells. Development 125:3935–3946.

Xiang M, Maklad A, Pirvola U, Fritzsch B (2003) Brn3c null mutant mice show long-term, incomplete retention of some afferent inner ear innervation. BMC Neurosci 4:2.

Xiong F, Tentner AR, Huang P, Gelas A, Mosaliganti KR, Souhait L, Rannou N, Swinburne IA, Obholzer ND, Cowgill PD, Schier AF, Megason SG (2013) Specified neural progenitors sort to form sharp domains after noisy Shh signaling. Cell 153:550–561.

Xu H, Viola A, Zhang Z, Gerken CP, Lindsay-Illingworth EA, Baldini A (2007) Tbx1 regulates population, proliferation and cell fate determination of otic epithelial cells. Dev Biol 302:670–682.

Yamada A, Hirose K, Hashimoto A, Iino M (2005) Real-time imaging of myosin II regulatory light-chain phosphorylation using a new protein biosensor. Biochem J 385:589–594.

Yang J, Weinberg RA (2008) Epithelial-Mesenchymal Transition: At the Crossroads of Development and Tumor Metastasis. Dev Cell 14:818–829.

Yeo SY, Kim M, Kim HS, Huh TL, Chitnis AB (2007) Fluorescent protein expression driven by her4 regulatory elements reveals the spatiotemporal pattern of Notch signaling in the nervous system of zebrafish embryos. Dev Biol 301:555–567.

Young PE, Pesacreta TC, Kiehart DP (1991) Dynamic changes in the distribution of cytoplasmic myosin during Drosophila embryogenesis. Development 111:1–14.

Zecca A, Dyballa S, Voltes A, Bradley R, Pujades C (2015) The Order and Place of Neuronal Differentiation Establish the Topography of Sensory Projections and the Entry Points within the Hindbrain. J Neurosci 35:7475–7486.

Zelarayan LC et al. (2007) Differential requirements for FGF3, FGF8 and FGF10 during inner ear development. Dev Biol 308:379–391.

Zheng JL, Gao WQ (2000) Overexpression of Math1 induces robust production of extra hair cells in postnatal rat inner ears. Nat Neurosci 3:580–586.

Zheng JL, Helbig C, Gao WQ (1997) Induction of cell proliferation by fibroblast and insulin-like growth factors in pure rat inner ear epithelial cell cultures. J Neurosci 17:216–226.

Zheng JL, Shou J, Guillemot F, Kageyama R, Gao WQ (2000) Hes1 is a negative regulator of inner ear hair cell differentiation. Development 127:4551–4560.

Zhong W, Feder JN, Jiang MM, Jan LY, Jan YN (1996) Asymmetric localization of a mammalian Numb homolog during mouse cortical neurogenesis. Neuron 17:43–53.

Zine A, Aubert A, Qiu J, Therianos S, Guillemot F, Kageyama R, de Ribaupierre F (2001) Hes1 and Hes5 activities are required for the normal development of the hair cells in the mammalian inner ear. J Neurosci 21:4712–4720.

Zirlinger M, Lo L, McMahon J, McMahon AP, Anderson DJ (2002) Transient expression of the bHLH factor neurogenin-2 marks a subpopulation of neural crest cells biased for a sensory but not a neuronal fate. Proc Natl Acad Sci U S A 99:8084–8089.

Zou D, Silvius D, Fritzsch B, Xu P-X (2004) Eya1 and Six1 are essential for early steps of sensory neurogenesis in mammalian cranial placodes. Development 131:5561–5572.

# 7. APPENDIX

194

## 7.1. Supplementary figures

## Chapter 1
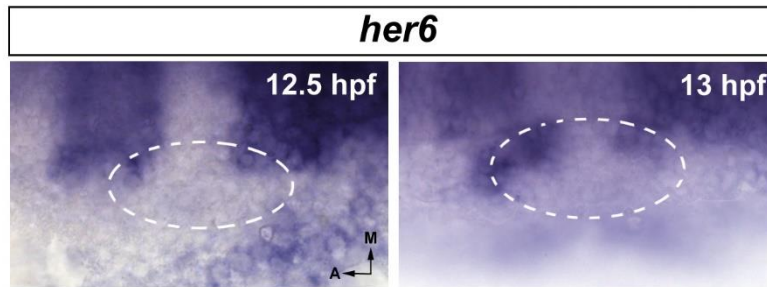


**Figure S1**. *her6* **is expressed in similar domains to** *her4.*

*her6* expression is restricted to the anterior and posterior sensory domains from its onset and is not induced at the CMD.

# Chapter 2



**A** 13 hpf Post-photoconversion  20 hpf

**B** *neurog1*:dsRedE *neurod*:GFP memb-GFP

16 hpf
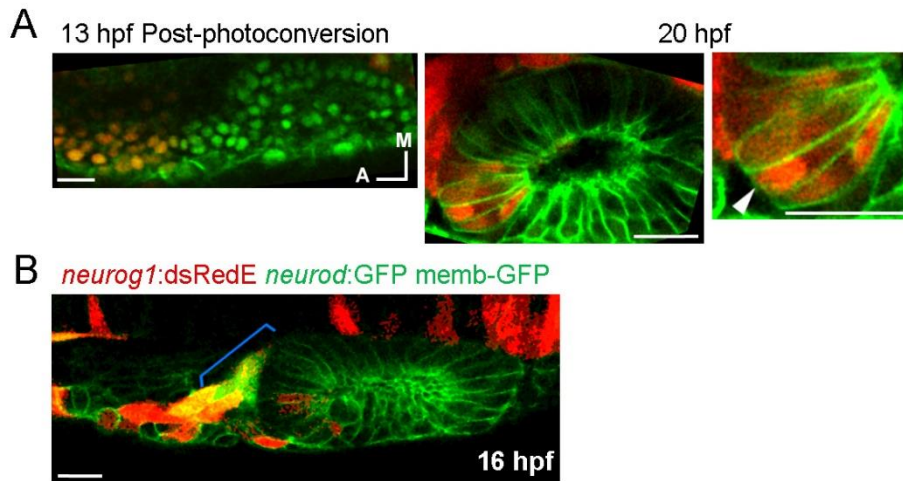
**Figure S2. Cell ingression and populations of ingressing cells. Related to Figure 22.**

**(A)** Photoconversion of a region anterior to the vesicle of NLS-Eos stained nuclei at 13 hpf in TgBAC(*neurog1*:DsRedE)[n16] embryos expressing memb-GFP. At 20 hpf photoconverted nuclei were observed in *neurog1*+ cells inside the vesicle (arrowhead). **(B)** GFP reporting *neurod* expression in the non-ingressing pool of cells at 16 hpf from Tg(*neurod:GFP*) embryos (blue bracket). Embryos are also TgBAC(*neurog1*:DsRedE)[n16] and express memb-GFP. Scale bars, 20 μm.
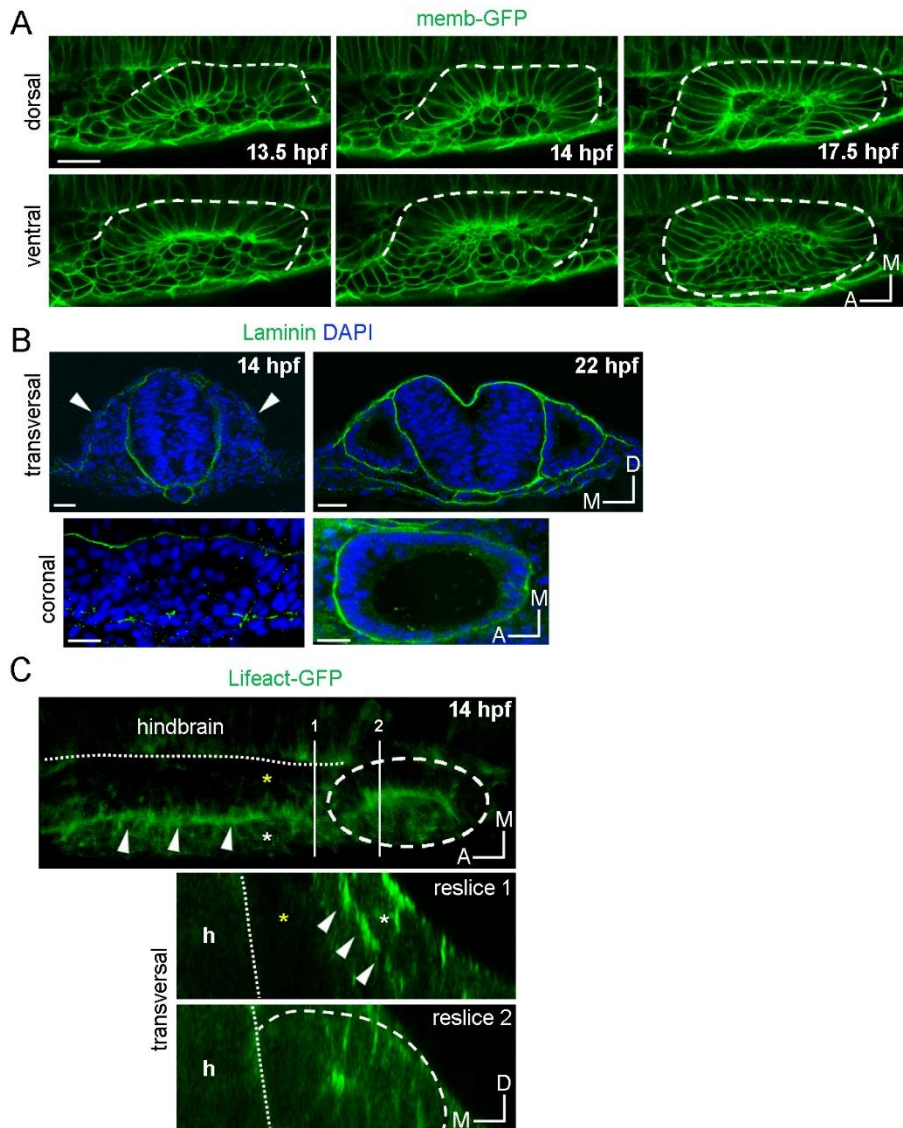
**Figure S3. Morphogenetic features related to ingression. Related to Figures 23-24.**

**(A-C)** As we previously reported, the otic placode is only epithelialized medially at these stages (Hoijman et al., 2015). Later, while the posterior part of the placode already presents an organized epithelial structure and has segregated from the surrounding cells, the anterior region of the placode does not (A). Moreover, the basal lamina at these early stages is only rudimentary and not continuous (contrary to the one present at later stages completely surrounding

the organ (B)). Therefore, the combination of these morphogenetic features could allow the migrating cells to be able to ingress into the primordium before is fully organized. The migrating cells are located in a region of the embryo that is converging medially together with the neural tube (Bhat and Riley, 2011) (see Figure 24). This lateral region of migrating cells is delimitated by an F-actin rich layer that runs anteroposteriorly until it reaches the placode (C), dividing mediolaterally this dense migratory cell region from the medial one presenting sparse cells (see Figure 24). **(A)** Early stages of otic epithelialization. Dashed line indicates the epithelialized part of the otic vesicle. The posterior part folds before the anterior. Membranes are stained with memb-GFP. **(B)** Laminin staining at 14 and 22 hpf in transversal and coronal sections. Nuclei are counterstained with DAPI. White arrowheads indicate where the otic placodes are located. **(C)** 3D reconstruction (dorsal view) of an otic vesicle and its anterior region at 14 hpf from a Tg(actb1:Lifect-GFP) embryo. An actin layer (white arrowheads) divides lateromedially the tissues lateral to the hindbrain in two regions (white and yellow asterisks, see also reslice 1). Reslices, built from the white bars 1 and 2 shown in the 3D reconstruction, show transversal sections anterior (reslice 1) or at the position (reslice 2) of the otic placode (dashed line). h: hindbrain (dotted line). Scale bars, 20 μm.
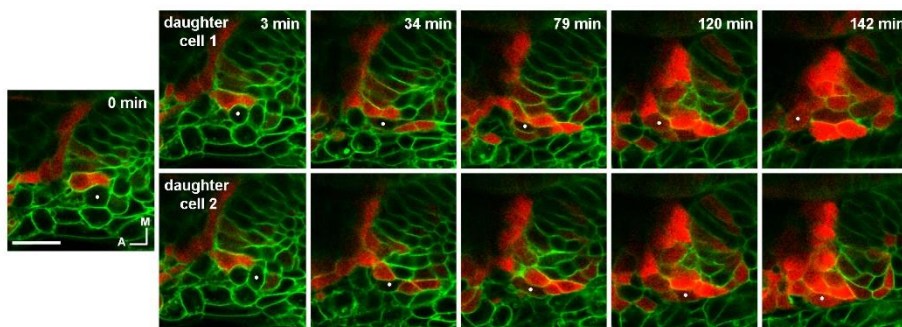


**Figure S4. Cell division can precede *neurog1* expression. Related to Figure 27.**

3D tracking of a *neurog1⁻* cell (white dot) that divides and subsequently their daughters express DsRedE and delaminate.
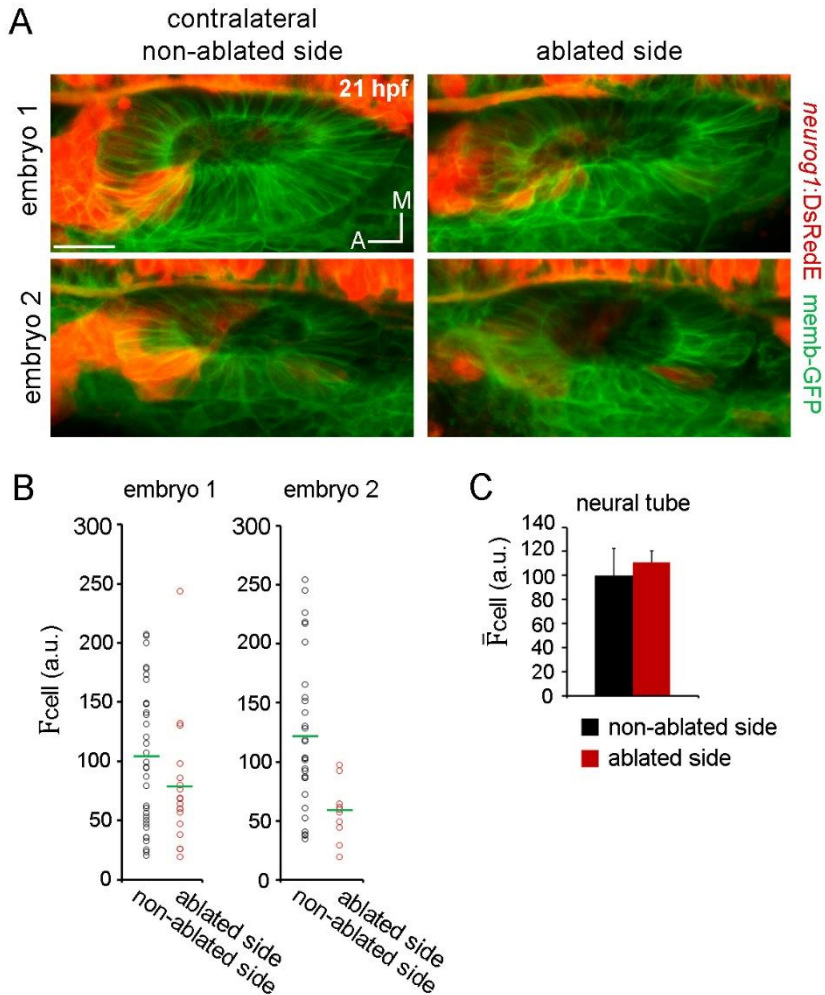
**Figure S5. Late *neurog1* expression pattern inside the vesicle after ablation. Related to Figure 29.**

**(A)** Images of the embryos shown in (Figure 29) 8 hours after ablation (21 hpf). The ablated side and their contralateral non-ablated side of the same embryo are shown. **(B)** Quantification of the mean DsRedE fluorescence in each *neurog1*+ cell of the vesicles shown in (A). Each dot indicates one cell. Green lines indicate the mean of each condition. **(C)** Quantification of the $\bar{F}_{cell}$ in a region of the neural tube adjacent to the otic vesicle 5 hours after ablation (18 hpf). Data are mean s.e.m. (n=3).

## 7.2. Supplementary movie legends

## Chapter 2

**Movie S1. 4D imaging of otic neuronal specification. Related to Figure 20.**
3D reconstructed time-lapse of the otic vesicle from a TgBAC(*neurog1*:DsRedE)[n16] embryo. Red: DsRedE fluorescence. Green: memb-GFP. Dorsal view. Time from the first frame is indicated.

**Movie S2. Specification dynamics visualized in individual cells. Related to Figure 20.**
Selected coronal ventral planes from the z-stacks used for 3D reconstructions in Movie S1.

**Movie S3. *neurog1* expressing cells locate in the SAG after delamination. Related to Figure 20.**
3D reconstruction of the otic vesicle at 21 hpf. White arrow indicates the position of the SAG.

**Movie S4. Early *neurog1* expressing cells located anterior to the otic vesicle. Related to Figure 22.**
3D reconstruction of an otic vesicle and the anterior region at 13 hpf, showing the presence of DsRedE expressing cells (white arrows).

**Movie S5. *neurog1* expressing cells ingress in the otic vesicle. Related to Figure 22.**
3D reconstructed time-lapse showing the ingression of *neurog1* expressing cells. Orange arrowheads indicate ingressing cells and white arrowheads cells that are outside the organ. Cells that will ingress are highlighted with a red bracket and the direction of movement by a red arrow. The group of *neurog1* expressing cells that do not ingress is

indicated by a blue bracket and arrow.

**Movie S6. 3D tracking of an individual cell during ingression, division and delamination. Related to Figure 22.**

Coronal ventral planes from z-stacks selected to track an ingressing cell (white dot). Note that it begins to express *neurog1* before epithelialization.

**Movie S7. 3D tracking of multiple cells during ingression. Related to Figure 23.**

Initially, the position of three cells anterior to the otic placode is shown (white, pink and blue dots). Tracking (upper panels) and 2D trajectory of each cell (lower panel, yellow track shows the position of the posterior vertex of the placode) are depicted. Insets highlight the mode of migration, with leading edge of the cell protruding (white arrowheads) before the forward displacement of the nucleus (yellow arrowheads).

**Movie S8. Real-time activation of *neurog1* expression in local specified cells. Related to Figure 25.**

Coronal ventral planes from z-stacks selected to follow the beginning of DsRedE expression in two individual cells that are being specified locally (white and blue dots). Insets show higher magnification images.

**Movie S9. Apical scaffold formation dynamics. Related to Figure 26.**

3D reconstructed time-lapse of Pard3-GFP (gray) localization during otic morphogenesis (dorsal view). Pard3-GFP in the otic vesicle (green arrows) or in the superficial external superficial (orange arrows) is shown. The anterolateral apical scaffold forms early during placode development and is transitory.

**Movie S10. Coordinated delamination after division of *neurog1* expressing cells. Related to Figure 27.**

In the upper panel, coronal planes tracking an individual cell before division (white dot) and their daughters after division and until delamination (white and blue dots) are shown. In the lower panel, 2D movement of the tracked cells is shown. Note the coordinated behavior of daughter cells moving in close contact to the periphery of the tissue and delaminating simultaneously.

**Movie S11. Visualizing quick delamination after division. Related to Figure 27.**

Same tracking as in Movie S10 but in this case sagittal planes are shown in the lower panel. Only one daughter is tracked (white dot). White lines indicate the limits of the vesicle.

**Movie S12. Ablation of pioneer cells before ingression affects *neurog1* expression in the NgD at later stages. Related to Figure 29.**

3D reconstruction of the DsRedE signal in the NgD (red) of otic vesicles at 21 hpf corresponding to the previously ablated (upper panel) and contralateral non-ablated (lower panel) sides of the same embryo. A single plane of the memb-GFP signal from each vesicle is shown for better 3D orientation (green).

## Chapter 3

**Movie S13. *neurog1* positive cells form blebs at the basal side during delamination. Related to Figure 37.**

Coronal planes from z-stacks selected to follow a *neurog1* expressing cell forming blebs prior to delamination. Green: memb-GFP.

**Movie S14. Cortical myosin recruitment during bleb retraction phase. Related to Figure 38.**

Time-lapse imaging of bleb formation from a Tg(β-actin:myl12.1-eGFP) embryo. Green: GFP fluorescence. Red: memb-mCherry. Dorsal view.

**Movie S15. Calcium accumulation during bleb formation. Related to Figure 38.**

Time-lapse imaging of $Ca^{2+}$ during bleb formation from a wild-type embryo. Green: GCaMP3.1 fluorescence. Red: memb-mCherry. Dorsal view. White arrows indicate calcium activation at the bleb.

## 7.3. Abbreviations

| | |
|---|---|
| *ace* | *acerebellar* |
| **AM** | anteromedial |
| **AP** | anteroposterior |
| *asc* | *achaete-scute* |
| *ato* | *atonal* |
| *atoh* | *atonal homologue* |
| **AV** | anteroventral |
| **bHLH** | basic Helix-Loop-Helix |
| **BMP** | Bone Morphogenetic Protein |
| **BSA** | Bovine Serum Albumin |
| *Dl* | *delta* |
| **CMD** | Central Medial Domain |
| **CNS** | Central Nervous System |
| **DIG** | digoxigenin |
| **DMSO** | dimethyl sulphoxide |
| **DNA** | deoxyribonucleic acid |
| **DV** | dorsoventral |
| **EB** | epibranchial |
| **EMT** | Epithelial-Mesenchymal Transition |
| *Espl* | *Enhancer of Split* |
| **EVL** | enveloping layer |
| **FGF** | Fibroblast Growth Factor |
| **FGFR** | Fibroblast Growth Factor Receptor |
| **GFP** | Green Fluorescent Protein |
| **HC** | Hair Cell |
| *her* | *hairy-related* |
| *Hes* | *Hairy and Enhancer of Split* |
| **hpf** | hours post-fertilization |
| **hr** | hours |
| *hsy* | *hearsay* |
| **INM** | Interkinetic Nuclear Migration |
| **ISH** | in situ hybridization |
| **MET** | Mesenchymal-Epithelial Transition |
| *mib* | *mind bomb* |
| **min** | minutes |
| **ML** | mediolateral |
| **N** | Notch |
| **NC** | Neural Crest |

204

| | |
|---|---|
| ***Neurog*** | *Neurogenin* |
| **NgD** | Neurogenic Domain |
| **NGS** | Normal Goat Serum |
| **OEPD** | Otic-Epibranchial Precursor Domain |
| **Pard3** | partitioning-defective complex protein 3 |
| **pax** | paired box |
| **PBS** | Phosphate Buffered Saline |
| **PBT** | Phosphate Buffered Saline with Tween-20 |
| **PCR** | Polymerase Chain Reaction |
| **PFA** | paraformaldehyde |
| **PGC** | Primordial Germ Cells |
| **pH3** | phospho-histone 3 |
| **PPR** | Pre-Placodal Region |
| **RA** | Retinoic Acid |
| **RNA** | ribonucleic acid |
| **SAG** | statoacoustic ganglion, gVIII$^{th}$ |
| **SC** | Supporting Cell |
| **Sdf1** | Stromal-derived factor 1 |
| **sec** | seconds |
| **Shh** | Sonic Hedgehog |
| **ss** | somite-stage |
| **Tbx** | T-box transcription factor |
| **VAL** | ventroanterolateral |
| **Wnt** | Wingless-related integration site |
| **Zeb** | zinc finger E-box-binding |
| **ZO-1** | zona occludens 1 |

# 8. ANNEX

During my PhD I also collaborate in other projects that result in the following publications:

Iturbide A, Pascual-Reguant L, Fargas L, Cebrià JP, Alsina B, García de Herreros A, Peiró S (2015) LOXL2 Oxidizes Methylated TAF10 and Controls TFIID-Dependent Genes during Neural Progenitor Differentiation. Mol Cell 58:755–766. doi: 10.1016/j.molcel.2015.04.012

Pujadas G, Cervantes S, Tutusaus A, Ejarque M, Sanchez L, García A, Esteban Y, Fargas L, Alsina B, Hartmann C, Gomis R, Gasa R (2016) Wnt9a deficiency discloses a repressive role of Tcf7l2 on endocrine differentiation in the embryonic pancreas. Sci Rep 6:19223. doi: 10.1038/srep19223